

UNIVERSITÉ DU QUÉBEC

**MÉMOIRE PRÉSENTÉ À
L'UNIVERSITÉ DU QUÉBEC À CHICOUTIMI
COMME EXIGENCE PARTIELLE
DE LA MAÎTRISE EN INGÉNIERIE**

PAR

ARUNIMA SARKAR

INVESTIGATION ON WETTING OF B₄C BY ALUMINUM ALLOYS

DECEMBER 2009

RÉSUMÉ

Les composites à matrices métalliques (CMM) ont intéressé l'industrie de l'aluminium (Al- Al_2O_3 , Al-SiC) à cause de la supériorité de leurs propriétés mécaniques comparée à celles d'alliage d'aluminium. Les composites d'aluminium- B_4C (CMM) sont devenue importante pour l'industrie de l'aluminium à cause de leurs utilisations dans des applications de haute performance telles que le stockage de rejets nucléaires radioactifs, les avions et les structures aérospatiales, dues à leur capacité d'absorber des neutrons, leur légèreté, leur haute résistance et leur rigidité. La production des matrices métalliques (CMM) de B_4C -aluminium n'est pas une tâche facile à cause de la faible mouillabilité de B_4C par l'aluminium. De plus, B_4C n'est pas stable quand il est en contact avec l'aluminium. Les analyses de l'interface basées sur la microscopie optique et la microscopie électronique à balayage ont indiqué la formation des particules d' Al_3BC et d' AlB_2 autour de la particule de B_4C . Cette réaction est incessante et elle a comme conséquence l'épuisement de la concentration de B_4C , la diminution de la fluidité de la fonte et la détérioration de ses propriétés mécaniques et physiques. Pour empêcher la perte de B_4C , le Ti est ajouté à l'aluminium. Le Ti a de l'affinité à réagir avec B_4C et forme une couche protectrice autour de la particule.

Les objectifs du projet sont d'étudier la mouillabilité des systèmes B_4C /aluminium et B_4C /alliage d'aluminium-titane et d'identifier d'autres éléments d'alliage potentiels pour protéger B_4C . Les expériences de mouillabilité sont effectuées pour mesurer les angles de contact de B_4C aussi bien que ceux des produits de réaction entre les éléments d'alliage et B_4C . Aussi, l'effet de la teneur en Ti de l'aluminium sur la mouillabilité de B_4C a été

étudié.

Les résultats des expériences montrent que l'addition de titane et de zirconium à l'aluminium a un effet positif fort sur le mouillage entre les particules de B_4C et le métal liquide. Afin de comprendre les effets que la réaction produit sur la mouillabilité, les angles de contact entre les produits de la réaction (particules de TiC , TiB_2 , AlB_2 and Al_4C_3) et l'aluminium ont été mesurés à $750^\circ C$ et $850^\circ C$. Les résultats démontrent également que la mouillabilité de B_4C augmente avec la température et le temps de contact.

On a constaté que les particules de AlB_2 disparaissent avec l'addition de Ti et de nouvelles particules en forme d'aiguille (TiB_2) riches en Ti se forment autour des particules de B_4C . Celles-ci agissent comme une barrière qui isole le B_4C de la matrice d'aluminium. On observe également que la formation d' Al_3BC diminue avec l'augmentation de la teneur en Ti. Cependant, si on continue d'augmenter la teneur en Ti, des plaques intermétalliques d' Al_3Ti se forment ce qui réduit la mouillabilité. Cette étude a démontré qu'il y a une teneur en Ti optimale où le mouillage est le meilleur. Cette valeur semble être autour de 1.5%Ti. L'augmentation de la teneur en Ti au delà de cette concentration détériore le mouillage.

L'aluminium est une des industries principales au Canada et au Québec, et les résultats de cette étude aideront à améliorer la qualité du produit grâce au transfert de la technologie vers l'industrie.

SUMMARY

Metal matrix composites (MMC) have been of interest to aluminum industry (Al-Al₂O₃, Al-SiC) because of their superior mechanical properties compared to aluminum alloys. Aluminum-B₄C composites (MMC) gained importance in aluminum industry because it can be used in high performance applications such as radioactive nuclear waste storage, aircraft and aerospace structures due to its neutron shielding capacity, light weight, high strength, and stiffness. It is difficult to mix B₄C powder with liquid aluminum to produce composites due to poor wettability of B₄C. In addition, B₄C is not stable when it is in contact with aluminum. The optical microscopy and scanning electron microscopy analyses of the interface revealed the formation of Al₃BC and AlB₂ particles around the B₄C particle. This reaction is continuous and results in the depletion of B₄C concentration, decrease in the fluidity of the melt, and deterioration in its mechanical and physical properties. To prevent B₄C loss, titanium is added to aluminum. Ti has affinity to react with B₄C and forms a protective layer around the particle.

Objectives of this project are to investigate the wettability of B₄C/aluminum and B₄C/aluminum-titanium alloy systems, and to identify other potential alloying elements to protect B₄C. The sessile-drop experiments have been conducted to measure the contact angles of B₄C as well as those of the interfacial reaction products forming due to the presence of alloying elements in aluminum. Also, the effect of Ti content on the wettability of B₄C by aluminum was studied.

The results of the experiments show that the titanium and zirconium addition to aluminum has a strong positive effect on wetting between B₄C particles and the liquid metal. In order

to understand the effects of the reaction products on wetting, the contact angles between the reaction products (TiC , TiB_2 , AlB_2 and Al_4C_3 particles) and aluminum have been measured at 750°C and 850°C . The results also show that wetting increases with increasing temperature and contact time.

It is found out that with Ti addition, AlB_2 particles disappear and new Ti-rich needle-like particles (TiB_2) are formed around the B_4C particles. These act as a barrier layer which isolates the B_4C from the aluminum matrix. It is also observed that with increasing Ti content, the formation of Al_3BC decreases. However, further increase in Ti content causes the formation of large plate-like Al_3Ti intermetallics which reduces the wettability. This study revealed that there is an optimum Ti content where the wetting is the highest. This value seems to be around 1.5wt%Ti. Further increase in Ti content deteriorates wetting.

Aluminum is one the major industries in Canada and Quebec and this knowledge will result in the improvement of product quality through technology transfer to the industry.

ACKNOWLEDGEMENTS

I would like to thank everyone who have helped and inspired me during my master's study.

I especially want to thank my Director, Prof. Duygu Kocafe, for her guidance during my research and study at University of Quebec at Chicoutimi. Her perpetual energy and enthusiasm in research had motivated all her advisees, including me. In addition, she was always accessible and willing to help her students with their research. As a result, research life became smooth and rewarding for me.

I am delighted to interact with Dr. X-G Chen by attending his classes and having him as my co-director. I would like to express my gratitude to him for his inspiring guidance and valuable help in research.

I would like to acknowledge Rio Tinto Alcan and National Science and Engineering Research Council (NSERC) of Canada for financial support. Special thanks to Mr. Patrice Paquet and Mr. Martin Bouchard for their technical supports, and Dr. Zhan Zhang for SEM analysis. I would also like to convey thanks to the Department of Applied Sciences of University of Quebec at Chicoutimi for providing the laboratory facilities.

A Special thanks to Dr. Ujjaini Sarkar and Dr Jayanta Guha for their support through the duration of my studies. I would like to express my love and gratitude to my parents for their understanding, & endless love. Also I wish to acknowledge the help provided, in every aspects, by the staff of the Engineering department of UQAC. I want to thank all my

colleagues and friends for their kindness and availability.

Table of Contents

CHAPTER 1	1
INTRODUCTION	1
1.1 Relationship between Wetting and Metal Matrix Composites	3
1.2 The Statement of the Problem	7
1.3 Scope	9
1.4 Objectives	10
CHAPTER 2	11
THEORY	11
2.1 Relationship between Wetting, Surface Tension and Contact Angle	11
2.1.1 Sessile -Drop System	13
2.1.2 Measurement of Surface Tension by Dorsey Method	13
2.2 Work of Adhesion	15
2.3 Wetting Model	15
2.4 Arrhenius Law	17
2.5 Phase Diagram of Aluminum-Titanium	17
CHAPTER 3	19
LITERATURE REVIEW	19

3.1 Wetting and Contact Angle	19
3.2 Surface Tension Measurement Methods.....	20
3.3 Sessile- Drop Technique	23
3.4 Effect of Different Factors on Wetting	23
3.4.2 Interfacial Reaction.....	26
3.4.3 Surface Roughness	27
3.4.4 Methods to Promote Wettability	28
3.5 Incorporation of Transition Metal Borides and Carbides.....	37
CHAPTER 4	39
EXPERIMENTAL SET-UP AND PROCEDURE.....	39
4.1 Sessile Drop Experimental Set-Up	39
4.2 Experimental Procedure of Sessile Drop Experiments	42
4.2.1 Sample Preparation.....	42
4.2.2 Experimental Procedure.....	44
4.2.3 Titanium Recycling	46
4.2.4 Sample Preparation for Analysis	47
4.2.5 Analysis of Samples Prepared.....	50
CHAPTER 5	52
RESULTS AND DISCUSSIONS	52

5.1 Experimental Results	52
5.1.1 Contact Angle Measurement of Al and Al-Ti Alloy on Different Ceramic Powders	57
5.1.2 Comparisons with Literature.....	70
5.1.3 Surface Tension Calculation for Al and Al-Ti Alloy	77
5.1.4 Microstructural Analyses	80
5.1.5 Calculation Work of Adhesion, Reaction Kinetics and Activation Energy of Different Ceramic Powders	92
CHAPTER 6	106
CONCLUSIONS AND RECOMMENDATION	106
6.1 Conclusions	106
6.2 Recommendations.....	108
REFERENCES.....	110

LIST OF FIGURES

Figure 1.1 Classification of composites material within the group of material [Kainer, 2006].....	3
Figure 1.2 Schematic presentation of an ideal melt infiltration of fiber preforms [Kainer, 2006].....	5
Figure 1.3 Schematic presentation of the infiltration process of an aluminum oxide preform with molten aluminum [Kainer, 2006].....	6
Figure 2.1 Schematic representation of wetting.....	12
Figure 2.2 Identification of geometric parameters of a sessile drop [Dorsey, 1928].....	15
Figure 2.3 Phase diagram for Al-Ti alloy.....	18
Figure 3.2 Comparison of dimensions used to determine surface tension from the shape of	21
Figure 4.2 (a) General view of metal injection system	40
Figure 4.1 Schematic diagram of Sessile Drop Experimental Set-up.....	40
Figure 4.3 Graphite sample crucible with three compartments	43
Figure 4.4 Furnace calibration curve.....	45
Figure 4.5 Contact angle of Al-1.5wt% Ti alloy on B ₄ C powder at 850°C after 20 min measured using FTA32 software	46
Figure 4.6 Schematical summary of sample preparation process	49
Figure 5.1 Change of contact angle of aluminum drop at different temperatures with time on boron carbide powder	58

Figure 5.2 Change of contact angle of Al-1wt%Ti drop at different temperatures with time on boron carbide powder	59
Figure 5.3 Comparisons between initial contact angles of pure aluminum and Al-1wt%Ti alloy on B ₄ C powder.	60
Figure 5.4 Change of contact angle B ₄ C powder with pure Al and Al-Ti alloy as a function of time and temperature.....	61
Figure 5.5 Initial contact angle of Al and Al-Ti alloy on B ₄ C powder at two different temperatures.....	62
Figure 5.6 Contact angle data after 20 minutes for Al and Al-Ti alloy on B ₄ C powder at two different temperatures.....	63
Figure 5.7 Initial contact angle of pure aluminum at different temperatures on different ceramic powders.....	65
Figure 5.8 Initial contact angle of Al-1%wtTi at different temperatures on different ceramic powders.....	66
Figure 5.9 Contact angle vs. time data for AlB ₂ and Al ₄ C ₃ powders with Al and Al-1wt% Ti alloy at different temperatures.....	67
Figure 5.10 Contact angle vs. time data for TiC and TiB ₂ powders with pure Al at different temperatures.	68
Figure 5.11 Change of contact angle with time for ZrC and ZrB ₂ powders with Al and Al-1wt% Ti alloy.....	69
Figure 5.12 Change of contact angle with time for VC and VB ₂ powders with Al and Al-Ti (1%) alloy at different temperatures.....	70

Figure 5.13 Comparisons of initial contact angles reported in literature and experimental results of the present work for pure aluminum on B_4C powder	71
Figure 5.14 Comparisons of initial contact angles reported in literature and experimental results of the present work for pure aluminum on TiC powder	73
Figure 5.15 Comparisons of initial contact angles reported in literature and experimental results of the present work for pure aluminum on TiB_2 powder.....	75
Figure 5.16 Densities of the pure Al and Al-Ti alloys at different temperatures	77
Figure 5.17 Surface tension of Al at two different temperatures and for different systems	79
Figure 5.18 Surface tension Al-1wt%Ti alloy at different temperatures and for different systems.....	79
Figure 5.19 Effect of Ti content on the surface tension Al-Ti alloy at different temperatures	80
Figure 5.20 (a) The interfacial product layer formation at the middle of the drop in Al/ B_4C system (b) Cross section of the sessile drop – B_4C powder interface obtained at $850^\circ C$ and after 20 minutes for pure Al using optical microscopy	82
Figure 5.21 SEM micrograph of Al/ B_4C interface showing formation of new phase at $850^\circ C$ and after 20 minutes	83
Figure 5.22 Cross section of the sessile drop/ B_4C powder interface obtained at $850^\circ C$ and after 20 minutes with different Ti levels using optical microscopy.....	86
Figure 5.23 SEM micrographs of different samples at $850^\circ C$ and after 20 minutes, showing barrier layer of TiB_2 particulates on B_4C powder surface	87
Figure 5.24 (a) Optical micrograph of Al/ Al_4C_3 interface after 20 minutes at $850^\circ C$	89

Figure 5.25 Optical micrograph of Al/VC interface after 20 minutes at 850°C.....	90
Figure 5.26 SEM observation of the Al/VC interface after 20 minutes at 850°C	90
Figure 5.27 EDX observation of the Al/VC interface after 20 minutes at 850°C	91
Figure 5.28 Optical micrograph of Al/ZrC interface after 20 minutes at 850°C	92
Figure 5.29 Comparisons of contact angle evolution measured experimentally and calculated with wetting model for Al/ B ₄ C powder system	98
Figure 5.30 Comparisons of contact angle evolution measured experimentally and calculated with wetting model for Al-1wt%Ti/ B ₄ C powder system.....	100
Figure 5.31 Comparisons of contact angle evolution measured experimentally and calculated with wetting model for Al-1.5wt%Ti/ B ₄ C powder system.....	101
Figure 5.32 Comparisons of contact angle evolution measured experimentally and calculated with wetting model for Al-3wt%Ti/ B ₄ C powder system.....	102
Figure 5.33 Arrhenius plot for Al/B ₄ C and Al alloys/B ₄ C systems.....	105

LIST OF TABLES

Table 3.1 An overview of surface tension data for pure aluminum cited in the literature ...	22
Table 3.2 An overview of change of contact angle of aluminum on B ₄ C powder with time and temperature.....	34
Table 3.3 An overview of change of contact angle of aluminum on TiC plate with time and temperature	35
Table 3.4 An overview of change of contact angle of aluminum on TiB ₂ powder with time and temperature.....	36
Table 3.5 Heat of formation for transition metal carbides and borides [Naidich <i>et al.</i> , 1983]	38
Table 4.1 Summary of impurities reported by the supplier of argon gas	42
Table 4.2 The bulk density and the approximate particle size for the ceramic powders used in the wetting test	43
Table 4.3 Summary of polishing procedure	50
Table 5.1 Experimental parameters for the experiments with different ceramic powders...	52
Table 5.2 Experimental conditions used by different researchers for pure aluminum and on B ₄ C powder.....	72
Table 5.3 Experimental conditions used by different researchers for pure aluminum and on TiC substrate.	74
Table 5.4 Experimental conditions used by different researchers for pure aluminum and on TiB ₂ powder.....	76
Table 5.5 Work of adhesion evaluated in function of the surface tension and contact angle	

for Al/ B ₄ C and Al-Ti alloy/B ₄ C powder systems	92
Table 5.6 Work of adhesion evaluated as a function of the surface tension and contact angle	94
Table 5.7 Contact angle change rate (K) for Al/B ₄ C powder system at different temperatures.....	97
Table 5.8 Rate constant (K) for Al-1wt%Ti/B ₄ C powder system at different temperatures	99
Table 5.9 Contact angle change rate (K) for Al-1.5wt%Ti/B ₄ C powder system at two different temperatures.....	101
Table 5.10 Rate constant (K) for Al-3wt%Ti/B ₄ C powder system at two different temperatures.....	102
Table 5.11 Activation energy of Al/B ₄ C and Al alloys/B ₄ C systems	105

CHAPTER 1

INTRODUCTION

Aluminum is one of the major industries in Quebec and Canada. This project will contribute to the fundamental understanding of interactions between the B₄C and aluminum alloys which form metal matrix composites (MMC). A MMC composed of at least two constituents, one of which is a metal. The other may be a different metal or another material, such as ceramic or organic compound to reinforce the metal matrix. They are used in many areas of daily life for quite some time. For many researchers the term metal matrix composites is often known as light metal matrix composites. Substantial progress in the development of light metal matrix composites has been achieved in recent decades and they are used in important applications. In traffic engineering, especially in the automotive industry, MMCs have been used commercially in fiber reinforced pistons and aluminum crank cases with strengthened cylinder surfaces as well as particle strengthened brake disk.

These innovative materials open up many possibilities in modern material science and development. These materials group become interesting as construction and functional materials, if the property profile of conventional materials do not meet the increased standards of specific demands. The composites materials have advantages over the conventional ones if their cost-performance relationship is reasonable.

The possibility of combining various material systems (metal-ceramic-non metal) gives the opportunity for unlimited variations (see Fig.1.1). The properties of these new materials can be predicted by the properties of each component [Kainer, 2006]. The light metal matrix composites have the following advantages:

- ✓ Reduction in weight
- ✓ Increase in yield strength and tensile strength at room temperature and above while maintaining the minimum ductility or rather toughness.
- ✓ Increase in creep resistance at higher temperatures compared to that of conventional alloys.
- ✓ Increase in fatigue strength, especially at high temperatures.
- ✓ Improvement in thermal shock resistance.
- ✓ Improvement in corrosion resistance.
- ✓ Increase in Young modulus.
- ✓ Reduction in thermal expansion.

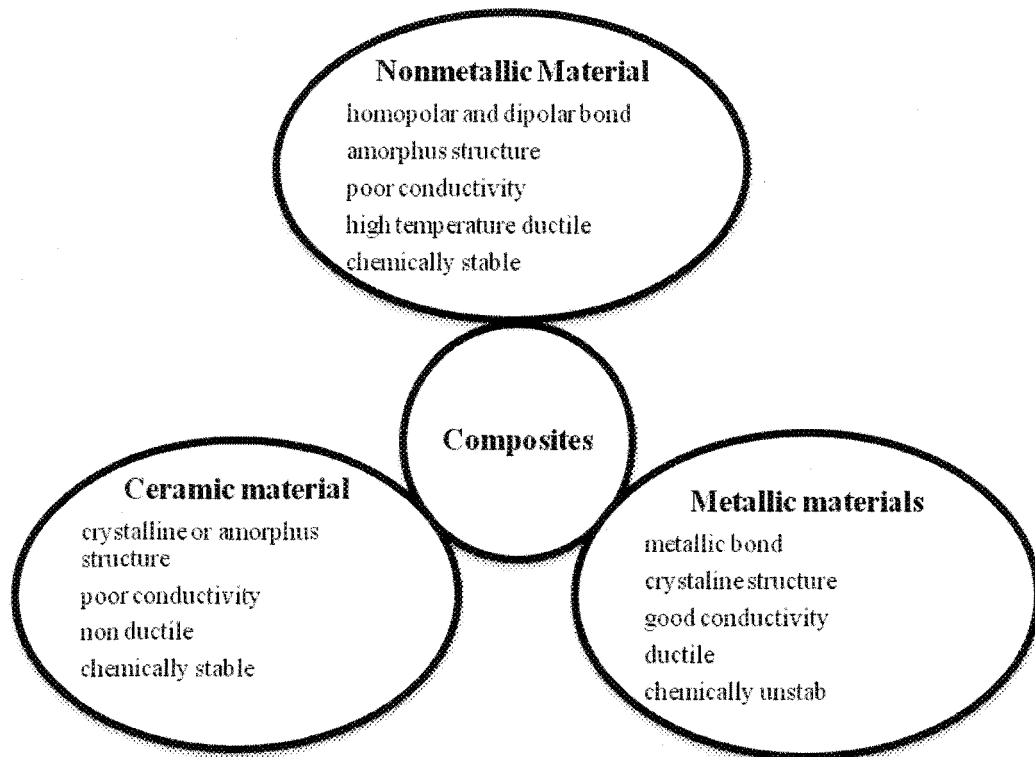


Figure1.1 Classification of composites material within the group of material [Kainer , 2006]

1.1 Relationship between Wetting and Metal Matrix Composites

Wetting is the contact between the liquid and the solid surface due to molecular interactions when they are brought together. Wetting studies can be classified into different groups according to the measurement methods (sessile-drop, infiltration etc), the type of substrate surface (smooth, rough, porous) or by the type of wetting (physical, chemical). Wetting is often defined in terms of contact angle, θ , which is defined as the angle between the tangent to the liquid–fluid interface and the tangent to the solid interface at the contact line between the three phases. Wettability of solid by liquid is required in many industrial applications.

Controlling and modifying wettability is a difficult task since it is affected significantly by different factors. This is the challenge of the wettability research.

Detailed understanding of interfaces in materials is of significant importance for many manufacturing industries. The wetting of ceramic surfaces by molten metal is one of the most important phenomena to consider when a metal matrix composite is produced. Contact angles as determined by the sessile-drop test are used to determine whether or not spontaneous incorporation is possible for a given metal-ceramic combination. Also wettability has a significant influence on the properties of the final product. In addition, wettability plays a key role in the improvement of reliability during application of these materials. The wettability of material interfaces has been studied widely in the field of material science [Conteras *et al.*, 2003; Hashim *et al.*, 2001].

Casting of MMCs is an attractive processing method for this advanced material since it is relatively inexpensive, and offers a wide variety of material and processing conditions. Generally these composites consist of a metal matrix, which is melted during casting, and discontinuous (particle, whisker, short fiber or other) or continuous (monofilament or multifilament) reinforcement which is added to the molten matrix material. MMCs with discontinuous reinforcements are usually less expensive to produce than continuous fiber reinforced MMCs, although this benefit is normally offset by their inferior mechanical properties. Consequently, continuous fiber reinforced MMCs are generally accepted as offering the ultimate in terms of mechanical properties and commercial potential [Kainer, 2006].

Good wetting between the solid ceramic phase and liquid metal matrix is an essential condition for the generation of a satisfactory bond between these two during casting. However ceramic materials are frequently not wetted by liquid metals. The basic reason is that most of the ceramics are ionic or covalent in nature and they are not compatible with the metallic species. Wetting is substantially important for infiltration procedure. This is shown in the schematic representation in Fig.1.2. When a solid-liquid system is wetting, a capillary effect occurs (Fig 1.2a). At large contact angles (non wetting or partially wetting systems) this phenomenon is inhibited (Fig 1.2b). In addition, this can also occur during an industrial process due to a reaction taking place between the melt and the surrounding atmosphere. Then, for example, an oxide film (or any other reaction product) can form, as in the case of magnesium alloys, which affects the wetting behavior by creating a new interface between the reinforcement and the melt (Fig 1.3).

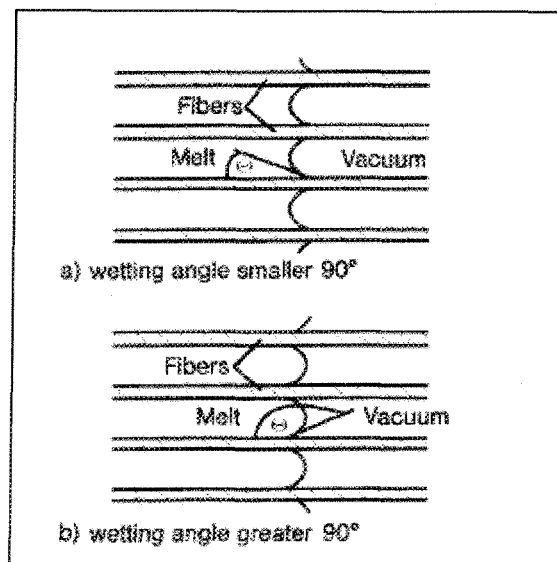


Figure1.2 Schematic presentation of an ideal melt infiltration of fiber preforms [Kainer, 2006]

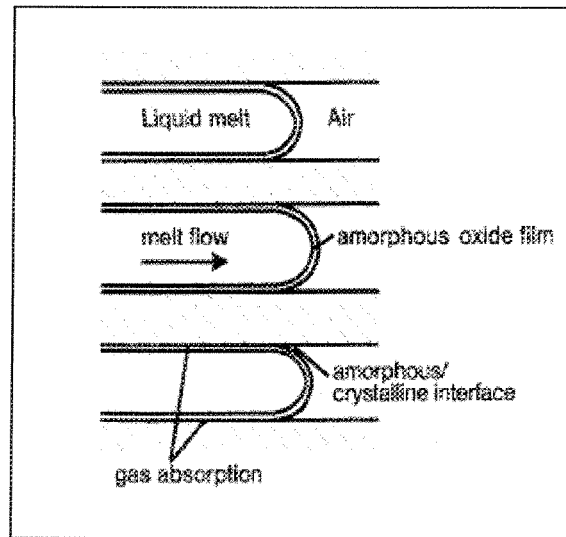


Figure 1.3 Schematic presentation of the infiltration process of an aluminum oxide preform with molten aluminum [Kainer, 2006]

Wettability and reactivity determine the quality of bonding between the constituents and thereby greatly affect the final properties of composites. The mechanical properties of MMCs are controlled to a large extent by the structure and properties of this reinforcement–metal interface. It is believed that a strong interface permits transfer and distribution of load from the matrix to the reinforcement, resulting in an increased elastic modulus and strength. From the metallurgical consideration the desired interfacial region in a composite relies on several factors: 1) an intimate contact between the reinforcement and the matrix to establish satisfactory wetting of the reinforcement by the matrix 2) a very low rate of chemical reaction at the interface, and 3) little or no inter diffusion between the component phases, so that the reinforcement is not degraded [Rajan, 1998]. The principal matrix materials for MMCs are aluminum and its alloys. To a lesser extent, magnesium and

titanium are also used, and for several specialized applications a copper, zinc or lead matrix may be employed.

1.2 The Statement of the Problem

The metal matrix composites have been of interest to aluminum industry because Al has high electrical conductivity, low density and aluminum metal matrix composites (Al MMCs) have superior mechanical properties compared to those of aluminum alloys. Al MMCs are a group of new advanced materials and they are known for their light weight, high strength, high specific modulus, low coefficient of thermal expansion and good wear resistance properties. Combination of these properties is not available in a conventional material [Contreras *et al.*, 2003]. The use of Al MMCs has been limited in very specific applications such as aerospace industry and military weapons due to high processing cost. Recently, Al matrix composites have been used for the automobile products such as engine piston, cylinder liner, brake disc/drum etc.

For critical control of spent nuclear fuel in dry storage and transport, special materials are used inside the containers to absorb thermal neutrons. Several elements with a high cross section can effectively capture thermal neutrons. In nuclear industry, boron is the most commonly used element as a neutron absorber. Boron has two kinds of isotopes. One is the thermal neutron absorbing ^{10}B boron isotope and the other is the thermal neutron reflecting ^{11}B isotope. The ^{10}B isotope is the principal neutron absorber because it possesses a high cross section for absorbing thermal neutrons. Naturally occurring boron typically contains 19.9% of atom % of ^{10}B and 80.1% of atom % of ^{11}B . The values of the absorption cross

sections are $3.835 \times 10^{-21} \text{ cm}^2$ and $5.5 \times 10^{-27} \text{ cm}^2$ for ^{10}B and ^{11}B , respectively [Viala *et al.*, 1997; Chen, 2005]. Boron can be typically incorporated into aluminum as AlB_2 , TiB_2 , B_4C or simply B. In recent works, aluminum - boron carbide composites gained importance due to 1) high boron concentration (78% B) in B_4C therefore high neutron absorption capacity, 2) light weight (2.52 g/cm^3) and 3) its commercial availability in large quantities. Also this composite can be used in high performance application such as aircrafts and aerospace structures, medical applications etc [Viala *et al.*, 1997; Chen, 2005].

During the preparation of Al- B_4C composite, B_4C particles has to be mixed with liquid aluminum. However, the poor wetting between B_4C and aluminum makes this task a difficult one. Also B_4C is not stable when it is in contact with aluminum. An interfacial reaction takes place extensively and Al continues to react with B_4C until the reaction is complete [see Eq. (3.3) and (3.5)]. This reaction decreases the fluidity of the melt and deteriorates its mechanical and physical properties. To prevent this, titanium is added to aluminum because of its high affinity to react with boron carbide. Consequently, titanium addition reduces the interfacial tension of the liquid metal, and thus it is said that it improves the wettability of the reinforcement by the metal matrix. Titanium also forms a protective layer on the B_4C particles through a reaction which facilitates the incorporation of B_4C into the melt. Titanium seems to be the most efficient alloying element cited in the literature because Ti-B and Ti-C compounds are much more stable in liquid aluminum than B_4C . However, there is no systematic study on the wetting of B_4C .

1.3 Scope

In this project, the wetting characteristics between the B_4C particles and pure aluminum as well as Al-Ti alloys were investigated. The molten metal/alloy drop has to be in contact with the solid for long time to form reaction products. This is difficult since aluminum oxides form easily at high temperatures in the presence of very low partial pressure of oxygen. In order to understand the effects of the reaction products on wetting, the contact angles between the reaction products (carbides and borides) shown in Eq. (3.3 and 3.5) such as (AlB_2 , Al_4C_3 TiC, TiB_2 powders) and aluminum have been measured .

The other alloying elements like zirconium and vanadium can also be incorporated to protect B_4C . Zirconium is group IV material (same as titanium) and vanadium is group V material. In order to evaluate their potential; the wetting experiments were carried out with some of the possible reaction products (ZrB_2 , ZrC , VB_2 , VC) which could form if these alloying elements were used during B_4C preparation [see Eq. (3.7)] and aluminum with and without Ti.

In the literature, different wetting studies are reported with these carbides and borides. However, each study has different experimental conditions and it is difficult to compare and withdraw conclusions from them. The originality of this project is to study the wetting behavior of boron carbide, transition metal carbides and borides by aluminum and aluminum alloys under same experimental environment.

1.4 Objectives

Objectives of the project are:

- To investigate the wettability between B_4C and liquid aluminum and Al-Ti as a function of temperature, time and Ti content.
- To identify potential alloying elements to protect B_4C other than titanium such as zirconium and vanadium.
- To study the effect of possible reactions products (AlB_2 , Al_4C_3 , TiC , TiB_2 , ZrB_2 , ZrC , VB_2 , VC) forming during the preparation of Al/ B_4C MMC on wetting.
- To investigate the reaction products formed during the wetting tests using optical microscope and SEM analysis.
- To study the surface tension of pure aluminum and aluminum-titanium alloys under argon gas.
- To contribute to the improvement of Al/ B_4C composite production technology.

CHAPTER 2

THEORY

In this study the interaction between aluminum and aluminum alloys with different ceramic materials were investigated. This requires the quantitative representation of interfacial phenomenon, which can be realized by measuring contact angle and surface tension, hence, wetting.

2.1 Relationship between Wetting, Surface Tension and Contact Angle

The wettability of reinforcement particles by a metal melt can be shown with the contact angle of a molten droplet on a solid ceramic surface as the degree of wettability according to Young [Kainer, 2006]. The first widely accepted relationship between interfacial tension and contact angle for a liquid drop on a solid surface is expressed by Young's Equation, suggested by Young in 1805 [Adamson, 1990]:

$$\gamma_{sv} = \gamma_{sl} + \gamma_{lv} \cos\theta \quad (2.1)$$

where γ_{sv} the interfacial tension of the solid-vapor interface γ_{sl} is the interfacial tension of the solid-liquid interface, γ_{lv} is the interfacial tension of the liquid-vapor interface and θ is the contact angle. γ_{lv} is also known as surface tension. These phases meet at a point called triple point. The force balance given by Young equation [Adamson, 1990; Kainer, 2006] at

the triple point determines the wettability of the solid phase by liquid phase in presence of vapor phase. Fig. 2.1 shows the possible contact angles between a liquid drop and a solid base.

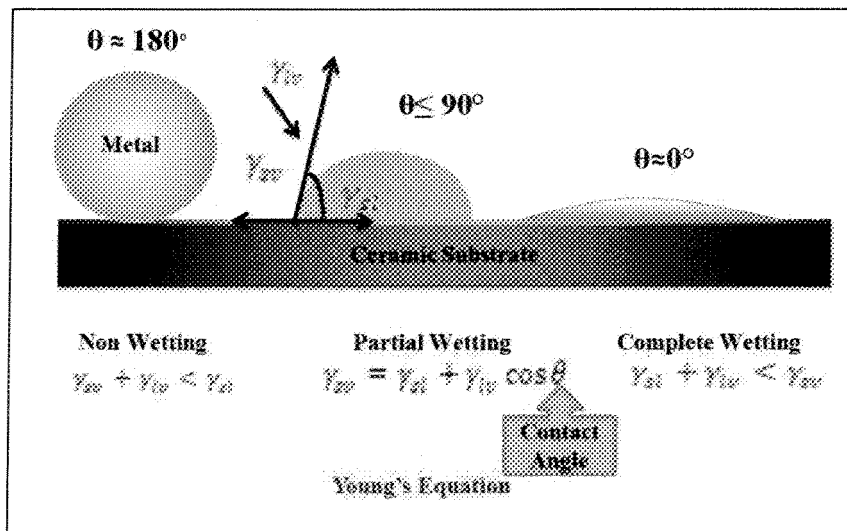


Figure 2.1 Schematic representation of wetting

If $\theta > 90^\circ$ a liquid-solid system is non wettable and if $\theta < 90^\circ$ the system is wettable (Fig.2.1). As the contact angle decreases the wettability improves [Kainer, 2006]. Wettability is significantly affected by the different factors such as type of alloying elements added to metal, roughness, crystal orientation of the solid (ceramic) material and its impurity.

The wettability can be determined by the optical methods known as *Goniometry* [Vainshtein, 1996] which analyses the shape of a liquid drop placed on a solid surface. Another approach to measure the wettability is the tensiometric methods. In this approach,

a solid sample is submerged into the liquid and the interfacial force is measured during their contact. The wetting behavior between aluminum and aluminum alloys with boron carbide is the main interest of this study. For this purpose sessile-drop technique which is a goniometric method was used.

2.1.1 Sessile -Drop System

The Sessile-drop technique is an optical contact angle measurement in order to determine the wetting behavior of solids by the liquids. This technique involves placing a drop of liquid metal on a solid substrate. During the measurements either the system is rapidly cooled in order to freeze the initial shape and measure the static contact angle or the change of contact angle with time can be monitored to measure the dynamic contact angle [Paddy, 1960; Murr, 1975; Eustathopoulos *et al.*,1999]. The surface tension (or surface free energy) of solids can also be determined from sessile-drop measurements using the shape of the drop.

2.1.2 Measurement of Surface Tension by Dorsey Method

Accurate information on the surface tension of aluminum and its alloys is necessary for many metallurgical and material related processes, such as casting, welding, brazing, sintering and fabrication of the metal matrix composites.

The Dorsey method [Dorsey, 1928] is one of the image analysis methods used to calculate the surface tension of a sessile drop or a bubble.

The empirical relationship which is proposed by Dorsey used during this study for calculating the surface tension using image analysis is given below:

$$\gamma_{lv} = \frac{gd_m^2 \rho_{liq}}{4} \left(\frac{0.0520}{k} - 0.1227 + 0.0481k \right) \quad (2.2)$$

$$k = \left(\frac{2H'}{d_m} \right) - 0.4142,$$

where, ρ_{liq} is the density of the liquid obtained from the reference [Assael *et al.*, 2006].

Density of the Al-Ti alloy is calculated using the following equation:

$$\rho_{Alloy} = \rho_{Al}x + \rho_{Ti}y \quad (2.3)$$

where x and y are the weight percentages of aluminum and titanium, respectively. The parameters H' and d_m are defined in Fig.2.2. It is not necessary to know the exact point of the tangency or the exact position of the horizontal plane at which the inclination of the surface is 135° . Considering that the surface is a sphere of diameter d_m then H' is given as:

$$H' = (\sqrt{2} - 1) \frac{d_m}{2} \quad (2.4)$$

Hence k may be regarded as a measure of the flattening of the drop or bubble. Dorsey also mentioned that an error of 0.001 in k can produce an error of 0.8 in the final result [Dorsey, 1928].

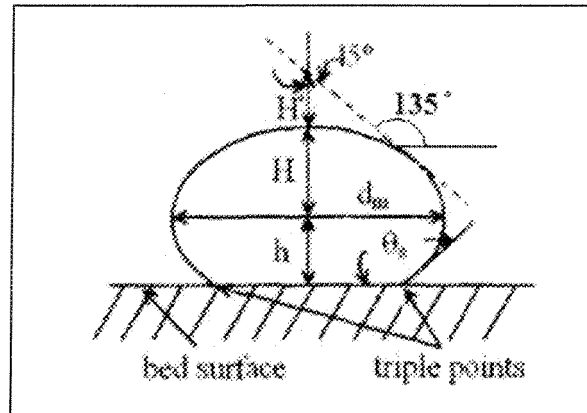


Figure 2.2 Identification of geometric parameters of a sessile drop [Dorsey, 1928].

2.2 Work of Adhesion

The work of adhesion of metal-ceramic systems is calculated as a function of the contact angle (θ) and the surface tension (γ_{lv}) using the following equation [Adamson, 1990; Hashim *et al.*, 2001]:

$$W_a = \gamma_{lv}(1 + \cos \theta) \quad (2.5)$$

Since the work of adhesion is the work per unit area of interface that must be performed to separate reversibly the two phases, it is a measure of the strength of binding between the phases.

2.3 Wetting Model

In the present study, the wetting model proposed by Shi and Gardner, 2001 was used to quantify the change of contact angle with time during different wetting experiments. Although this model is developed for measuring adhesive wettability, it can be applied to any liquid-solid system. The wetting model describes that when a liquid drop is formed on

a solid surface, liquid penetration and spreading takes place simultaneously [Stehr *et al.*, 2001]. In general, the contact angle decreases rapidly at initial times, however, as the time increases, the contact angle decrease slows down and finally it reaches a relative equilibrium. For an ideal liquid and solid system, the penetration and spreading rate depends on the drop shape at a particular moment in time which can be expressed as:

$$\frac{d\theta}{dt} = -K\theta \quad (2.6)$$

where K can be considered as the contact angle change rate constant. K shows how fast the liquid metal spreads and penetrates into the ceramic powders or plate. By knowing the K value, interaction of solid with liquid can be quantified.

According to Equation 2.6, the rate of change of contact angle is proportional to time and it approaches to zero at infinity. This does not represent the reality; therefore, a term to limit the decrease of the contact angle is added to this equation as shown below:

$$\frac{d\theta}{dt} = -K\theta \cdot \left(1 - \frac{\theta_i - \theta}{\theta_i - \theta_e}\right) \quad (2.7)$$

where θ_i represents the initial contact angle, and θ_e represents the apparent equilibrium contact angle. Rearranging the Eq. (2.6), the following expression is obtained:

$$\frac{d\theta}{dt} = K\theta \cdot \left(\frac{\theta_i - \theta}{\theta_i - \theta_e}\right) \quad (2.8)$$

After integration, the final expression of the wetting model is given as:

$$\theta = \frac{\theta_i \theta_e}{\theta_i + (\theta_e - \theta_i) \exp \left[K \left(\frac{\theta_e}{\theta_e - \theta_i} \right) t \right]} \quad (2.9)$$

2.4 Arrhenius Law

For many reactions, particularly elementary reaction, the rate expression can be written as a product of the temperature dependent term and a composition dependent term. For such reactions, the reaction rate constant which is a function of temperature has been found to be well represented by Arrhenius law [Levenspiel, 1999] as shown below:

$$K = K_0 e^{-E/RT} \quad (2.10)$$

where K_0 is the frequency or pre-exponential factor and E is the activation energy of the reaction and K is reaction rate constant of the system.

i) Activation Energy and Temperature Dependency

1. From Arrhenius' law a plot of $\ln K$ vs $1/T$ gives a straight line. E and K_0 can be determined from the slope and the intercept, respectively [Levenspiel, 1999].
2. Reaction with high activation energies are very temperature sensitive. Reaction with low activation energies are relatively temperature-insensitive [Levenspiel, 1999].

2.5 Phase Diagram of Aluminum-Titanium

The phase equilibria of the Al-Ti system have been determined experimentally in the last years. Figure 2.3 shows Al-Ti alloy phase diagram [Onuhama *et al.*, 2000 ; Okamoto, 2000] showing the different thermodynamically possible phases depending on the Al-Ti wt%. In this study Al-1wt%Ti, Al-1.5wt%Ti and Al-3wt%Ti alloys were used. It is clear from the Figure 2.3 within the temperature range used (700-900°C) there is only possibility of formation of Al_3Ti . The crystal structure of the Al_3Ti is discussed below.

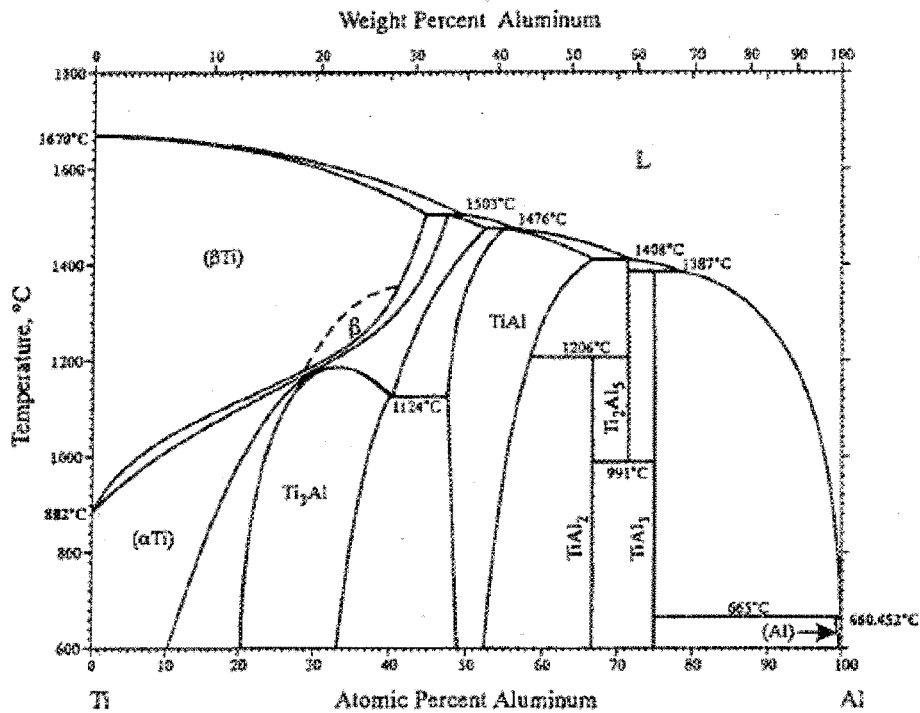


Figure 2.3 Phase diagram for Al-Ti alloy

Crystal structure:

Al₃Ti (h): Its structure is tetragonal (TiAl₃ – type); superstructure with $a = 0.38488$ nm, and $c = 0.85982$ nm. Braun determined: $a = 0.3849$ nm and $c = 0.8609$ nm. The lattice parameters are function of temperature [Onuhama *et al.*, 2000 ; Okamoto, 2000].

Al₃Ti (r): This intermediate phase has a tetragonal structure (TiAl₃ – type). At about 840 K the lattice constants are: $a = 0.38771$ nm and $c = 0.3828$ nm [Onuhama *et al.*, 2000 ; Okamoto, 2000].

CHAPTER 3

LITERATURE REVIEW

3.1 Wetting and Contact Angle

Wettability can be defined as the ability of a liquid to spread on a solid surface and represents the extent of intimate contact between a liquid and solid. It can be described by the angle of contact between a drop of liquid resting on a solid substrate [Marmur, 2006; Liptáková, Kúdela and Sarvaš *et al.*, 2000;]. The contact angle at equilibrium, θ , is determined by the Young-Dupre equation [Hashim *et al.*, 2001; Kwok *et al.*, 2000 and Neumann *et al.*, 1979]:

Cassie *et al.*, 1944 proposed an equation describing the contact angle θ at a heterogeneous surface composed of two different materials. If the surface fractions of these materials are f_1 and f_2 , and the contact angles are θ_1 and θ_2 , the overall contact angle on the surface can be expressed by the following equation:

$$\cos\theta' = f_1\cos\theta_1 + f_2\cos\theta_2 \quad (3.1)$$

When f_2 represents the area fraction of trapped air, equation (3.1) can be modified as follows:

$$\cos\theta' = f\cos\theta + (1 - f)\cos 180^\circ = f\cos\theta + f - 1 \quad (3.2)$$

Where f is the remaining area fraction, i.e., liquid-solid interface. This equation can also be used for rough hydrophobic surfaces trapping air in the hollows of the rough surface.

3.2 Surface Tension Measurement Methods

Two methods are commonly used to determine the surface tension from the shape of a sessile drop (Fig.3.2). The Basforth and Adams method [Bashforth *et al.*, 1883] involves the precise location of distance, Z , between the maximum drop diameter and apex of the drop. The Dorsey method avoids the determination of Z , but still relies on the precise drop dimensions at a few locations [Dorsey, 1928]. Kingry and Humenick in 1953 stated that the Basforth and Adams, and Dorsey Methods should yield deviations of $\pm 2\%$ - 3% and $\pm 5\%$, respectively, for metallic and ionic melts with drop diameters of approximately 0.8cm.

There is recent revival in shape evaluation methods due to the accessibility, speed, reduced cost and ease of application of modern computers. Computerized methods have the advantage over the previously mentioned methods of deriving the best fit to the drop profile over the entire pertaining section instead of the precise dimensions at a few points [Sangiorgi *et al.*, 1982; Rotenberg *et al.*,1983]. Drop symmetry, contact angles, and the local shape variations can be readily determined, thereby permitting the detection of experimental errors. C. Maze and G. Burnet in 1969 developed a numerical procedure for generating a best fit to a drop profile. Rotenberg *et al.* in 1983 improved their method and generalized it to both sessile and pendant drops. Passerone *et al.*, 1979; Weirauch *et al.*, 1993; and Askari *et al.*,1990 have used computerized drop shape fitting techniques to determine the surface tension.

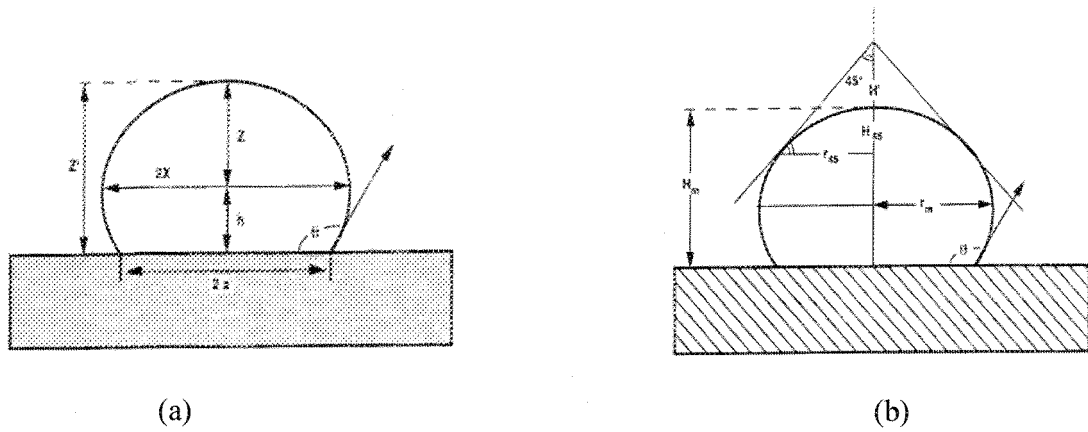


Figure 3.1 Comparison of dimensions used to determine surface tension from the shape of a Sessile Drop [Weirauch *et al.*, 1996] (a) Basforth and Adams method (b) Dorsey Method

Table 3.1 An overview of surface tension data for pure aluminum cited in the literature

Author	Temp. (°C)	γ_{lv}(dyne/cm)	Method	Environment
Saravanan <i>et al.</i>, 2002	670-930	680-840	SD	Ar
Saravanan <i>et al.</i>, 2002	670-950	670-800	SD	Ar + H ₂
Saravanan <i>et al.</i>, 2002	670-950	870	SD	N ₂
Saravanan <i>et al.</i>, 2002	670-950	860-650	SD	N ₂ + H ₂
Sarou-Kainan <i>et al.</i>, 2003	1477-1827	850-750	SD	Air+10% H ₂
Sarou-Kainan <i>et al.</i>, 2003	1527	810	SD	He
Sarou-Kainan <i>et al.</i>, 2003	1627-1727	790-710	SD	Ar
Rhee, 1970	707-817	760-720	SD	Vacuum
Eegin, 2006	720	850	SD	Ar

3.3 Sessile- Drop Technique

More than 80% of the wetting studies at high temperatures are conducted by using different variants of the classic drop method [Kennedy *et al.*,1999; Ergin, 2006] such as in situ formation of alloy, dispensed drop, such as in situ formation of alloy transferred drop, double substrate, tilted plate[Rhee,1970; Halverson,1989; Contreras,2003]. A classic sessile drop experimental set-up mainly consists of a close end, horizontal quartz [Lebeau *et al.*, 1991] or metal tube heated by an appropriate resistance furnace. Generally a quartz window is fitted to one end of the tube furnace to capture the image of sessile drop. This technique involves placing a drop of liquid metal on a solid substrate (Fig.3.1) [Contreras *et al.*, 2003; Contreras *et al.*, 2004; Ergin, 2006] or placing a sessile drop on the substrate and then heating the furnace at desired temperature [Rhee, 1970; Halverson *et al.*,1989]. To measure the angle, the system is rapidly cooled in order to freeze the equilibrium shapes or the change of contact angle with time can be monitored to measure the dynamic contact angle. In measuring the contact angle θ , great care must be exerted to tightly control several important parameters including the composition and surface finish of the solid, the purity of the melt, and the composition and pressure of the vapor phase. All these can exert a significant influence on θ . Such control is often difficult to achieve, and the literature contains many contradictions and inaccuracies attributable to error in experimental conditions.

3.4 Effect of Different Factors on Wetting

Contact angles are used to determine whether or not a spontaneous incorporation of a

ceramic is possible into a given metal. When trying to predict wetting behavior, experimental conditions should be representative of the composite fabrication process, particularly with respect to temperature, time and environment. However, sessile droplet test data reported in the literature is inconsistent due to the variations of time, temperature and environment used [Contreras *et al.*, 2003; Kennedy *et al.*, 1999]. In the absence of reliable wetting angle data, there are some rules of thumb that can be followed to predict wetting behavior. For a given liquid metal, transition metal carbides, borides and nitrides are better wetted than covalently and ionically bonded ceramics and the tendency for a ceramic to be wetted by metal decreases as its heat of formation becomes more negative [Kennedy *et al.*, 1999]. Most solid surfaces (with the exception, perhaps, of single crystals) are seldom consistent and clean, with different surface domains possessing different chemistries and wetting properties. Such chemical inhomogeneity could result from oxidation, corrosion, coatings, multiple phases (e.g., eutectic), adsorbed films, ledges, kinks, dislocations and grain-boundary intersections with the surface, and crystallographic anisotropy (planes having different packing density and exposing different molecular groups). Wettability and spreading are sensitive to such chemical and structural inhomogeneities [Neumann *et al.*, 1979; Drelich *et al.*, 1994; Cassie *et al.*, 1944]

3.4.1 Oxidation

Contact angles for reactive metals such as Al are sensitive to oxygen contamination. This is due to the formation of a tenacious oxide skin on the surface of the metal droplet that obstructs wetting [Kennedy *et al.*, 1999]. For liquid Al, contact angles $< 90^\circ$ are sometimes

observed if tests are conducted above 1000°C [Contreras *et al.*, 2003; Kennedy *et al.*, 1999; Weirauch *et al.*, 2005; Halverson *et al.*, 1989; and Rhee, 1970]. This is commonly explained as being due to the degradation of the metal oxide film on the droplet surface at high temperatures, enabling the molten metal to pierce the oxide skin. Measurements under these conditions may indicate the true wetting nature of the ‘clean’ liquid metal with respect to the ceramic substrate.

Generally to solve the oxidation problem a diffusion pump is attached to the system and oxygen partial pressure reduced to 10^{-7} - 10^{-9} atm [Contreras *et al.*, 2001; Toy *et al.*, 1997; Weirauch *et al.*, 1990; Schoennahl *et al.*, 1984; Landy *et al.*, 1997; and Nizhenko *et al.*, 2001]. It is also important to control the experimental environment to achieve practically sound results [Saiz *et al.*, 1999]. Most of the experiments are conducted under vacuum [Halverson *et al.*, 1989; Weirauch *et al.*, 2005; and Rhee, 1970]. Some of the experiments are conducted under different gas atmospheres. Environment of ultra high purity argon (99.999%) [Contreras *et al.*, 2001; Toy *et al.*, 1997; and Saiz *et al.*, 1999] is also very popular for these experiments. Nowok *et al.*, 1997 maintained an atmosphere of purified argon gas together with 2% hydrogen gas, Weirauch *et al.*, 2005 used ultra high pure hydrogen environment. Lai, 1994 used nitrogen gas during the experiments, and Landry *et al.*, 1997 utilized helium. Sometimes titanium [Contreras *et al.*, 2001; and Schoennahl *et al.*, 1984;] and /or copper [Toy *et al.*, 1997] are also placed in the vicinity of the samples in order to reduce the oxygen potential around the metal sample further [Schoennahl *et al.*, 1984].

3.4.2 Interfacial Reaction

The nature of interface between matrix and reinforcement has a strong influence over the properties of the metal matrix composites. An interfacial behavior plays an important role on the mechanical and physical properties of the MMCs such as neutron shielding capacity, weight, toughness, fatigue, strength, stiffness, ductility, creep and coefficient of thermal expansion. During the wetting of ceramic by molten metal, a chemical reaction occurs at the interface which changes the composition of the melt and ceramics. These interfacial reactions change all of the solid-liquid, liquid-vapor and solid-vapor interfacial free energies and improve adhesion through chemical bonding. Interfacial reactions and type of reaction products are function of temperature, experimental time, pressure, atmosphere, matrix composition and surface chemistry of the ceramics. Temperature and time promotes the interfacial reactions even if there is no reaction products at the interface, the tensile properties are dependent on the nature of the bonding.

The strength of the composites is dependent on the strength of the interfacial bond between the matrix and the reinforcement. A strong interfacial bonding permits transfer and distribution of the load from the matrix to the reinforcement [Contreras *et al.*, 2003; Rajan *et al.*, 1998].

Wetting is also function of interfacial reactions. Depending on the type of reactions, wettability may increase or decrease with time and temperature.

3.4.3 Surface Roughness

Young-Dupre equation can be applied only to a flat surface and not to a rough one [Hashim *et al*, 2001]. The Young equation assumes a perfectly flat surface, and in many cases surface roughness and impurities causes a deviation in the equilibrium contact angle from the contact angle predicted by Young's equation. Thus, several models describing the contact angle at a rough solid surface have been proposed so far. Wenzel proposed a theoretical model describing the contact angle θ at a rough surface [Wenzel, 1936]. He modified Young's equation as follows:

$$\cos\theta' = \frac{r(\gamma_{sv} - \gamma_{sl})}{\gamma_{lv}} \quad (3.6)$$

r is roughness factor, defined as the ratio of the actual area of a rough surface to the geometric projected area. This equation indicates that the surface roughness enhances the hydrophilicity of hydrophilic surfaces or enhances the hydrophobicity of hydrophobic ones because r is always larger than 1. These trends are generally (not always) observed, but Wenzel's relation implies that there is no limitation of the effect: The roughness factor is arbitrarily large, which results in complete wetting ($\cos\theta'=1$) but further increase in r does not affect the wetting as the surface is already completely wet. Quere, 2008 elucidated that often Wenzel's assumptions are not satisfied.

The complete wetting becomes more difficult to achieve as particle size decreases. This is due to surface energy increase required for metal to have an intimate contact with the solid. The smaller particles are more difficult to disperse because of their inherently greater

surface area. These finely divided powders show an increasing tendency to agglomerate or clump together as particle size decreases. So it is clear that surface roughness affects contact angle, hence, wetting [Myres, 1999]. Also, if the particle size is too big, surface roughness will increase and this will hinder the spreading of the liquid metal. Therefore, particle size should be optimum for good wetting. Excessive roughness in micro scale contributes to poor wettability and it serves as the fracture initiation site close to the interface [Keisler *et al.*, 1995]. Surface roughness also affects the rate of spreading [Cazabat *et al.*, 1986]. Wettability increases as the micro roughness decreases [Semal *et al.*, 1990] and this is also supported by the molecular kinetic theory of wetting [Himbeault *et al.*, 1989]. To reduce the surface roughness and increase the wettability, hot pressed ceramic plates were used [Contreras *et al.*, 2003; Halverson *et al.*, 1989; Weirauch *et al.*, 2005; and Rhee, 1970].

3.4.4 Methods to Promote Wettability

Several methods have been used to promote wetting of reinforcement particles with a molten alloy [Himbeault *et al.*, 1989; Tafto *et al.*, 1988]. These include:

3.4.4.1 The coating of the ceramic particles,

3.4.4.2 Treatment of the ceramic particles,

3.4.4.3 The addition of alloying elements.

Different approaches which can be used to improve wetting are: to increase the surface energy of the solid, to decrease the surface tension of the liquid alloy, or to decrease the solid–liquid surface energy at the particle–matrix interface [Hashim *et al.*, 2001].

3.4.4.1 Particle Coating

In general, the surface of non-metallic particles is difficult to wet by a liquid metal. Wetting has been achieved, however, by first coating the particles with a wettable metal. Coatings are applied in a variety of ways including chemical vapor deposition (CVD), several forms of plasma vapor deposition (PVD), electroplating, cementation, plasma spraying [Chou *et al.*, 1985]. Nickel and copper are wetted well by many alloys, and these metals have been used as coating materials. Silver, copper and chromium coatings have also been proposed [Pai *et al.*, 1975; Hashim *et al.*, 2001; Ishikawa *et al.*, 1981; and Zhou *et al.* 1997] as coatings. However, nickel is the most frequently used metal for coating reinforcement particles used with aluminum-based composites [Hashim *et al.*, 2001; Ishikawa *et al.*, 1981]. It is important to note that the interaction of coatings with a liquid metal during infiltration or stirring, and the influence of this on the solidification microstructure and the mechanical properties of a composite are not well understood.

3.4.4.2 Particle Treatment

It has been observed that a ceramic particle surface is generally covered with a gas layer [Roy, 1996]. Zhou and Xu, 1997 have proposed that this gas layer may be the main reason for their poor wettability. This layer prevents molten matrix material from coming into contact with the surface of individual particles. In addition, when the particle concentration in a melt reaches a critical level, the gas layers can form a bridge, leading to total rejection of particles from the melt [Warren *et al.*, 1984]. Hence, it is essential that gases from the

surface of particles are desorbed prior to composite synthesis, or alternatively that gas layers are broken by mechanical means. Depending on the density of the ceramic material, completely wetted particles may tend to sink to the bottom, rather than float to the surface of a melt.

Heat treatment of particles before dispersion in the melt aids their wetting because of desorption of adsorbed gases from the particle surface. The importance of preheating on the incorporation of graphite particles to an aluminum alloy has also been mentioned. There was no retention when the graphite particles were not preheated, whereas the particles were retained when preheated but it is not mentioned as to how much particle is retained after preheating [Hashim *et al.*, 2001]. Heating silicon carbide particles to 900°C helps to remove surface impurities, promotes desorption of gases, and alters the surface composition by forming an oxide layer on the surface. The ability of this particle oxide layer to improve the wettability of SiC particles by an alloy melt has been reported by several investigators. This layer is distinctly different from that of a melt oxide layer which is a barrier to wetting. The addition of preheated alumina particles in an Al–Mg melt has also been found to improve the wetting of alumina [Hashim *et al.*, 2001].

A clean surface provides a better opportunity for melt–particle interaction, and thus enhances wetting. Ultrasonic techniques, various etching techniques and heating in suitable atmosphere can be used to clean the particle surface [Hashim *et al.*, 2001]. Also, aluminum was cleaned by NaOH solution, deionized water, and ethanol or acetone [Weirauch *et al.*,

2005] during experimental studies.

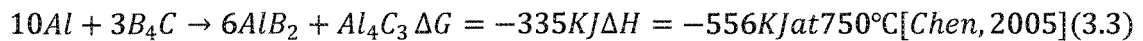
3.4.4.3 Addition of Alloying Elements

The composites produced by liquid metallurgy techniques generally show excellent bonding between ceramic and molten matrix when reactive elements are added to induce wettability [Hashim *et al.*, 2001]. For example, the addition of magnesium, calcium, titanium, or zirconium to the melt may promote wetting by reducing the surface tension of the melt, decreasing the solid–liquid interfacial energy of the melt, or by the negative free energy of the chemical reaction [Hashim *et al.*, 2001]. It has been found that for aluminum-based composites, magnesium has a greater effect in incorporating reinforcement particles in the melt and improving their distribution more than other elements tested including cerium [Hashim *et al.*, 2001; Werren *et al.*, 1984], lanthanum, zirconium, and titanium, bismuth, lead, zinc, and copper [Hashim *et al.*, 2001]. The addition of magnesium to molten aluminum has been found to be successful in promoting wetting of alumina [Hashim *et al.*, 2001], and indeed it is concluded that magnesium is suitable for most reinforcements [Hashim *et al.*, 2001] in aluminum. The possible alloying elements for aluminum-B₄C MMC are presented below.

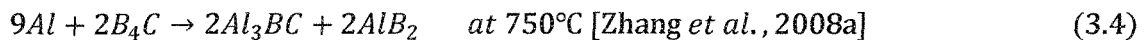
3.4.4.3.1 Addition of Titanium

Boron carbide and Al have been interspersed to produce MMCs by powder metallurgy method [Hashim *et al.*, 2001; Chen, 2004]. However, the poor wetting between Al and B₄C

below 1100°C [Kennedy *et al.*,2001] makes it difficult to produce Al-B₄C composites by mixing particles in the liquid phase [Kennedy *et al.*,1999]. In order to enhance the wettability of ceramics and improve their incorporation behavior into Al melts, particles are often heat treated or coated [Kennedy *et al.*, 2001]. The B₄C reacts with aluminum forming different components which decreases B₄C concentration in aluminum and decreases the fluidity. The thermodynamic reactions taking place are [Chen, 2005]:



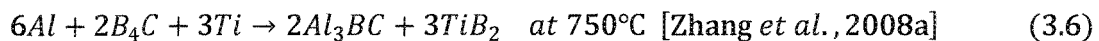
Later it has been proposed that secondary reactions phases Al₃BC and AlB₂ formed by following equation [Zhang *et al.*, 2008a; Zhang *et al.*, 2007; Viala *et al.*,1997].



To protect the B₄C particles and prevent the reactions, Ti is added to aluminum. Titanium can improve the uniformity of the particulate distribution within aluminum matrix if the titanium content in the composites is more than 0.5%. Coating and reacting B₄C particles with Ti particles results in the formation of complex surface layers of titanium borides and titanium carbide [Kennedy *et al.*, 2001] outside the B₄C particles and prevents its further consumption of B₄C. The thermodynamic reactions taking place are:



Later it has been proposed that secondary reactions phases Al₃BC and TiB₂ formed by following equation [Zhang *et al.*, 2008a].



As seen above, it is reported in the literature that Ti addition increases the wettability of B₄C particles by aluminum but there is no systematic study on the wetting characteristics of

all the borides and carbides involved under the same experimental condition.

Halverson *et al.*, 1989 studied the boron carbide-aluminum composites. High purity industrial grade aluminum and hot pressed B₄C substrate made of commercial grade B₄C particles were used. During the experiment, sessile drop of aluminum was placed on B₄C substrates which were polished to a 1- μ m finish. The experiment was conducted in a tungsten-mesh, resistance heated vacuum furnace at pressure less than 5×10^{-3} Pa but greater than 10^{-4} Pa and kept for 10,000 minutes between 900 to 1300°C (see Table 3.2). It was observed that the wetting increased with increasing time. After that, the specimen was vacuum cooled under the room temperature. Kennedy *et al.*, 1999 studied the incorporation of ceramic particles in molten aluminum and its relationship to contact angle data but the experimental conditions were not specified in the publication (see Table 3.2).

Table 3.2 An overview of change of contact angle of aluminum on B₄C powder with time and temperature

Author	Temperature (°C)	Time (min)	Initial Contact Angle(°)	Final Contact Angle(°)
Halverson <i>et al.</i>, 1989	900	10,000	145	20
	1000	1000	110	5
	1100	200	45	5
	1200	90	30	2
	1300	30	10	1
Kennedy <i>et al.</i>, 1999	900	N/A	135	N/A

Contreras *et al.*, 2003 studied the wettability and spreading kinetics of Al and Mg on TiC. He used hot pressed TiC plate (1 μ m diamond polish) and pure Al (99.99%). The wetting experiments were conducted under ultra high purity argon (99.999%) at atmospheric pressure between 800 to 1000°C in a set-up specially designed for this experiment (see Table 3.3). Rhee, 1970 used sessile drop apparatus which is a horizontal resistance furnace consisting of a fused silica tube with standard taper joints. The furnace was evacuated by a mechanical pump in conjunction with a three stage oil diffusion pump and a nitrogen cold trap. The furnace was operated at pressure 2×10^{-7} torr or less between 700-800°C. High Purity 99.99% of aluminum and TiC plaque (1 μ m alumina polished) was used (see Table

3.3). The sessile drop was allowed to rest on the plaque for about 30 min at a given temperature and then the drop was photographed. He also elicited that in general contact angle assumes a constant value after 30 minutes, and this value was taken as an equilibrium contact angle. He did not mention the oxidation of aluminum which certainly takes place under these conditions.

Table 3.3 An overview of change of contact angle of aluminum on TiC plate with time and temperature

Author	Temperature (°C)	Time (min)	Initial Contact Angle(°)	Final Contact Angle(°)
Contreras <i>et al.</i> 2003	800	150	130	60
	850	150	130	58
	900	150	118	55
	1000	55	132	10
Rhee 1970	700	30	110	N/A
	750	30	90	N/A
	800	30	66	N/A

Weirauch Jr. *et al.*, 2005 studied the wettability of titanium diboride by molten aluminum drops. The experiments were conducted under the vacuum atmosphere. He also used the TiB₂ plate (see Table 3.4). Rhee, 1970 deliberated that with increasing temperature contact

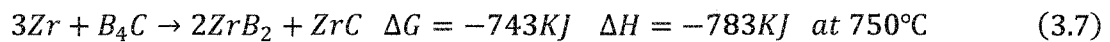
angle is decreasing significantly in case of liquid Al-TiB₂ system (see Table 3.4).

Table 3.4 An overview of change of contact angle of aluminum on TiB₂ powder with time and temperature

Author	Temperature (°C)	Time (min)	Initial Contact Angle(°)	Final Contact Angle(°)
Weirauch Jr <i>et al.</i> 2005	1025	300	95	10
Rhee 1970	700	30	90	N/A
	750	30	84	N/A
	800	30	69	N/A
	850	30	53	N/A

3.4.4.3.2 Addition of Zirconium

The reactions of the interface between B₄C–Zr are published very rarely. The reaction is given as [Zhang *et al.*, 2004]:



3.4.4.3.3 Addition of Vanadium

The interface reactions between boron carbide and vanadium are not yet published. There is no information regarding direct reaction between boron carbide and vanadium in the

present literatures.

3.5 Incorporation of Transition Metal Borides and Carbides

Kennedy *et al.*, 1999 reported that several transition metal compounds are successfully incorporated into aluminum. They said that it is impossible to incorporate VB_2 , ZrN and VN particle to the molten aluminum due to their high contact angle at temperatures ranging from 700°C to 900°C. All the other particles were readily incorporated but the particle yield was different for different ceramics. If the magnitudes of the particle yield are considered, it was observed that it is easier to add metal carbides to molten aluminum than borides and it is easier to add metal borides than nitrides [Kennedy *et al.*, 1999] to the same metal. Transition metal carbides and borides tend to have more uniform distribution of electron densities and hence the bonding is more metallic in character [Kennedy *et al.*, 1999]. The list of transition metal ceramic and their heat of formations are given below in Table 3.5. It is said that less thermodynamically stable compounds are easier to incorporate in to the liquid aluminum and the yield is higher for these components [Kennedy *et al.*, 1999] as shown in Table 3.5.

Table 3.5 Heat of formation for transition metal carbides and borides [Naidich *et al.*, 1983]

Ceramic Powder	$\Delta H_{f,298K}(\text{kJ/mol}^{-1})$	Particle Yield
ZrC	-207	>95%
VC	-102	75-85%
TiC	-185	>96%
ZrB ₂	-324	55-65%
VB ₂	-204	<1%
TiB ₂	-316	50-60%

The variation in incorporation behavior of different transition metal compounds is very complex and does not seem to relate to trends in the values of the heat of formation. There are a lot of exceptions to the above rule. For example, VB₂ which has a lower heat of formation than that of TiC is not easily incorporated in to a metal. On the other hand, ZrC which has a lower heat of formation than that of TiC but particle yield is very high (see Table 3.5). Therefore, the heat of formation (ΔH_f) values for ceramic phases are only a rough indication of trends in reactivity and wettability [Kennedy *et al.*, 1999].

CHAPTER 4

EXPERIMENTAL SET-UP AND PROCEDURE

In this project the sessile-drop method was used to measure the wetting between ceramic powders (B_4C , AlB_2 , Al_4C_3 , TiC , TiB_2 , ZrB_2 , ZrC , VB_2 , VC) and aluminum as well as aluminum alloys. Details about the experimental set-up and procedure are given below.

4.1 Sessile Drop Experimental Set-Up

The experimental system for the sessile-drop measurements is shown in Fig.4.1. The experimental system consists of a tube furnace (Thermolyne 21100), a digital video camera (B/W) (APPRO, model KC), a secondary rotary vacuum pump (GE, Precision Vacuum Pump, Model D25), and an inconel tube with a metal injection system (see Fig.4.2a), and a graphite sample crucible with three compartments (see Fig.4.2b). The sample to be tested is placed in the middle compartment of the sample crucible. The other two compartments contain titanium particles which were used for the removal of residual oxygen. The graphite injection chamber holds the solid aluminum sample. This chamber has a small hole at the bottom and is placed just above the ceramic sample.

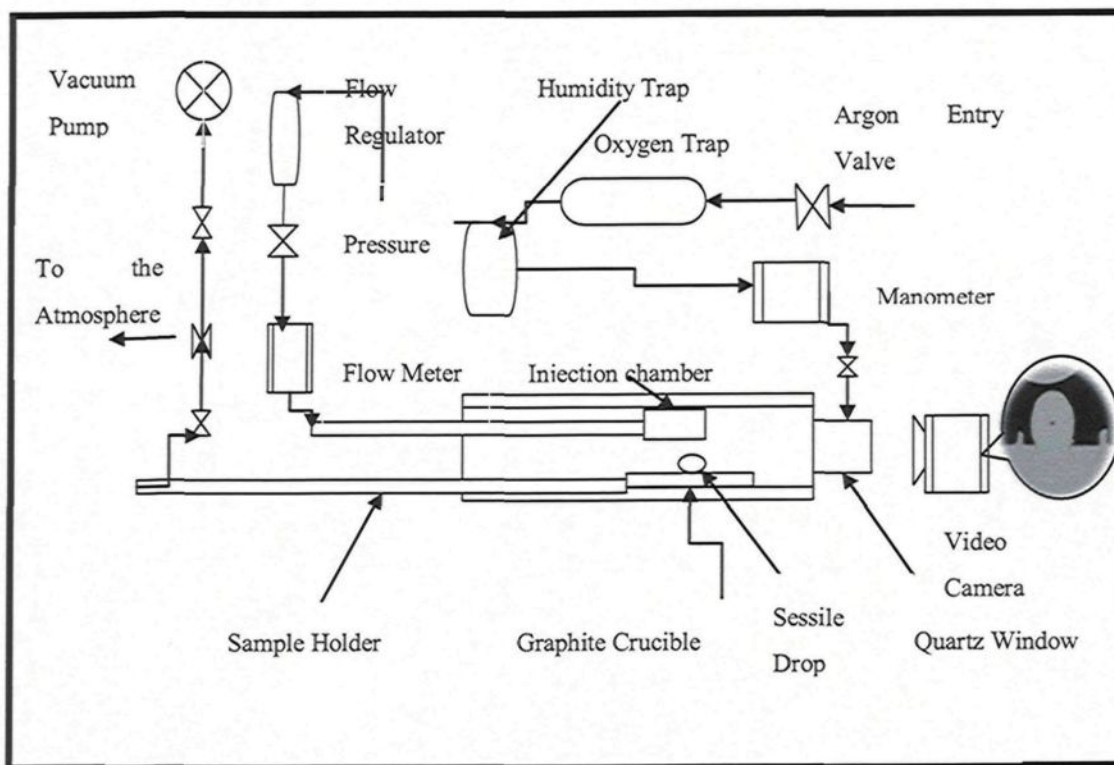


Figure 4.1 Schematic diagram of Sessile Drop Experimental Set-up

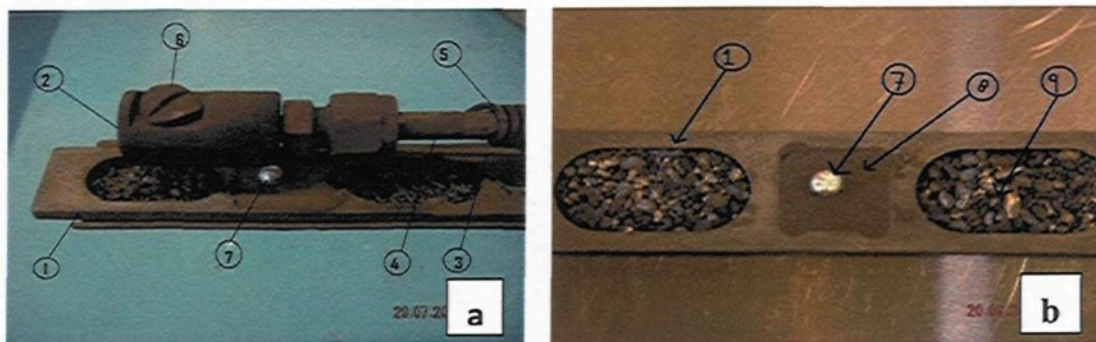


Figure 4.2 (a) General view of metal injection system

(b) View of sample crucible

- | | |
|---|--|
| 1. Sample crucible with three compartments. | 6. Cap of injection chamber charging hole. |
| 2. Injection chamber charged with solid aluminum. | 7. Aluminum drop. |
| 3. Thermocouple. | 8. Compartment for ceramics. |
| 4. Sample removing mechanism. | 9. Compartment for titanium. |
| 5. Argon supplying line for pushing the metal. | |

The experiments are conducted under argon atmosphere. There are two entry lines for argon. The main line was directly connected to the inconel tube to maintain the inert atmosphere inside. The other line, which connects the injection chamber to inert gas supply, carries the necessary argon for pushing the liquid metal out of the injection chamber on to the solid sample. Research grade (RG) argon (99.999%) is used during the experiments. The impurities certified by the supplier (Praxair) for argon gas are given below in Table 4.1. In order to decrease the oxygen and humidity content of the argon, it is passed through oxygen (Chromatographic Specialties, Big Oxygen Trap (C36084), humidity traps (Chromatographic Specialties, Glass Moisture Trap - C36150) before it enters the system. Pressure of argon is measured on the argon entry lines by manometers. A simple system is installed on the secondary line, which is connected to the injection chamber, for generating a higher pressure with respect to the main line and depressurizing it when necessary. A compressed gas regulator which can regulate a maximum supply of 160 psi was used to pressurize the secondary line and a pressure gauge (Winter's Economy Gauge, 0-5 psi) with 0.1 psi accuracy was connected in order to prevent the liquid metal to overflow over the powders and damage the furnace. The formation of the sessile drop is carried out in a controlled manner by relieving the pressure of the secondary line gently with a desired flow rate by means of a flow regulator (Nupro Company, Cleveland, Ohio).

Table 4.1 Summary of impurities reported by the supplier of argon gas

Argon Gas Type	O ₂ [ppm]	H ₂ O [ppm]	CO ₂ [ppm]	CO [ppm]	TCH ₄ [ppm]	N ₂ [ppm]	H ₂ [ppm]
Research Grade	< 0.2	< 1	< 0.1	< 0.1	< 0.1	< 1	< 1

* TCH₄ is total hydrocarbon

4.2 Experimental Procedure of Sessile Drop Experiments

4.2.1 Sample Preparation

In this experimental system the sessile drop of Al or Al alloys were formed on the different ceramics powders (B₄C, TiB₂, TiC, AlB₂, Al₄C₃, ZrC, ZrB₂, VC, VB₂). The sample preparation methods are explained below in detail.

4.2.1.1 Packed powders

In the first series of experiments, the ceramic particles are packed in the graphite sample crucible and the sessile drop is formed directly on them. The middle compartment of the sample crucible is filled with ceramics powders and compressed with an aluminum weight. To reduce the oxidation of the drop, the other two compartments are filled with titanium particles (see Fig.4.3). The particle size distributions and bulk densities of the ceramic used are given in Table 4.2



Figure 4.3 Graphite sample crucible with three compartments

Table 4.2 The bulk density and the approximate particle size for the ceramic powders used in the wetting test

Ceramic Powder	Bulk Density (kgm⁻³)	Approximate Particle Size (μm)
B ₄ C	2500	23
ZrC	6730	≤ 44
VC	5770	≤ 44
TiC	4900	≤ 44
Al ₄ C ₃	2360	≤ 44
ZrB ₂	6090	≤ 44
VB ₂	5100	≤ 44
TiB ₂	4500	13-15
AlB ₂	3190	≤ 250

4.2.1.2 Preparation of Al and Al Alloys

A piece of aluminum(99.99% pure) or aluminum alloys (0.25-0.26 g) is initially cleaned with 10% NaOH solution to remove the upper oxide layer from the metal skin, next it is washed with fresh cooled distilled water until it is cleaned properly. Then it is cleaned with acetone and dried with ultra high pure argon (UHP).

In this study Al-1wt%Ti, Al-1.5wt% and Al-3wt%Ti alloys with 99.99% purity aluminum are used. It is always necessary to choose an optimum Ti level because there was possibility of formation of intermettals at operating temperatures (see Fig.2.3).

4.2.2 Experimental Procedure

To know the gas temperature in the different region of the furnace, a calibration has been carried out at the beginning of the study. Fig 4.4 shows the furnace calibration data. The sample is placed in the region where the temperature is uniform during the sessile-drop experiments.

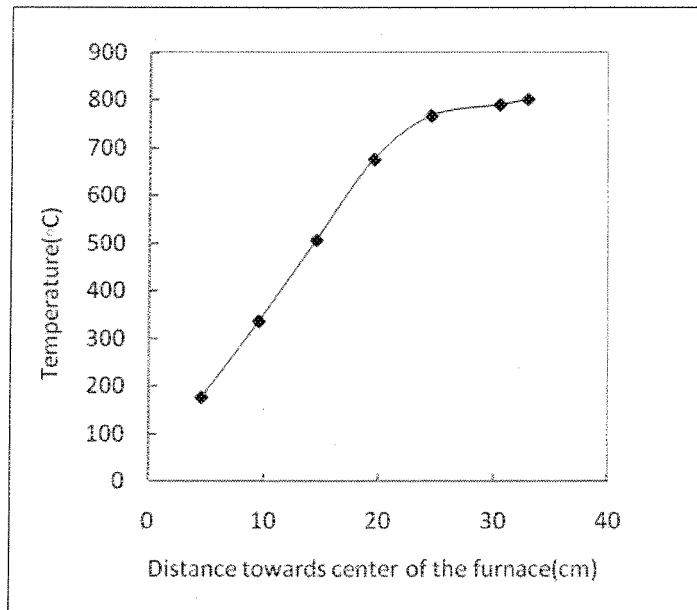


Figure 4.4 Furnace calibration curve

Before starting the experiments, RG argon is passed through the furnace for 5 min. Then, all of the argon in the lines and inside the tube furnace is evacuated using diffusion pump and the system is purged with RG argon for another 30-45 minutes. After a steady RG argon flow is maintained, the set-up was heated to 600°C. When the temperature stabilized at 600°C, a secondary argon line is opened to purge the injection chamber with RG argon for 30 minutes. After closing the secondary line the furnace is heated to the desired temperature, and the liquid aluminum in the injection chamber is pushed down gently by applying a small pressure to the line leading to the injection chamber. A sessile drop forms, and the experiment starts. The video of the drop is captured for 20 minutes. The form of the drop appears live on the computer screen and the salient images are captured to the computer's memory for later image analysis. The system can capture both static and

dynamic behavior of liquid interactions. FTA 32 (video 2) software is used to measure the contact angle. The analysis is based on the drop size and shape. In this study, the contact angle is measured by curve fitting (spherical fit) method using manual mode of image analysis (see Fig.4.5). Then, the furnace is shut down, and the sample crucible is pulled back by using a specially designed sample removing mechanism from the hot region of the furnace. This way, the sample is quenched for further analysis and the experiment terminated.

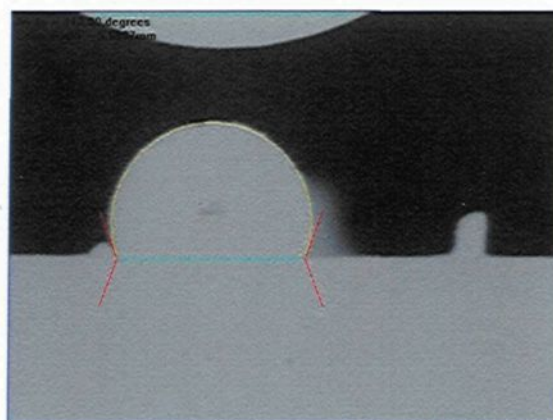


Figure 4.5 Contact angle of Al-1.5wt% Ti alloy on B_4C powder at $850^\circ C$ after 20 min measured using FTA32 software

4.2.3 Titanium Recycling

When the industrially pure grade titanium particles are used once in an experiment, their outer surfaces are oxidized and titanium oxide is formed. Titanium oxide is extremely stable and difficult to remove when formed but it is not economical to dispose of these oxidized titanium particles because under the oxidized layer there still significant amount of titanium left. The oxidized titanium particles are cleaned and recycled by particle cleaning procedure which is optimized by trial and error. In this procedure, a batch of

oxidized titanium particles is added to 75 ml 10% NaOH solution (by volume) which is dispensed into a 100 ml quartz bottle with air tight cap. The liquid level in the bottle is marked. The solution is slightly heated and magnetically stirred for two days onto a hot magnetic stirring plate (Fisher Thermix, Model 210T). During the cleaning procedure, if the liquid level decreased, distilled water is poured to keep the liquid level as same. After hot leaching, the solution is decanted and the titanium particles are washed with fresh cold distilled water until the distilled water stayed clean. Then it is place in a vacuum oven (Precision 110-F4-021) at 104°C to evaporate the moisture.

4.2.4 Sample Preparation for Analysis

While the furnace is cooling down to ambient temperature, the metal drop (sessile drop) on the powder bed solidifies. The sessile drop (sample) is taken out of the graphite crucible together with the sample holder. Then, it is prepared for optical microscope and SEM analyses.

4.2.4.1 Sectioning and Mounting

The first step of sample preparation is sectioning the sessile drop for proper mounting. Since the samples are aluminum or aluminum-titanium alloy, they are not difficult to cut. The samples are cut vertically from one side of the sessile drop. When sectioning is completed, samples are mounted by using cold mounting method. Cold mounting procedure is chosen for proper placement of samples because they were very small and round in shape. Cold mounting is done using epoxy resins mix with resin hardener which is liquid at the start but becomes solid after few hours. Initially, the mixture is evacuated for 8 hours in an evacuator to remove air bubbles from the mixture. Cold mounting requires very

simple equipment consisting of a cylindrical ring (cup) which serves as a mould and a flat piece which serves as the base of the mould. Samples were placed on the flat piece within the mould and the mixture is poured in and allowed to set for 12 hours. After curing, the sample can be taken out of the cup and analyzed. Cold mounting takes few hours to complete.

4.2.4.2 Grinding and Polishing

Samples are grounded and polished using a variable speed grinder-polisher (Buehler, Ecomet 4 with Automet 2 Power Head assembly). Grinding and polishing are semi-automatic processes. The force to be exerted by the power head, the rotation speed and direction of the platen, the type of the cooler to be used, and the process duration are entered into the Automet 2 assembly. If a solution other than water is used, it is added manually while the grinder-polisher is running. First 340 and 500 grains of silicon carbide per square inch papers are used and then 40 μ diamond paper is used. All the samples are grinded by hand. During grinding light pressure was applied at the centre of the sample. Grinding is continued until all the blemishes have been removed, the sample surface is flat, and all the scratches are in a single orientation. The sample is washed in water and it is moved to the next grade of polishing, orienting the scratches from the previous grade normal to the rotation direction. This makes it easy to see when the coarser scratches have all been removed. After the final grinding operation on the 40 μ paper, the samples are washed in water and dried before being moved to the polishers.

The polishers consist of rotating discs covered with soft cloth impregnated with diamond particle suspensions and oily lubricants (the size ranges are 15, 3 and 1 μm) and finally with the final polishing cloth. The polishing is started with the coarse slurry and it is continued until the grinding scratches have been removed. The polishing procedure is given schematically in Fig.4.6 It is of vital importance that the sample is thoroughly cleaned using soapy water, and dried before moving onto the final stage. Any contamination of the final polishing disc will make it impossible to achieve a satisfactory polish. Examining the specimen in the microscope after polishing should reveal mirror like surface. The polishing procedure was summarized below in Table 4.3.

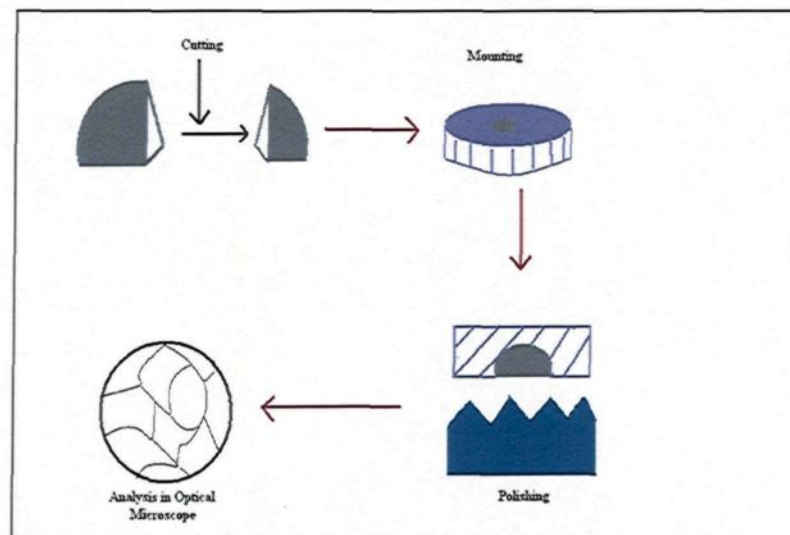


Figure 4.6 Schematical summary of sample preparation process

Table 4.3 Summary of polishing procedure

Platen	Polishing Cloth	Polishing Suspension	Polishing Media	Duration (min)	RPM
Plain	Textmet 1000	15 μ , diamond	Alcohol	10	150
Plain	Textmet 1000	3 μ ,diamond	Alcohol	5	150
Plain	Textmet 1000	1 μ ,diamond	Buehler Masterpolish 2	10	150
Plain	Final Polishing Paper	-	Colloidal Silica Polishing Suspension	3	60

4.2.5 Analysis of Samples Prepared

Prepared samples are analyzed in optical microscope and SEM.

4.2.5.1 Optical Microscope Analysis

The optical microscope (Nikon Eclipse ME600P) and image analysis software (Clemex Vision 4.0) is used to study the interface.

4.2.5.2 SEM Analysis

High performance scanning electron microscopy (JEOL-JSM-6480LV) is used for Microstructural analysis of the sessile drop/powder interface. The JEOL-JSM-6480LV is incorporated with Standard automated features include Auto Focus/Auto Stigmator, Auto Gun (saturation and alignment), and Automatic Contrast and Brightness. The operating voltage is 20kV and WD is 10 mm.

In order to facilitate SEM analysis, samples are coated with gold and platinum coating using Polaron Sputter Coater. During the coating the vacuum pressure is maintained at 10^{-4} mPa and operating current was 9mA.

CHAPTER 5

RESULTS AND DISCUSSIONS

5.1 Experimental Results

The experimental conditions for the experiments with different powders are summarized in Table 5.1. The parameters investigated during the sessile drop experiments are the type of powders, temperature, amount of titanium in alloy, experiment duration, and experimental environment (type of gas).

Table 5.1 Experimental parameters for the experiments with different ceramic powders

Exp.No	Temp. (°C)	Powder	Chemical Composition of Sample Metal	Atm.	Duration (min)
1	700	B ₄ C	Al	RG Ar*	20
2	700	B ₄ C	Al	RG Ar	20
3	750	B ₄ C	Al	RG Ar	20
4	750	B ₄ C	Al	RG Ar	20
5	800	B ₄ C	Al	RG Ar	20

Exp.No	Temp. (°C)	Powder	Chemical Composition of Sample Metal	Atm.	Duration (min)
6	800	B ₄ C	Al	RG Ar	20
7	850	B ₄ C	Al	RG Ar	20
8	850	B ₄ C	Al	RG Ar	20
9	900	B ₄ C	Al	RG Ar	20
10	900	B ₄ C	Al	RG Ar	20
11	700	B ₄ C	Al-1wt%Ti	RG Ar	20
12	700	B ₄ C	Al-1wt%Ti	RG Ar	20
13	750	B ₄ C	Al-1wt%Ti	RG Ar	20
14	750	B ₄ C	Al-1wt%Ti	RG Ar	20
15	800	B ₄ C	Al-1wt%Ti	RG Ar	20
16	800	B ₄ C	Al-1wt%Ti	RG Ar	20
17	850	B ₄ C	Al-1wt%Ti	RG Ar	20
18	850	B ₄ C	Al-1wt%Ti	RG Ar	20
19	900	B ₄ C	Al-1wt%Ti	RG Ar	20
20	900	B ₄ C	Al-1wt%Ti	RG Ar	20
21	750	B ₄ C	Al-1.5wt%Ti	RG Ar	20
22	750	B ₄ C	Al-1.5wt%Ti	RG Ar	20
23	850	B ₄ C	Al-1.5wt%Ti	RG Ar	20

Exp.No	Temp. (°C)	Powder	Chemical Composition of Sample Metal	Atm.	Duration (min)
24	850	B ₄ C	Al-1.5wt%Ti	RG Ar	20
25	750	B ₄ C	Al-3wt%Ti	RG Ar	20
26	750	B ₄ C	Al-3wt%Ti	RG Ar	20
27	850	B ₄ C	Al-3wt%Ti	RG Ar	20
28	850	B ₄ C	Al-3wt%Ti	RG Ar	20
29	750	AlB ₂	Al	RG Ar	20
30	750	AlB ₂	Al	RG Ar	20
31	850	AlB ₂	Al	RG Ar	20
32	850	AlB ₂	Al	RG Ar	20
33	750	AlB ₂	Al-1wt%Ti	RG Ar	20
34	750	AlB ₂	Al-1wt%Ti	RG Ar	20
35	850	AlB ₂	Al-1wt%Ti	RG Ar	20
36	850	AlB ₂	Al-1wt%Ti	RG Ar	20
37	750	Al ₄ C ₃	Al	RG Ar	20
38	750	Al ₄ C ₃	Al	RG Ar	20
39	850	Al ₄ C ₃	Al	RG Ar	20
40	850	Al ₄ C ₃	Al	RG Ar	20
41	750	Al ₄ C ₃	Al-1wt%Ti	RG Ar	20

Exp.No	Temp. (°C)	Powder	Chemical Composition of Sample Metal	Atm.	Duration (min)
42	750	Al ₄ C ₃	Al-1wt%Ti	RG Ar	20
43	850	Al ₄ C ₃	Al-1wt%Ti	RG Ar	20
44	850	Al ₄ C ₃	Al-1wt%Ti	RG Ar	20
45	750	TiB ₂	Al	RG Ar	20
46	750	TiB ₂	Al	RG Ar	20
47	850	TiB ₂	Al	RG Ar	20
48	850	TiB ₂	Al	RG Ar	20
49	750	TiC	Al	RG Ar	20
50	750	TiC	Al	RG Ar	20
51	850	TiC	Al	RG Ar	20
52	850	TiC	Al	RG Ar	20
53	750	ZrC	Al	RG Ar	20
54	750	ZrC	Al	RG Ar	20
55	850	ZrC	Al	RG Ar	20
56	850	ZrC	Al	RG Ar	20
57	750	ZrC	Al-1wt%Ti	RG Ar	20
58	750	ZrC	Al-1wt%Ti	RG Ar	20
59	850	ZrC	Al-1wt%Ti	RG Ar	20

Exp.No	Temp. (°C)	Powder	Chemical Composition of Sample Metal	Atm.	Duration (min)
60	850	ZrC	Al-1wt%Ti	RG Ar	20
61	750	ZrB ₂	Al	RG Ar	20
62	750	ZrB ₂	Al	RG Ar	20
63	850	ZrB ₂	Al	RG Ar	20
64	850	ZrB ₂	Al	RG Ar	20
65	750	ZrB ₂	Al-1wt%Ti	RG Ar	20
66	750	ZrB ₂	Al-1wt%Ti	RG Ar	20
67	850	ZrB ₂	Al-1wt%Ti	RG Ar	20
68	850	ZrB ₂	Al-1wt%Ti	RG Ar	20
69	750	VC	Al	RG Ar	20
70	750	VC	Al	RG Ar	20
71	850	VC	Al	RG Ar	20
72	850	VC	Al	RG Ar	20
73	750	VC	Al-1wt%Ti	RG Ar	20
74	750	VC	Al-1wt%Ti	RG Ar	20
75	850	VC	Al-1wt%Ti	RG Ar	20
76	850	VC	Al-1wt%Ti	RG Ar	20
77	750	VB ₂	Al	RG Ar	20

Exp.No	Temp. (°C)	Powder	Chemical Composition of Sample Metal	Atm.	Duration (min)
78	750	VB ₂	Al	RG Ar	20
79	850	VB ₂	Al	RG Ar	20
80	850	VB ₂	Al	RG Ar	20
81	750	VB ₂	Al-1wt%Ti	RG Ar	20
82	750	VB ₂	Al-1wt%Ti	RG Ar	20
83	850	VB ₂	Al-1wt%Ti	RG Ar	20
84	850	VB ₂	Al-1wt%Ti	RG Ar	20

*RG Ar: Research Grade Argon

5.1.1 Contact Angle Measurement of Al and Al-Ti Alloy on Different Ceramic Powders

5.1.1.1 Contact Angle Measurement of Al and Al-Ti Alloy on B₄C Powder

The wettability of B₄C powder by pure Al as well as by Al alloys have been studied using sessile-drop system. Initially the wetting experiments were carried out in the temperature range of 700°C to 900°C with Aluminum (99.99% pure) and Al- 1wt%Ti alloy (Figure 5.1 and 5.2). The each contact angle data is average of two.

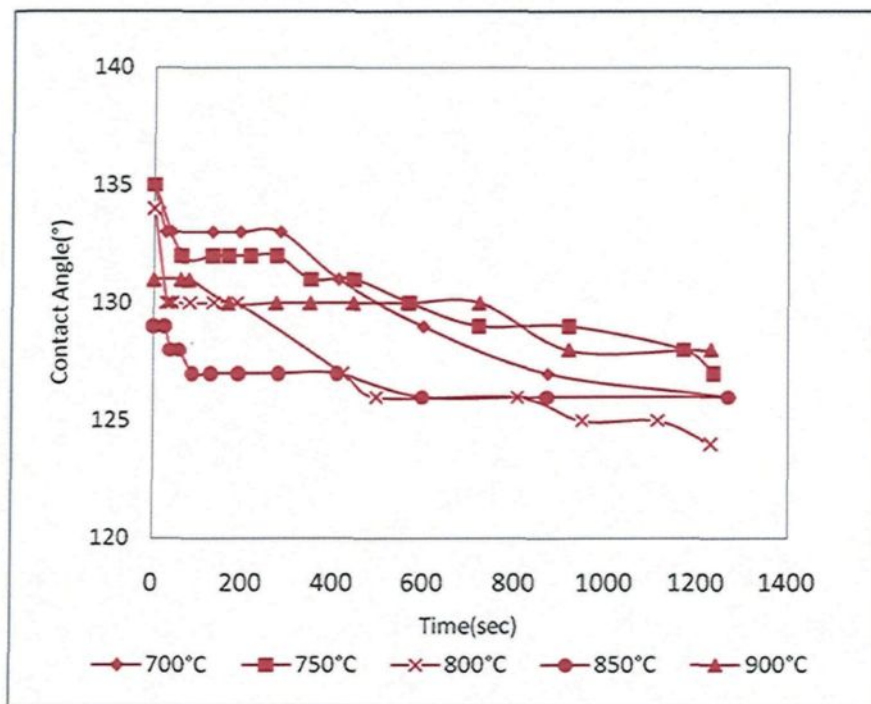


Figure 5.1 Change of contact angle of aluminum drop at different temperatures with time on boron carbide powder

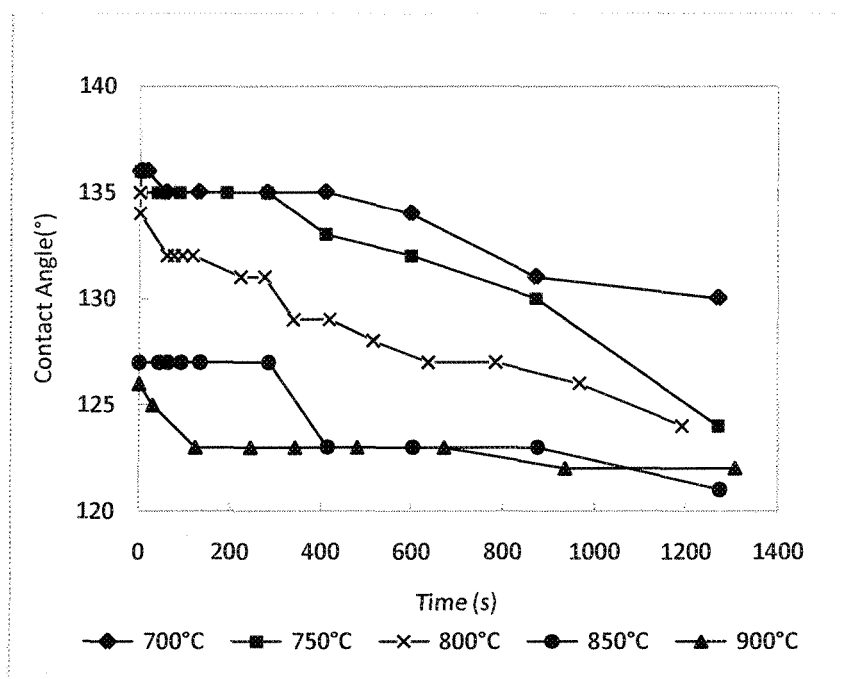


Figure 5.2 Change of contact angle of Al-1wt%Ti drop at different temperatures with time on boron carbide powder

Fig.5.1 and Fig.5.2 show the contact angle data for Al/ B₄C as well as Al-1wt%Ti /B₄C alloy. In general, it is observed that the contact angle decreases with increasing temperature. It is a clear from these figures that the contact angle decreases as the time increases. It can also be seen from the same figures that the contact angle decreases initially but after some time it stays constant at the highest temperature (900°C). This is probably due to the oxidation of the drop which prevents its spreading. Therefore, the initial contact angles were also studied (see Fig.5.3). It is observed that the initial contact angles measured with the alloy are lower than the contact angles measured with pure aluminum at high temperatures. This indicates that Al-1wt%Ti alloy wets B₄C powder

better than pure Al. When B_4C is in contact with Al-1wt%Ti alloy or with pure Al the initial contact angles decrease with increasing temperature (see Fig.5.3).

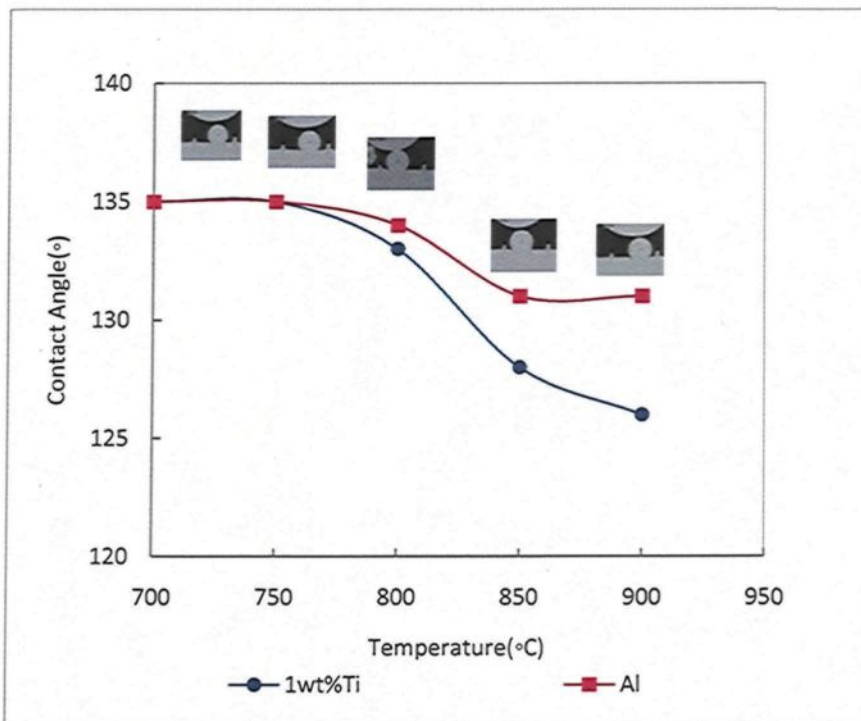


Figure 5.3 Comparisons between initial contact angles of pure aluminum and Al-1wt%Ti alloy on B_4C powder.

Fig. 5.4 shows the variation of the contact angle for Al-Ti alloys with different Ti content on boron carbide (B_4C) powder as a function of time and temperature. It is observed that B_4C is partially wetted by Al. At lower temperature ($750^\circ C$), initial contact angle for pure aluminum and Al-1wt% Ti alloy are the same. Pure aluminum wetted the particles more compared to the alloy up to 1000 seconds at this temperature. After, Al -1wt% Ti alloy wetted the powders more than pure Al and the contact angle decreased to 125° at the end of

the experiment. The profile of the contact angle for pure aluminum (Al-0wt%Ti) is included as reference to observe the effect of Ti in the wetting phenomenon. At higher temperatures, Ti addition improved the wetting.

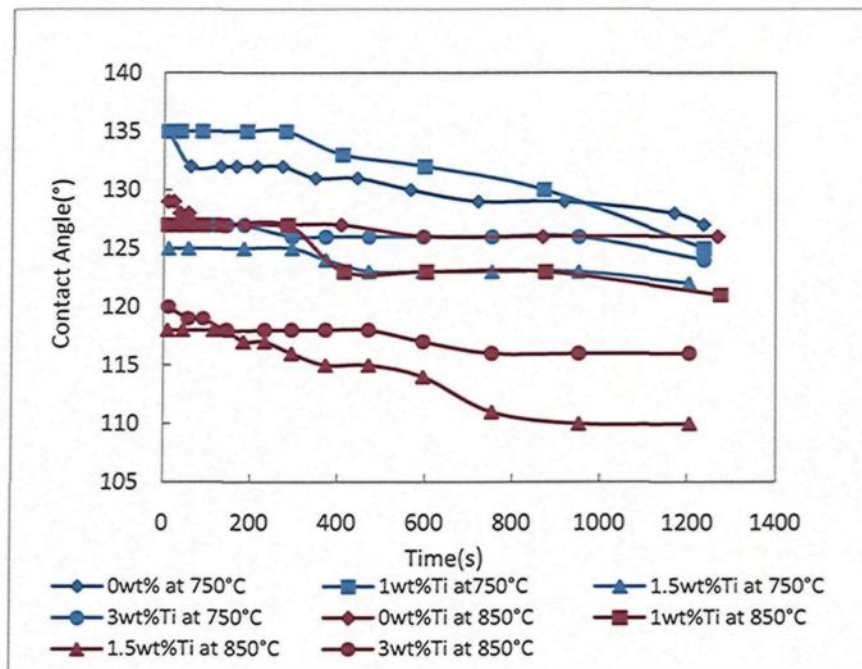


Figure 5.4 Change of contact angle B_4C powder with pure Al and Al-Ti alloy as a function of time and temperature

It is observed that increasing the titanium content of the alloy to 1.5wt% improves the wetting compared to wetting with the Al-1wt%Ti alloy. When Ti content is increased to 3wt%, the contact angles also increased compared to those obtained with 1.5wt% Ti. Although the wetting is still better with Al-3wt%Ti alloy compared to the wetting with pure Al and Al-1%Ti alloy, it cannot be improved further by increasing Ti content. The wetting

is better with 1.5wt% Ti alloy at both temperatures; however, B_4C powder is best wetted by Al-1.5wt% Ti alloy at 850°C (see Fig.5.4). These trends can be seen clearly if initial contact angle data and contact angle data after 20 minutes are compared at both temperatures (see Fig.5.5 and Fig.5.6).

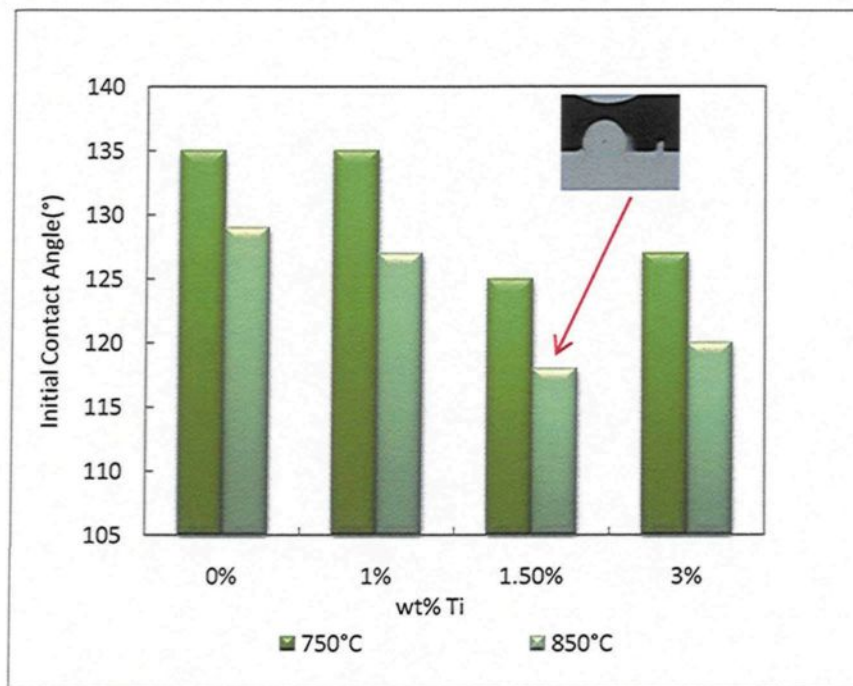


Figure 5.5 Initial contact angle of Al and Al-Ti alloy on B_4C powder at two different temperatures

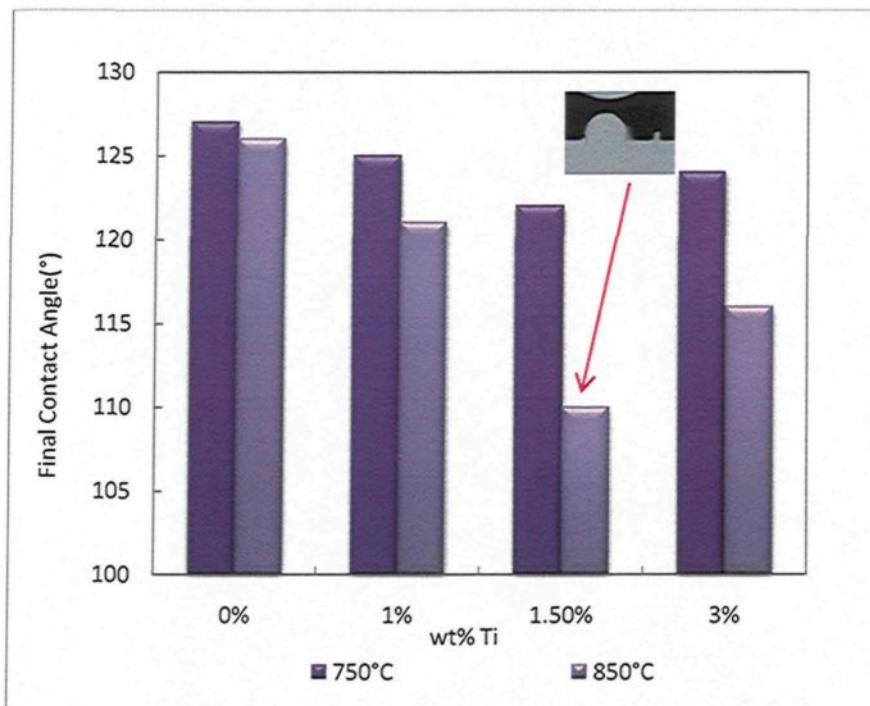


Figure 5.6 Contact angle data after 20 minutes for Al and Al-Ti alloy on B₄C powder at two different temperatures

These figures clearly show that best wetting is obtained for Al-1.5wt% Ti alloy at both temperatures. As the Ti levels increase further, the wettability of the boron carbide no longer improves but rather decreases. It is evident that the Ti addition greatly improves wetting of the boron carbide. However, it is important to select an appropriate Ti level to obtain the best results.

5.1.1.2 Contact Angle Measurement of Al and Al-Ti Alloy on other Ceramic Powders

In order to understand the effects of the reaction products on wetting, the contact angles

between the reaction products (TiC, TiB₂, AlB₂, Al₄C₃, ZrB₂, ZrC, VB₂, VC powders) and pure aluminum were initially measured at 750°C and 900°C (see Fig.5.7). But at 900°C, there was a problem of extensive oxidation. Also at this temperature, the sessile drop system itself was affected by oxidation. Therefore, the maximum temperature was lowered and the experiments were carried out at 750°C and 850°C. The results obtained up to now show that VC is most wetted (lowest contact angle) at 750°C and AlB₂ is most wetted at 850°C by pure aluminum. B₄C is the least wetted (highest contact angle) by pure aluminum at 750°C. ZrC and B₄C are least wetted at 850°C whereas AlB₂ has the highest contact angle at 900°C as shown in Fig.5.7. The initial contact angles measured at 900°C for all the particles are consistently higher than their corresponding contact angles measured at 850°C. This is probably due to oxidation of aluminum at this high temperature. The drop oxidizes right away and this prevents the spreading of the drop. The data taken at 750°C and 850°C show that wetting increases (contact angle decreases) with increasing temperature. It was impossible to place a liquid aluminum drop on ZrC particles at 750°C and on VB₂ powder within the temperature range studied. The drops rolled away from the particle surface showing that aluminum does not wet at all these ceramics at those temperatures.

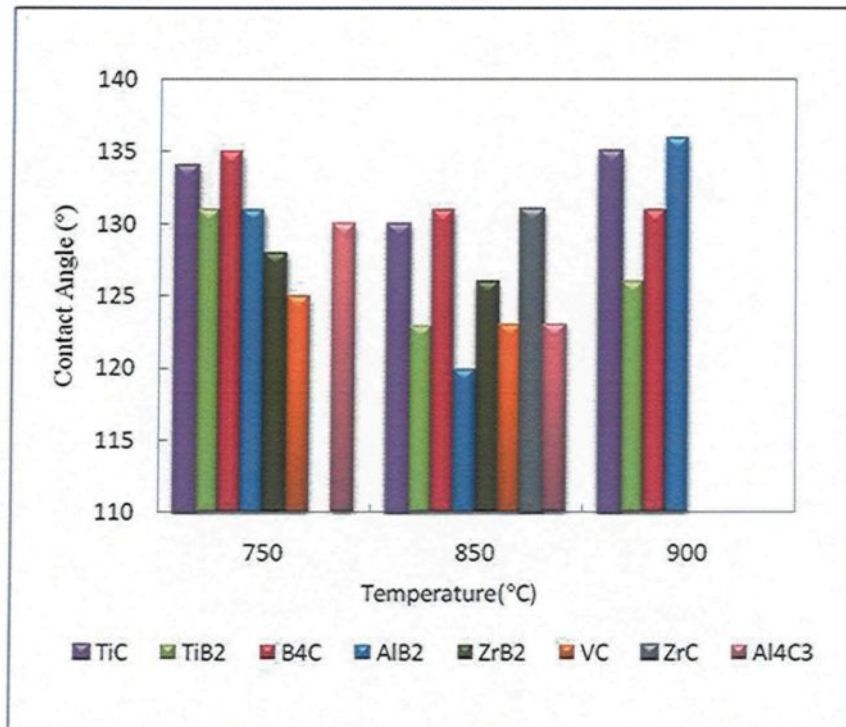


Figure 5.7 Initial contact angle of pure aluminum at different temperatures on different ceramic powders

Fig.5.8 presents the initial contact angles for different powders and Al-1wt%Ti alloy. This figure shows that ZrB₂ and ZrC are most wetted at 750°C and 850°C, respectively. The initial contact angle of AlB₂ is slightly higher than that of ZrC at 850°C. Although, ZrC is not wetted at all by the pure aluminum at 750°C (see Fig.5.7) addition of titanium improved its wetting. This figure also shows that the temperature has an important impact on wetting. VB₂ is only wetted at 850°C by Al-1wt%Ti but it is not wetted by pure aluminum at all within the experimental temperature range studied (see Fig.5.8).

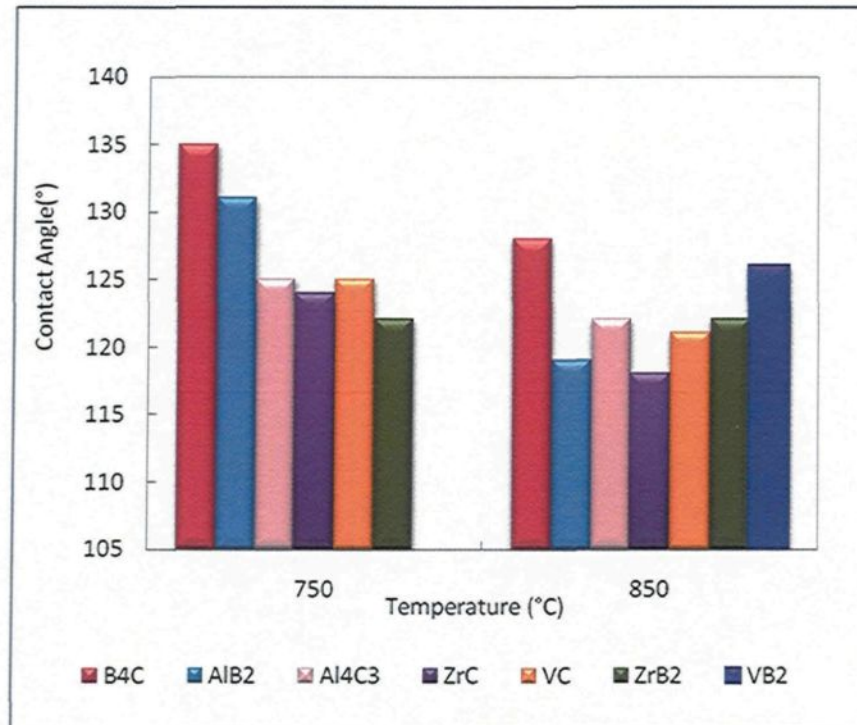


Figure 5.8 Initial contact angle of Al-1wt%Ti at different temperatures on different ceramic powders

The contact angle vs. time data is presented in Fig.5.9 for AlB₂ and Al₄C₃ powders with Al and Al-1wt%Ti alloy at 750°C and 850°C. The contact angles decrease with increasing temperature and time. They are lowest for both particles at 850°C with Al-1wt%Ti alloy (112° for Al₄C₃ and 114° for AlB₂). It can be seen that addition of titanium is not affecting the wettability of AlB₂. This could be due to no reaction at the interface.

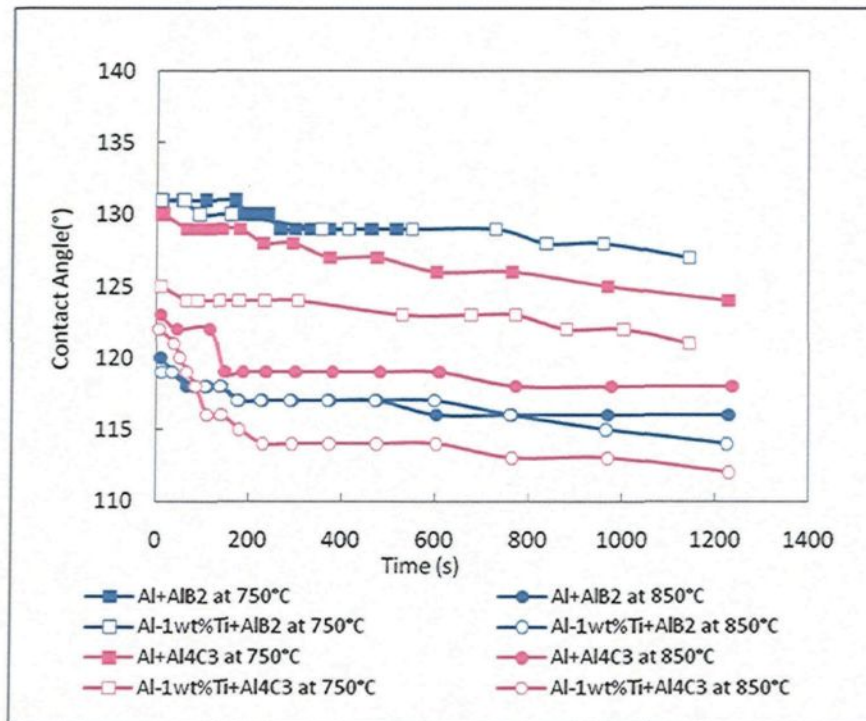


Figure 5.9 Contact angle vs. time data for AlB_2 and Al_4C_3 powders with Al and Al-1wt% Ti alloy at different temperatures

Fig.5.10 shows the variation of contact angle with time for TiC and TiB_2 with pure aluminum at two temperatures. As it is shown, the contact angle, in general, decreases with time. At 850°C , the initial contact angle of TiC is higher than that of TiB_2 but they approach one another with increasing time. At lower temperature (750°C), the initial contact angles of these powders are similar but TiB_2 is wetted better than TiC by Al as the time increases.

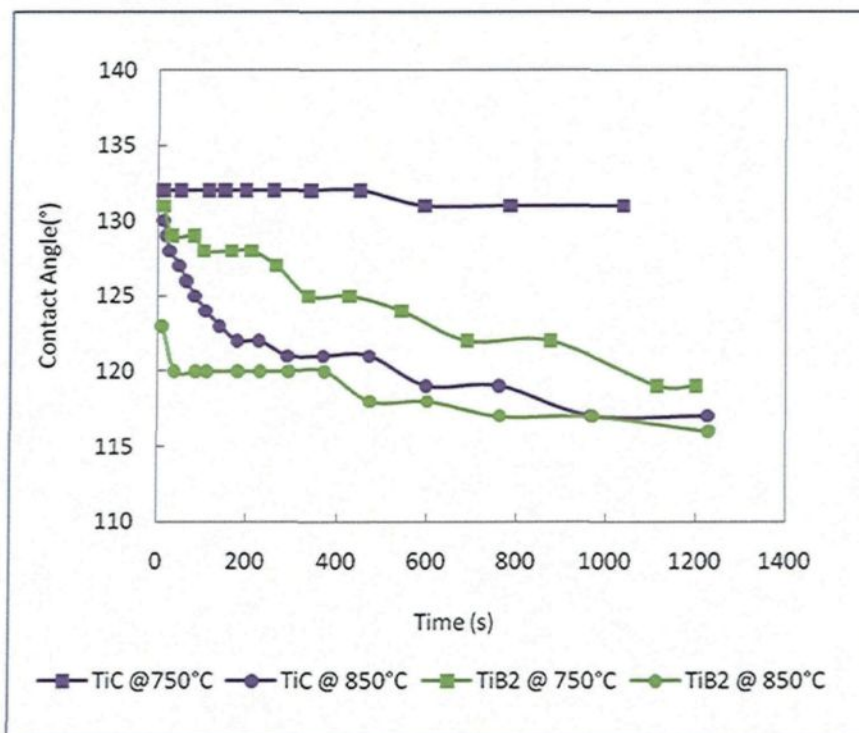


Figure 5.10 Contact angle vs. time data for TiC and TiB₂ powders with pure Al at different temperatures.

In the following figure (see Fig.5.11) effects of Zr and Zr-Ti addition to aluminum on the wetting of B₄C are demonstrated using some of the possible reaction products between Zr and B₄C as the substrate and pure Al and Al-1wt%Ti alloy. ZrC is wetted most by Al-1wt%Ti alloy at 850°C and after 20 min the contact angle reduces to 109° which is lowest contact angle obtained among the all powders studied. Addition of Ti to the metal improves the wetting for all cases shown in these figures. It can be said that presence of Ti together with Zr seems to increase the wetting at 850°C. The results also show that carbide is more wetted than boride by Al-Zr-Ti system at both temperatures. However, ZrC was not wetted at all by pure Al at 750°C.

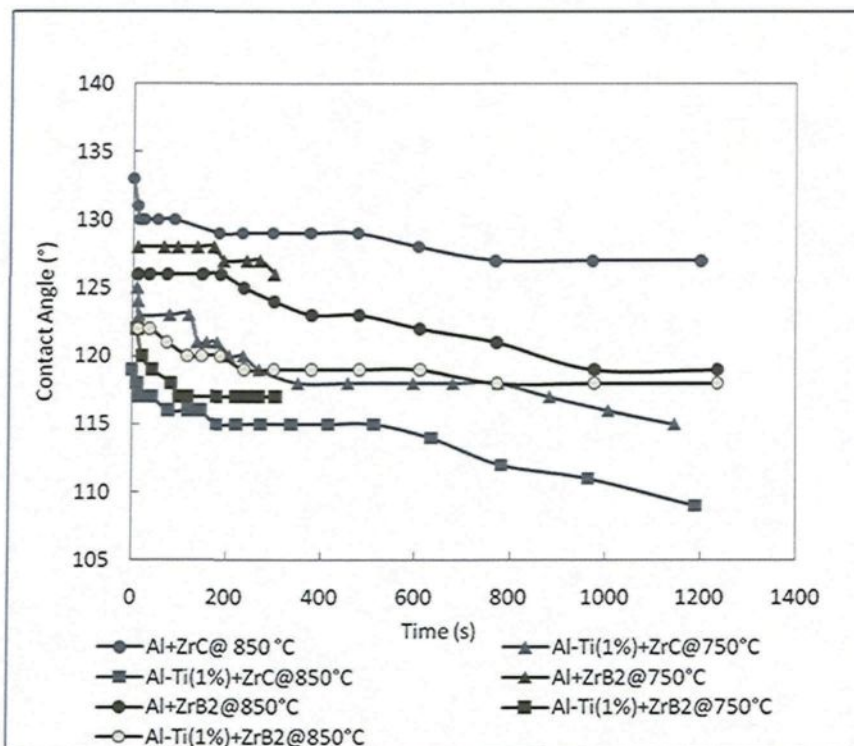


Figure 5.11 Change of contact angle with time for ZrC and ZrB₂ powders with Al and Al-1wt% Ti alloy

As shown in Fig.5.12, the change of contact angle with the both pure Al and Al-1wt%Ti on VC is almost the same at 750°C. The initial angles for both systems are also nearly the same. Therefore, it can be said that at this temperature Ti does not seem to have a significant effect on wetting of VC. This carbide seems to be wetted more by pure Al at 850°C compared to the alloy. This is an opposite trend observed with all the other powders. Pure Al does not wet VB₂ powder. The metal drop rolls over the powder bed. Al-1wt%Ti alloy wets it only at 850°C.

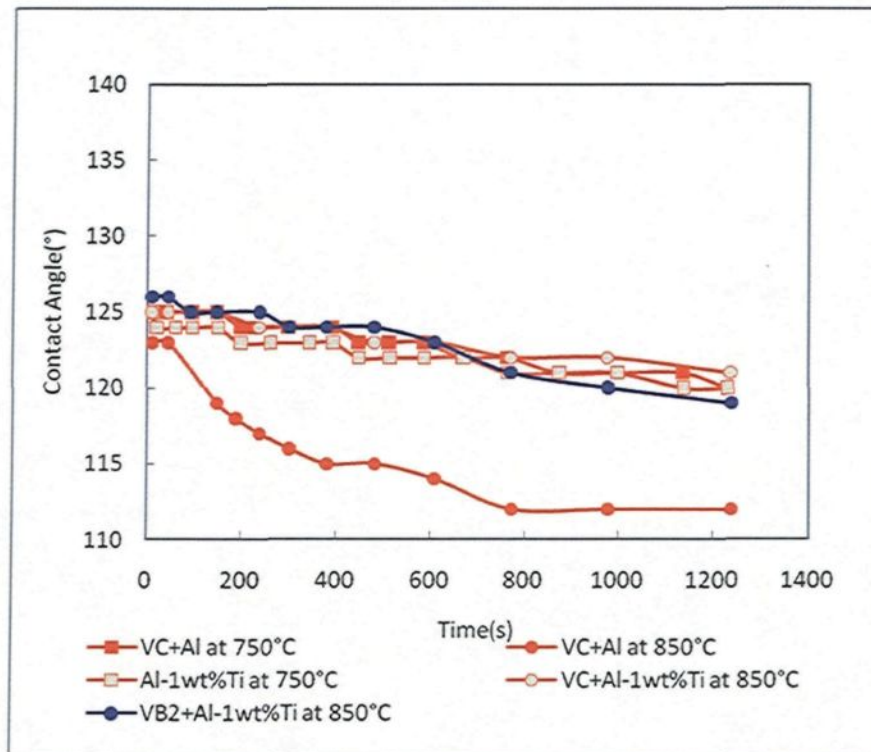


Figure 5.12 Change of contact angle with time for VC and VB_2 powders with Al and Al-Ti (1%) alloy at different temperatures.

5.1.2 Comparisons with Literature

Experimental conditions, such as, experiment duration, surface roughness, gas atmosphere have a great impact on the wetting characteristics. Fig.5.13 compares the initial contact angles measured during this study with the results of other researchers for B_4C -pure aluminum system. The experimental results are in good accordance with the cited literature in spite of the differences in experimental conditions used (see Table 5.2).

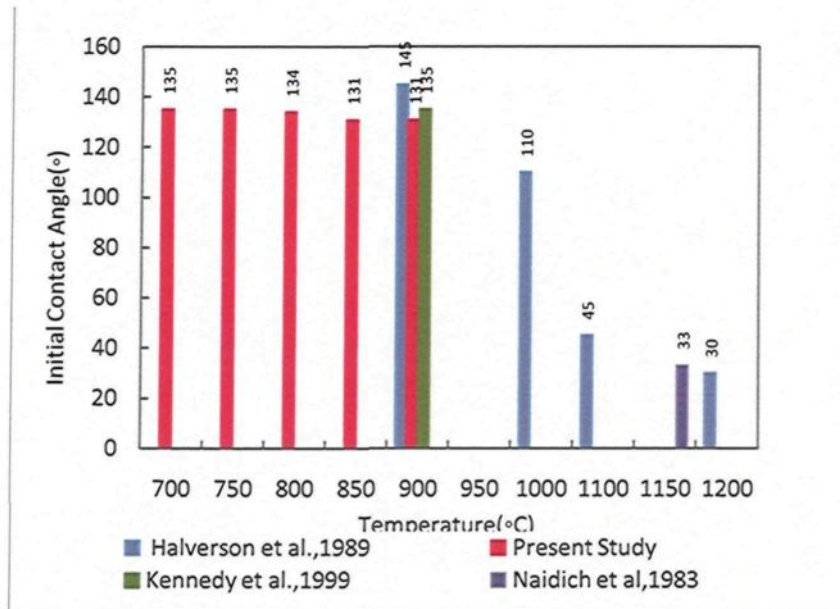


Figure 5.13 Comparisons of initial contact angles reported in literature and experimental results of the present work for pure aluminum on B₄C powder

Table 5.2 Experimental conditions used by different researchers for pure aluminum and on B₄C powder

Author	Experimental Environment	Metal (Al) Purity	Ceramic Substrate	Temperature (°C)	Contact Angle(°) with Respective Temperatures
Halverson et al., 1989	< 5×10^{-3} and $>10^{-4}$	99.99%	Hot Pressed	900-1300	145,110, 45,30,10
Present Study	Argon(RG) 99.999%	99.99%	Particles	700-950	135,135,134, 131,131,131, 131
Kennedy et al., 1999	Not reported	Not reported	Not reported	900	135
Naidich et al., 1983	Vacuum	Not reported	Not reported	1150	33

Fig. 5.14 compares the initial contact angles measured with those found in the literature for TiC substrate and pure Aluminum system. The experimental conditions used are also shown in Table 5.3. In general, it was observed that the experimental data of this work was in agreement with those of Contreras *et al.*, 2003 although they used plates instead of

powders. The differences are possibly due to different experimental conditions used. For example the angles obtained by Naidich *et al.*, 1983 are lower as expected because the experiments were carried out under vacuum (see Table 5.3) compared to argon gas used in this work and by Contreras *et al.*,2003 and for Rhee , 1970 the angles are much lower because the contact angle data is measured after 30 min.

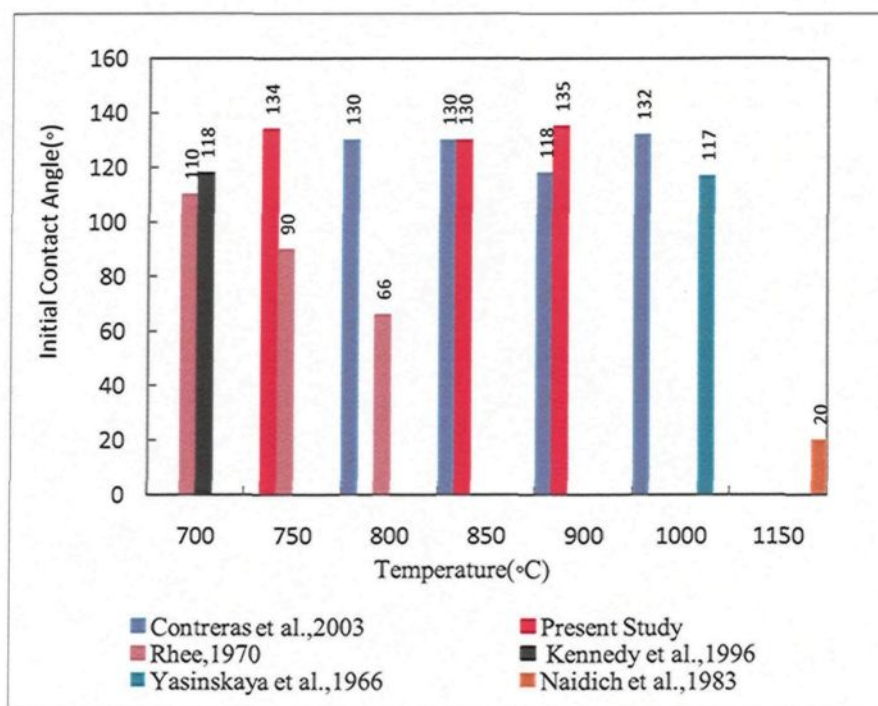


Figure 5.14 Comparisons of initial contact angles reported in literature and experimental results of the present work for pure aluminum on TiC powder

Table 5.3 Experimental conditions used by different researchers for pure aluminum and on TiC substrate.

Author	Exp. Environment	Metal (Al) Purity	Ceramic Substrate	Temp (°C)	Contact Angle(°) with Respective Temp
Contreras et al., 2003	Argon 99.999%	99.99%	TiC Plate	800 -1000	130,130, 118,132
Present Study	Argon 99.999%	99.99%	TiC Powder	750,850, 900	134,133
Rhee, 1970	Vacuum, 2×10^{-7} torr	99.99%	TiC Plate	700-800	110,90,66
Kennedy et al., 1999	Not reported	Not reported	Not Reported	700	118
Yasinskaya et al., 1965	Not reported	Not reported	Not reported	1000	117
Naidich et al., 1983	Vacuum	Not reported	Not reported	1150	20

Similar comparison is shown for TiB₂ substrate and pure aluminum system in Fig.5.15 and

the experimental conditions are shown in Table 5.4. The discrepancy between the results of this work and the literature data is larger for this system. This is most probably due to the fact that almost all the literature data is taken under vacuum whereas argon is used for experiments at UQAC which can undermine the result. The gas atmosphere was not provided in two of the references [Naidich *et al.*,1983; Yasinkaya *et al.*, 1965].

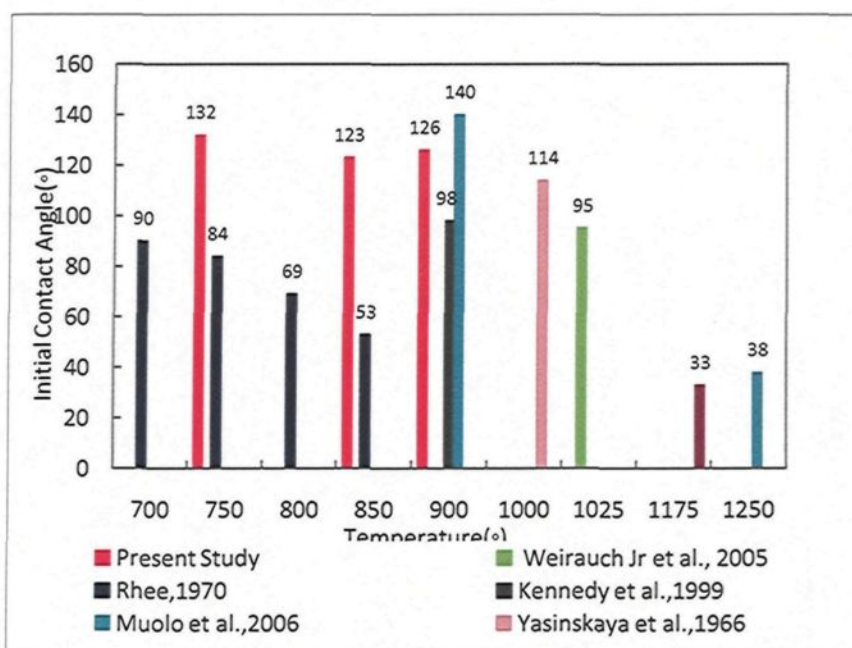


Figure 5.15 Comparisons of initial contact angles reported in literature and experimental results of the present work for pure aluminum on TiB_2 powder

Table 5.4 Experimental conditions used by different researchers for pure aluminum and on TiB₂ powder

Author	Exp. Environment	Metal (Al) Purity	Ceramic Substrate	Temp (°C)	Contact Angle(°) with Respective Temperature
Present Study	Argon 99.999%	99.99%	TiB ₂ Powder	750,850, 900	132,123, 126
Weirauch Jr. et al., 2005	Ultra High Vacuum	Single Crystal Aluminum	TiB ₂ Plate	1025	95
Rhee, 1970	Vacuum, 2×10^{-7} torr	99.99%	TiB ₂ Plate	700-850	90,84,69, 53
Kennedy et al., 1999	Not reported	Not reported	Not reported	900	98
Muolo et al., 2006	Vacuum	Not reported	Not reported	900,1250	140,38
Yasinskaya et al., 1965	Not reported	Not reported	Not reported	1000	114
Weirauch Jr. et al., 1995	Vacuum 1.9×10^{-4} to 9×10^{-3} torr	99.99%	Not reported	1175	33

5.1.3 Surface Tension Calculation for Al and Al-Ti Alloy

Accurate information on the surface tension of aluminum and its alloys are necessary for many metallurgical and material related processes, such as casting, welding, brazing, sintering and fabrication of the metal matrix composites. In this study, the effect of titanium addition on the surface tension has been investigated.

In the present study, the surface tensions are calculated by image analysis using the empirical relationship proposed by Dorsey, 1928 (see Eq.2.2). Densities of the Al-Ti alloys are required to calculate the surface tension by Dorsey method. They are calculated using Eq.2.3 and presented in Fig.5.16.

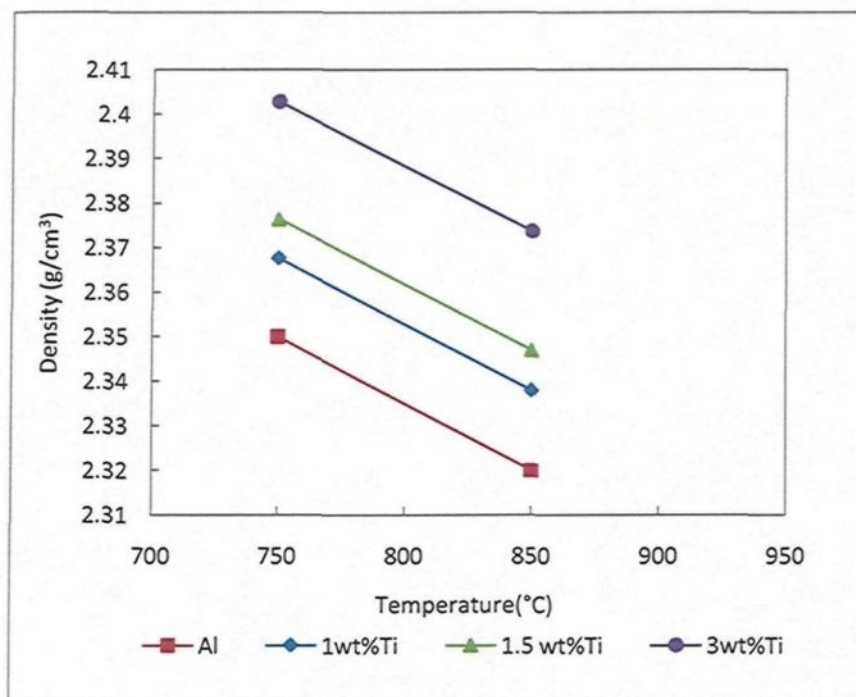


Figure 5.16 Densities of the pure Al and Al-Ti alloys at different temperatures

The calculated surface tension of liquid aluminum and Al-1wt%Ti alloy at 750°C and 850°C under argon atmosphere are shown in Fig.5.17 and 5.18, respectively, for B₄C and for different ceramic powders which represent possible reaction products. The results of the wetting experiments carried out with these powders are given in Section 5.1.1. These results are generally in agreement with the results reported in the literature which are shown in Table 3.1. As can be seen from these figures, the calculated surface tension values are similar under similar experimental conditions for different solid substrates. This is expected since the surface tension is a function of liquid and vapor properties (type of gas used, the purity of aluminum, presence of oxide layer on the liquid drop), experimental conditions (temperature, pressure). The results indicate that the experimental system is working properly.

The surface tensions of pure aluminum measured in this study are in perfect agreement with the results of Ergin, 2006, who also measured the surface tension of pure aluminum under argon atmosphere.

The results show the surface tension decreases with increasing temperature. Ti content changes the liquid properties, therefore, affect the surface tension. Surface tension of Al-1wt% Ti alloy is lower than that of pure aluminum. The average surface tension of the pure aluminum and Al-1wt%Ti alloy calculated under argon at two temperatures. The values for pure aluminum at 750 and 850°C, are found as **837** dyne /cm and **795** dyne/cm respectively. For Al-1wt%Ti alloy the calculated average surface tensions are **810** dyne /cm and **784** dyne /cm at the same temperatures

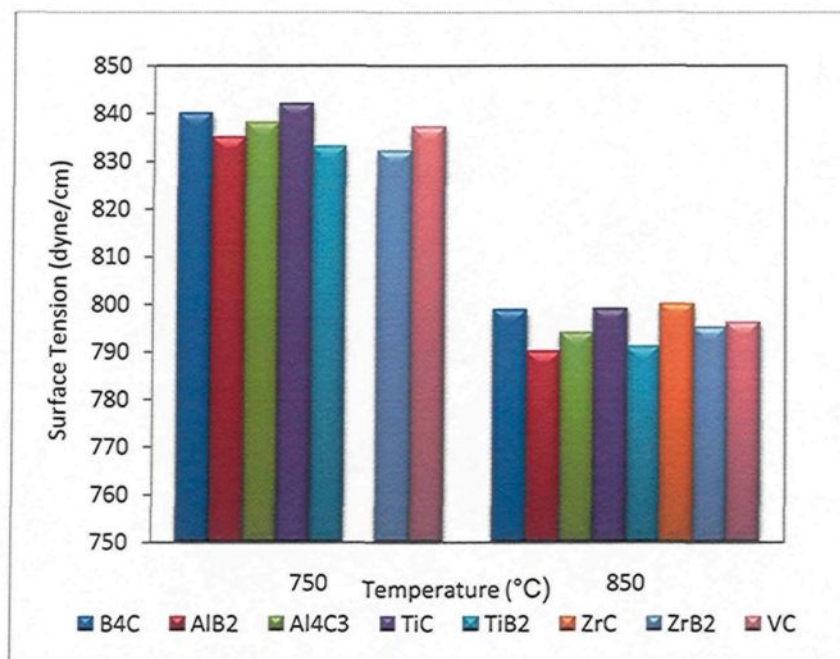


Figure 5.17 Surface tension of Al at two different temperatures and for different systems

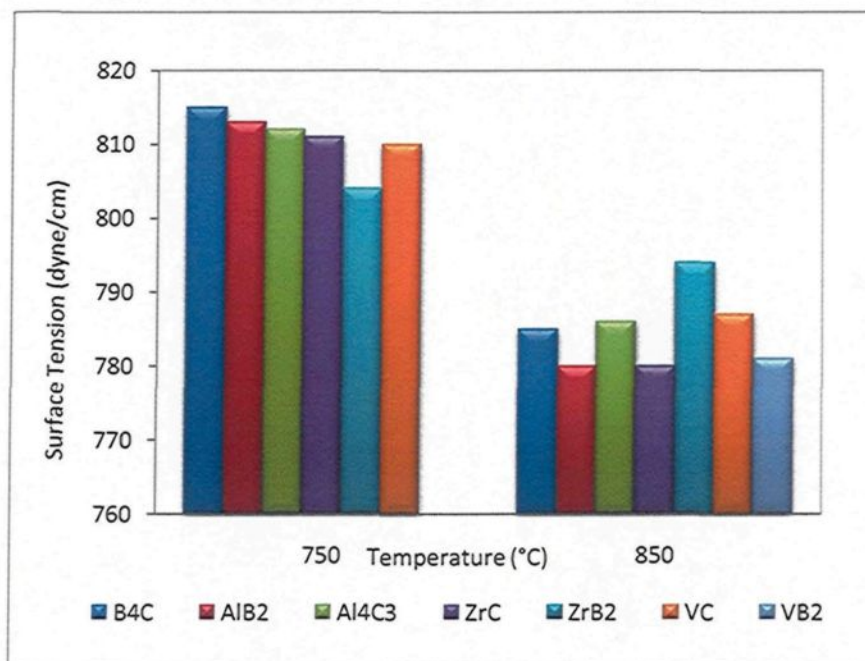


Figure 5.18 Surface tension Al-1wt%Ti alloy at different temperatures and for different systems

Fig.5.19 shows the surface tension values for different Al-Ti alloys with different Ti content at 750 and 850°C. The surface tension of pure aluminum is also given as a reference. As shown in this figure, surface tension decreases with increasing Ti wt% up to 1.5wt%Ti. However, at both temperatures, surface tension starts to increase when Ti content of the alloy is increased to 3wt%. This is in agreement with the contact angle data.

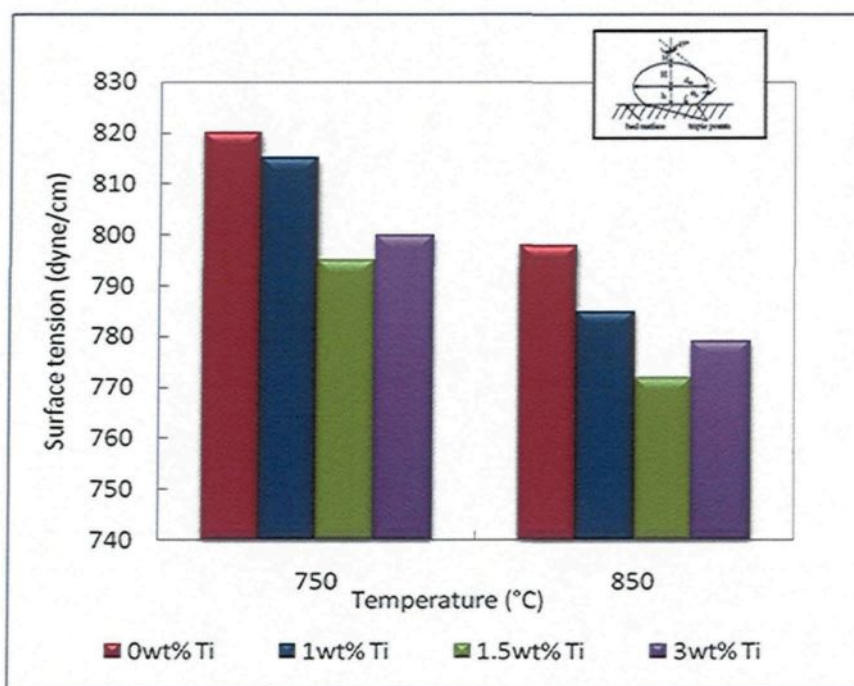


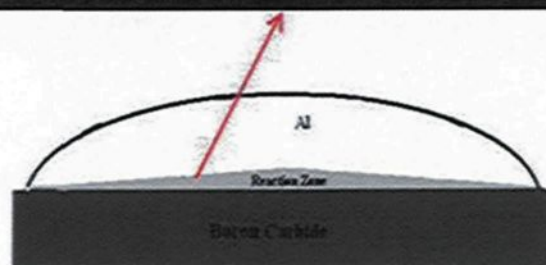
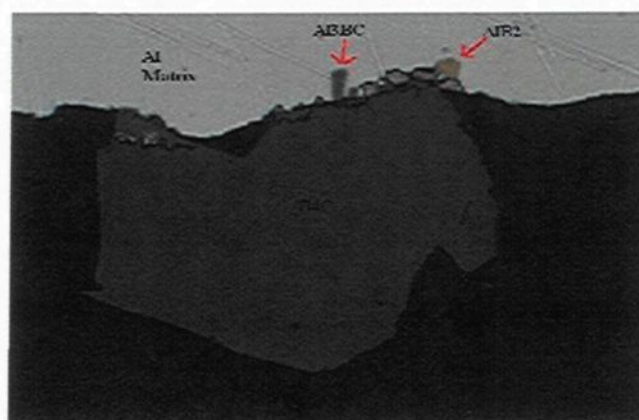
Figure 5.19 Effect of Ti content on the surface tension Al-Ti alloy at different temperatures

5.1.4 Microstructural Analyses

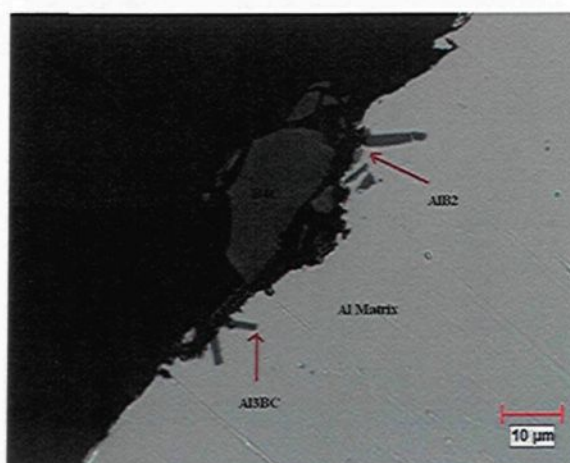
5.1.4.1 Al/B₄C and Al-Ti alloy/B₄C interface

In this study, the microstructural analyses were carried out only for the samples obtained from 20 minute wetting tests conducted at 850°C. Figure 5.20a shows the cross sections of

the drop-substrate interfaces for Al/B₄C system acquired with an optical microscope. Wetting frequently occurs because of the chemical reactions taking place in a reactive system. Due to these interfacial reactions, new solid compounds form on the interface of metal and ceramic substrate. For Al/B₄C system, the formation of a new discontinuous interface layer of 2-3 μm thickness was clearly observed (see Fig.5.20b) but due to reduced volume of the interface, it was not possible to examine accurately the cross section of the samples using XRD. Therefore, it was not possible to identify any phase other than B₄C and Al by this technique. As can be seen from these micrographs, interfacial reactions formed solid particles around the boron carbide powders. Two kinds of particles, a gray and yellow, were observed under the optical microscope. Most of the gray particles were attached or very close to the B₄C powder but yellow particles were not often attached to the B₄C powders. Quantitative determination performed by EDX of the reaction product revealed the presence of Al, B and C elements which could be Al₃BC. However the sizes of the particles were too small to obtain accurate quantitative data (see Fig.5.21).



(a)



(b)

Figure 5.20 (a) The interfacial product layer formation at the middle of the drop in Al/B₄C system (b) Cross section of the sessile drop – B₄C powder interface obtained at 850°C and after 20 minutes for pure Al using optical microscopy

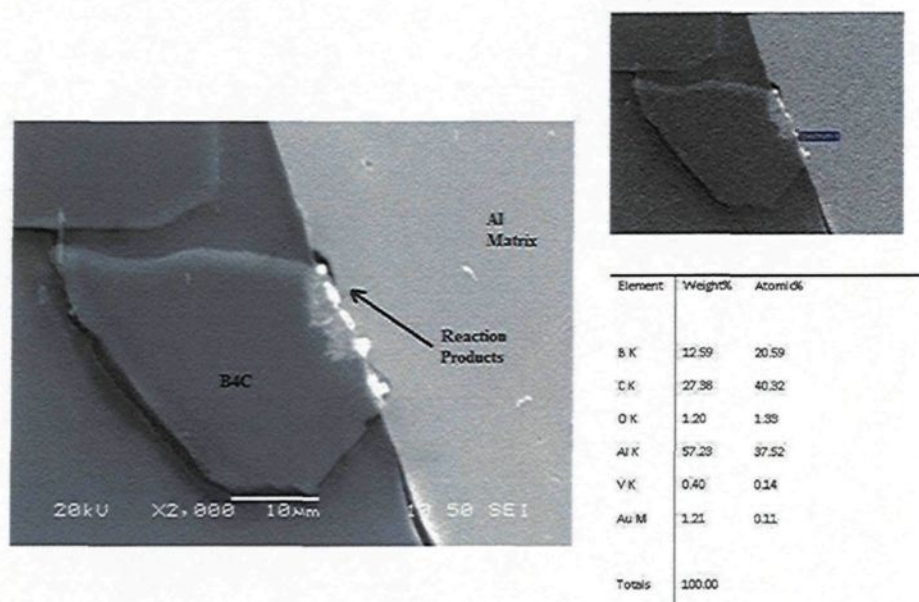


Figure 5.21 SEM micrograph of Al/B₄C interface showing formation of new phase at 850°C and after 20 minutes

The nature of the reaction between Al and B₄C has been well established. Several yellow particles were examined using EDX and the results compared with stoichiometric composition of the AlB₂ phase. The yellow particles were identified as AlB₂. The gray particles were identified as Al₃BC by TEM dark field image analysis. It has been proposed that secondary reaction phases Al₃BC and AlB₂ are formed [see Eq. 3.4] [Zhang *et al.*, 2008a; Zhang *et al.*, 2007; Viala *et al.*, 1997].

B₄C is not stable in the aluminum melt [Zhang *et al.*, 2008a; Zhang *et al.*, 2007; Viala *et al.*, 1997] and forms Al₃BC and AlB₂ as reaction products. Therefore, it can be said that the interfacial reaction (Eq.3.4) can help the wetting of the B₄C with aluminum with prolonged time (see Fig. 5.1). Microstructural analyses revealed that the formation of Al₃BC and AlB₂

enhances the wettability, due to the better wettability of the reaction products by aluminum. This phenomenon is in good accordance with the measured contact angles which are presented in Section 5.1.1.2, that is, the wettability of AlB_2 by aluminum is better than wettability of B_4C by aluminum (see Fig.5.10). However, B_4C reacts continuously with Al. The presence of these reaction products causes deterioration in certain mechanical and chemical properties of the melt [Chen, 2005; Chen, 2006].

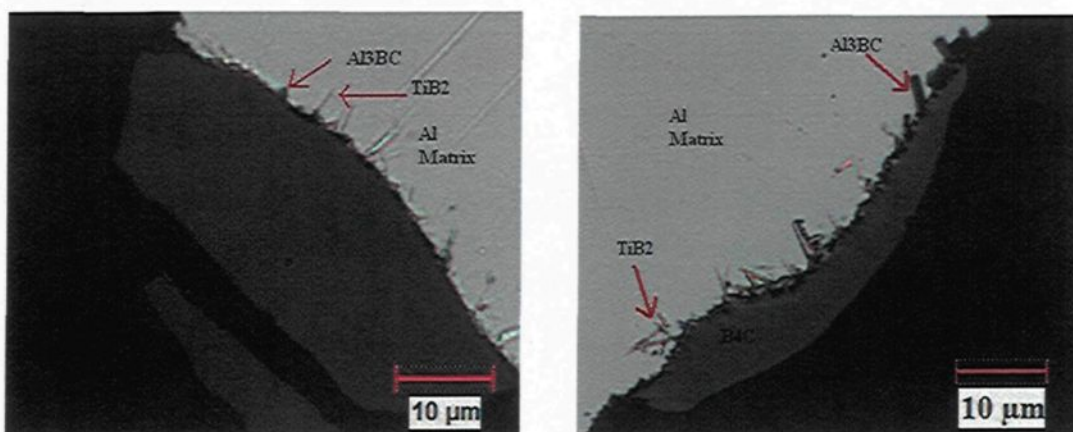
To control the interfacial reaction, a novel technique was developed. It was reported in the literature that the presence of titanium increase the stability of the B_4C powders in the aluminum matrix [Zhang *et al.*, 2008a; Zhang *et al.*, 2008b; Zhang *et al.*, 2007]. Fig.5.22a shows the micrograph of B_4C with 1wt% Ti addition after 20 min of contact time at 850°C. It is observed that, AlB_2 particles disappear and a new Ti rich needle like particles are formed around the B_4C powders. This layer acts as a barrier layer and isolates the B_4C from the matrix. Outside the needle like particle layer, there is no layer of gray particles. The sizes of the needle like particles are approximately 0.1-3 μm which are too small for obtaining accurate quantitative data (see Fig.5.22 b and Fig.5.23). However, quantitative determination performed by EDX of the reaction product revealed the presence of Al, B, C and Ti elements which could be Al_3BC or TiB_2 (see Fig. 5.23b). It is impossible to get accurate data because the phases are so close to each other that EDX scanning cannot differentiate the two phases. This thin dense needle-shaped particle layer not only prevents the further reaction of the boron carbide with aluminum but also improves the wettability of the B_4C by aluminum (see Figures 5.3-5.6). It is also observed that with increasing Ti

level, the amount of gray particles (Al_3BC) formation is decreased (see Fig.5.22b and c). However, further increase in Ti levels toward 3wt% Ti cause formation of large plate like Al_3Ti intermettals (see Fig.5.22c). This might explain the decrease in wetting (increased contact angle and surface tension) at this Ti percentage.

The nature of the reaction between Al-Ti alloy and B_4C has been well established in the literature. The transmission electron microscopy test has been conducted to identify the Ti rich layer. Results showed that the Ti rich layer is composed of fine TiB_2 crystals and other gray particles are Al_3BC [Zhang *et al.*, 2008a; Zhang *et al.*, 2008b; Zhang *et al.*, 2007; Chen,2006]. Also it has been proposed that secondary reactions phases Al_3BC and TiB_2 formed (see Eq.3.6)[Zhang *et al.*, 2008a].

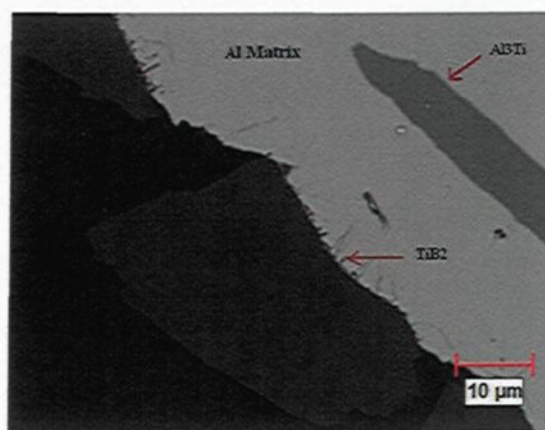
Based on the previous discussions, it is implied that during the wetting test of B_4C by Al, a B_4C particle constantly reacts with the liquid aluminum to form AlB_2 and Al_3BC reaction phases. This results in continuous depletion of B_4C . The addition of Ti results in formation of TiB_2 which is more stable than AlB_2 since the Gibbs free energies of the formation of the two compounds are -331.0 and -108.8 KJ/mol at 750°C, respectively [Zhang *et al.*, 2008b]. AlB_2 is gradually replaced by TiB_2 as Ti content of the alloy increases. Microstructural analyses revealed that the formation of TiB_2 is the cause of reactive wetting. It is clear from the Fig. 5.22a, 5.22b and 5.22c that TiB_2 forms a protective layer on B_4C surface which prevents the further reaction of B_4C with aluminum. Moreover, TiB_2 is wettable by Al, therefore the wetting of B_4C by Al improves remarkably with prolonged time. This result

also agrees well with the results of the wetting tests that the wettability of TiB_2 by Al is much better than that of B_4C by Al (see Fig.5.7 and Fig.5.10). However when an excess amount of Ti is added, large plate like Al_3Ti intermetallics appear due to the less solubility of Ti in Al. This results in reduced wettability of B_4C powder by the alloy.



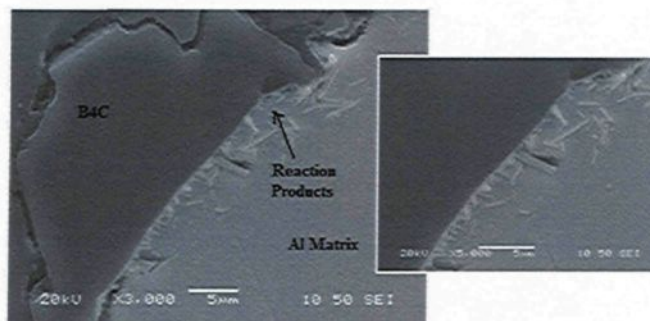
(a) 1wt% Ti

(b) 1.5wt% Ti

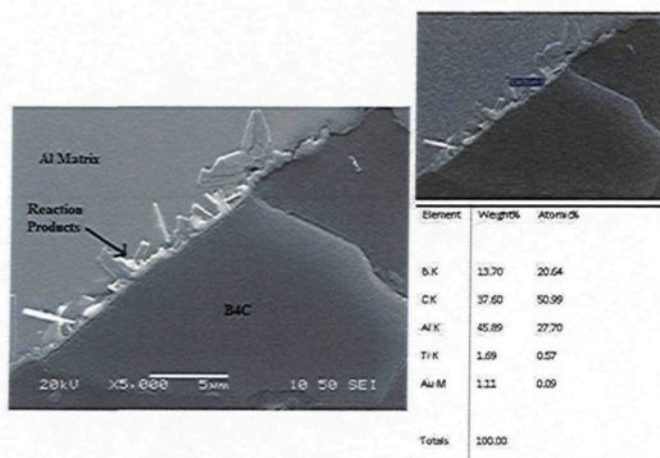


(c) 3wt% Ti

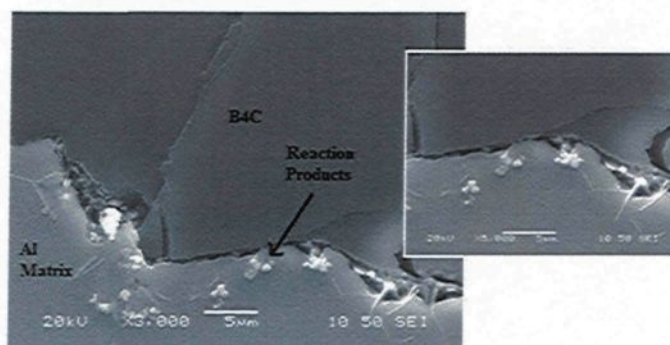
Figure 5.22 Cross section of the sessile drop/ B_4C powder interface obtained at $850^\circ C$ and after 20 minutes with different Ti levels using optical microscopy



(a) 1wt% Ti



(b) 1.5wt% Ti



(c) 3wt% Ti

Figure 5.23 SEM micrographs of different samples at 850°C and after 20 minutes, showing barrier layer of TiB_2 particulates on B_4C powder surface

5.1.4.2 Al/other ceramic powders and Al-Ti alloy/other ceramic powders interface

In order to understand the effects of the reaction products on wetting, the contact angles between the reaction products (TiC, TiB₂, AlB₂, Al₄C₃, ZrB₂, ZrC, VB₂, VC powders) and pure aluminum were measured at 750°C and 850°C. As explained in Section 5.1.1.2, it was found that the presence of zirconium also enhances the wetting in most of the cases (see Fig.5.11). Effect of vanadium on wetting is not very clear. It was observed that vanadium boride is not at all wetted by aluminum and vanadium carbide is wetted only at 850°C (see Fig 5.12).

During the second part of this study, morphological analysis of all the carbides used were carried out. The nature of reaction between Al and TiC is well established. Different studies have been reported in the literature on the interfacial reaction taking place at this interface. It was found that Al₄C₃ formed as a reaction product [Contreras *et al.*, 2004].

In the Al/Al₄C₃ system there is no traces of interfacial reaction (see Fig.5.24). The nature of the solid surface is not significantly modified by its contact with the metallic phase. It is confirmed by the wetting tests that Al does not react with Al₄C₃.

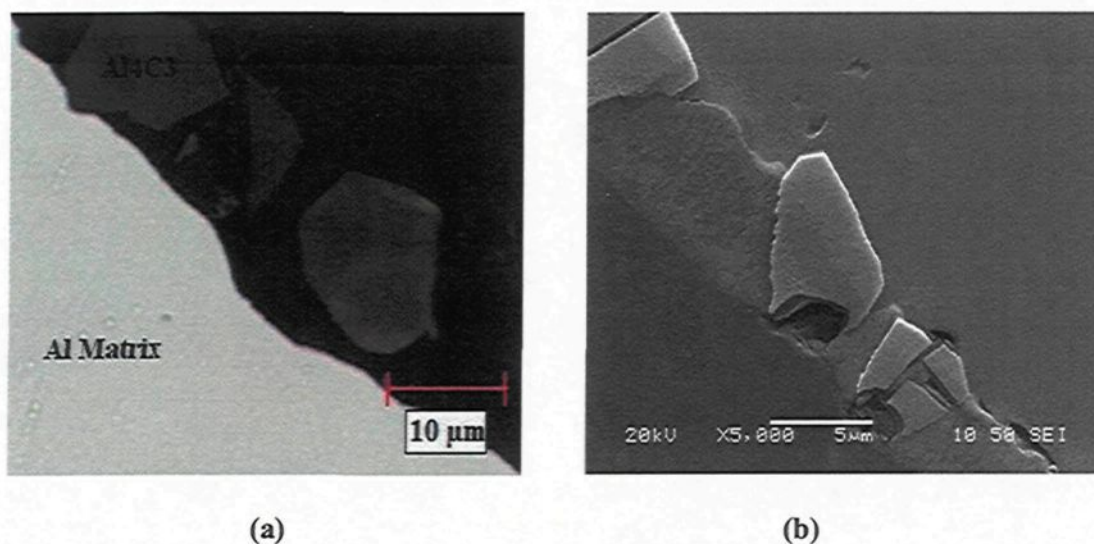


Figure 5.24 (a) Optical micrograph of Al/Al₄C₃ interface after 20 minutes at 850°C
 (b) SEM analysis of Al/Al₄C₃ interface after 20 minutes at 850°C

Fig.5.25 shows the cross sectional view of Al/VC drop-substrate interfaces obtained with optical microscope after 20 min of contact time at 850°C. Formation of small amount of reaction products can be seen from this micrograph. Fig.5.26 shows a SEM micrograph of a cross-section of Al/VC sample under the same conditions. The observed area is situated near the center of the drop. The vanadium carbide powder is covered by a discontinuous layer of reaction product with 0.1-1μm thickness. The thickness varied in different zones. Because of the reduced volume of the interface, it was not possible to perform X-ray diffraction studies. During the quantitative analysis of the samples only aluminum and carbon and gold were detected by EDX in the reaction layer, and no significant amount of oxygen was found (see Fig.5.27). The reaction product is possibly aluminum carbide (Al₄C₃). Traces of gold were due to the coating of gold on insulator substrates prior to SEM

analysis. These results are in agreement with the contact angle data which showed that VC is wetted by aluminum at this temperature.

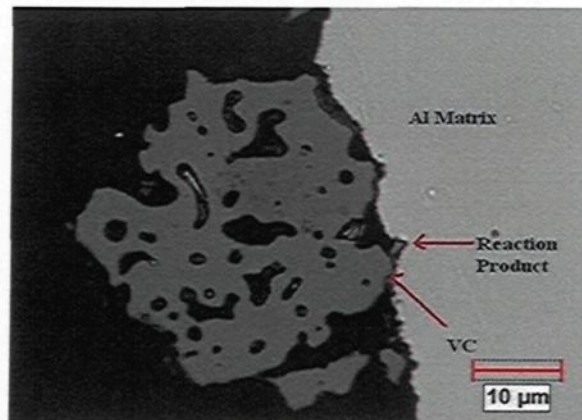


Figure 5.25 Optical micrograph of Al/VC interface after 20 minutes at 850°C

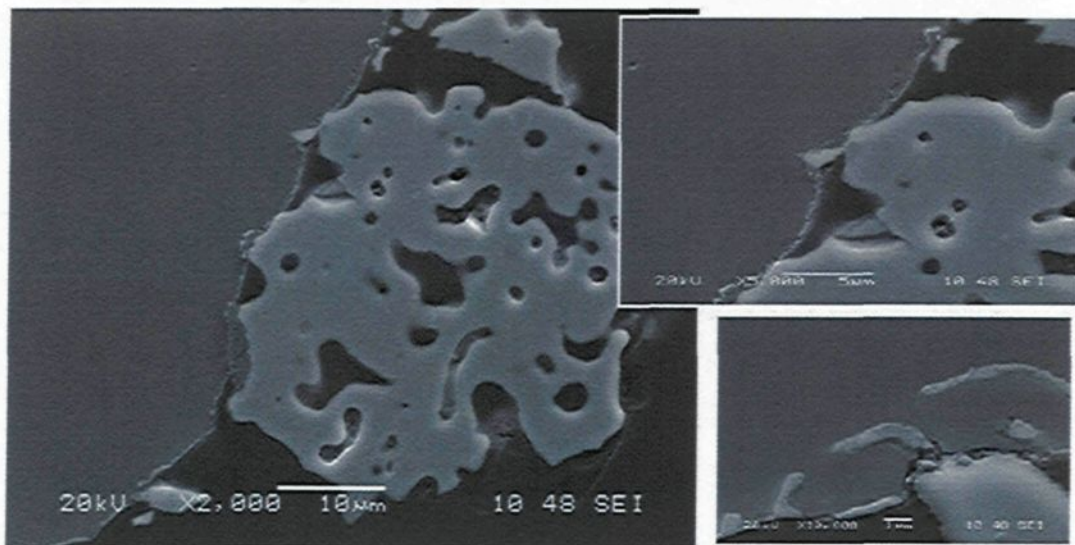


Figure 5.26 SEM observation of the Al/VC interface after 20 minutes at 850°C

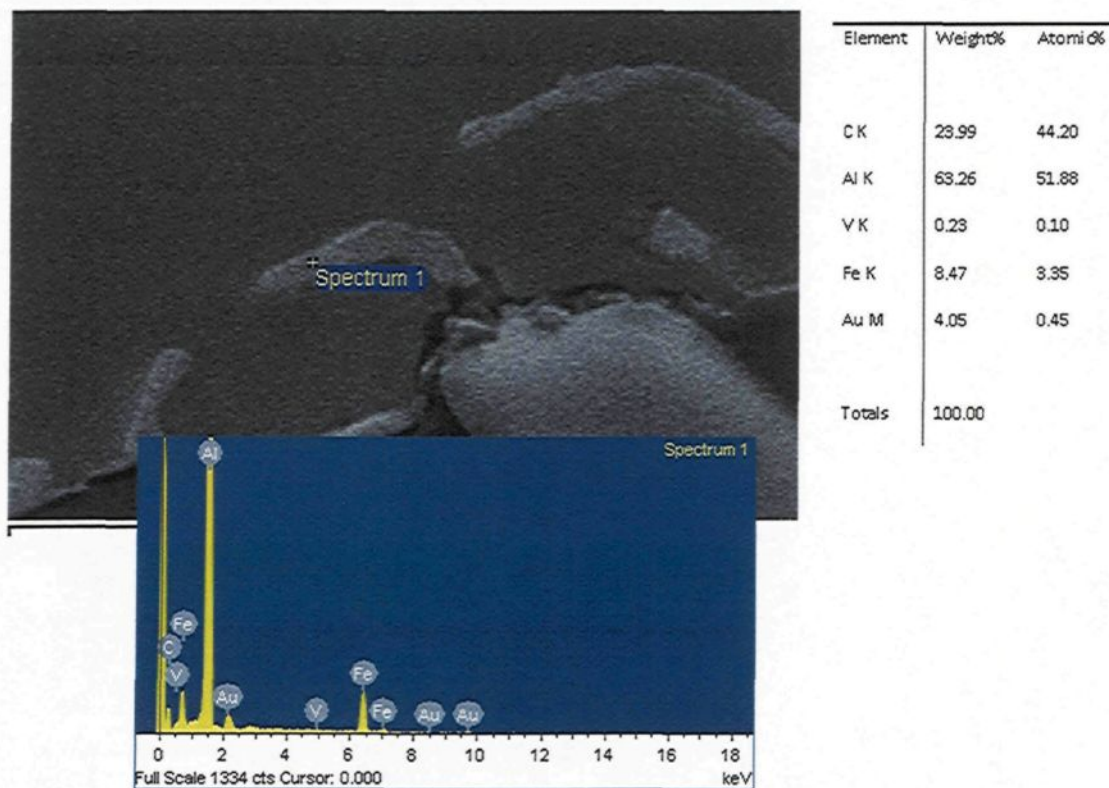


Figure 5.27 EDX observation of the Al/VC interface after 20 minutes at 850°C

Examination of the Al/ZrC interface afterwards disclosed the presence of small reaction layer at the interface shown in Fig.5.28. It appears from the morphology of the Al/ZrC interface that some other phases nucleate on the solid ZrC surface and grow towards the liquid aluminium. This morphology strongly indicates that the molten aluminium reacted with ZrC during the wetting studies so that wetting and spreading are possibly occurring due to chemical reaction. This is once again in agreement with the contact angle data. It is clearly observed that the thickness of the interface is about 1-3 μm (see Fig.5.28). Because of the reduced volume of the interface, it was not possible to perform X-ray diffraction studies.

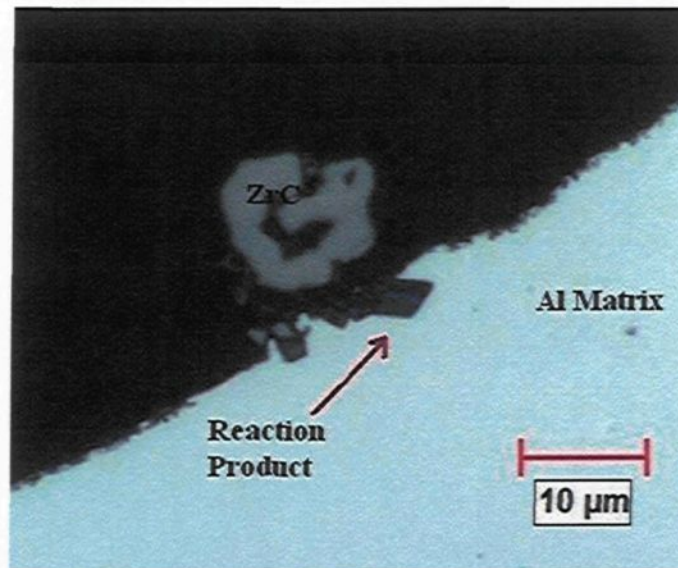


Figure 5.28 Optical micrograph of Al/ZrC interface after 20 minutes at 850°C

5.1.5 Calculation Work of Adhesion, Reaction Kinetics and Activation Energy of Different Ceramic Powders

5.1.5.1 Work of Adhesion

Table 5.5 Work of adhesion evaluated in function of the surface tension and contact angle for Al/ B₄C and Al-Ti alloy/B₄C powder systems

T (°C)	θ_i (°)*	Al W_a (dyne/cm) $W_a = \gamma_n(1 + \cos \theta)$	θ_i (°)*	1wt%Ti W_a (dyne/cm) $W_a = \gamma_n(1 + \cos \theta)$	θ_i (°)*	1.5wt%Ti W_a (dyne/cm) $W_a = \gamma_n(1 + \cos \theta)$	θ_i (°)*	3wt%Ti W_a (dyne/cm) $W_a = \gamma_n(1 + \cos \theta)$
750	135	245.15	135	237.24	125	339	127	318.5
850	131	273.43	128	301.32	118	409.56	120	389.5

*The contact angle used is the value of initial contact angle

The condition for perfect wetting is given by $W_a \geq 2\gamma_{lv}$ [Contreras *et al.*, 2003]. This means that the adhesion energy between the ceramic and the melt should be more than twice of the surface tension of the liquid which is mainly due to cohesive forces. The W_a is 273.43 dyne/cm and γ_{lv} is 795 dyne/cm for aluminum calculated at 850°C. This represents only 34.39% of the cohesion work of the liquid Al, which suggests that Al/B₄C will be weak energetically. In the case of Al-1wt%Ti/B₄C at that same temperature, the work of adhesion represents around 38.43% of the cohesion work of Al-1wt%Ti indicating another weak interface. The work of adhesion is 53.05% of the cohesion work of Al-1.5 wt% Ti/B₄C system at 850°C indicating the strongest interface among the systems studied.

The results for surface tension versus temperature obtained under argon atmosphere for both Al and Al alloy produced in Table 5.6 shows the work of adhesion of different ceramic powders, which are calculated using surface tension values obtained for Al/B₄C and Al-Ti alloy /B₄C system (Fig. 5.17 and Fig.5.18).

Table 5.6 Work of adhesion evaluated as a function of the surface tension and contact angle

Powder	Temperature (°C)	Aluminum			Al-1wt%Ti		
		θ_i (°)*	γ_{lv} (dyne/cm)	W_a (dyne/cm)	θ_i (°)*	γ_{lv} (dyne/cm)	W_a (dyne/cm)
ZrC	750	-	-	-	124	810	357.01
	850	131	795	273.43	118	784	415.93
ZrB ₂	750	128	837	321.69	122	810	380.76
	850	126	795	327.71	122	784	368.09
VC	750	125	837	356.91	125	810	345.40
	850	123	795	362.01	121	784	380.21
VB ₂	750	-	-	-	-	810	-
	850	-	-	-	126	784	323.17
AlB ₂	750	131	837	287.87	131	810	278.59
	850	120	795	397.5	119	784	403.9
Al ₄ C ₃	750	130	837	298.98	125	810	345.40
	850	123	795	362.01	122	784	368.54
TiB ₂	750	131	837	287.87	-	-	-
	850	123	795	362.01	-	-	-
TiC	750	134	837	255.57	-	-	-
	850	130	795	283.98	-	-	-

The W_a for Al/ZrC powder system calculated at 850°C is 273.43 dyne/cm and γ_{lv} is 795 dyne/cm at the same temperature. This is about 34.4% of the cohesion work of the liquid Al, which suggests that Al/ ZrC interface will be weak energetically. In the case of Al-1wt%Ti/ZrC powder system at that same temperature, the work of adhesion represents around 53% of the cohesion work of Al-1wt%Ti indicating comparatively stronger interface.

For Al/ZrB₂ powder system the cohesion work of liquid Al is about 41.2% of the work of adhesion and for Al-1wt%Ti/ZrB₂ powder system is about 47% of Al alloy at same temperature.

The W_a for Al/VC powder system is 45.5% of the cohesion work of liquid Al whereas for Al-1wt%Ti/VC powder system is 48.5% of liquid Al-1wt%Ti alloy at 850°C. This indicates that at that temperature for both the system have same weak interface.

For Al-1wt%Ti/VB₂ powder system, work of adhesion is only 41.22 % of the cohesion work of liquid Al-1wt%Ti alloy indicates a very weak interface.

The work of adhesion for Al/AlB₂ and Al-1wt%Ti/AlB₂ powder systems are 50% and 51.5% of the cohesion work of liquid aluminum and Al-1wt%Ti alloy at 850°C respectively, which suggests Al/AlB₂ and Al-1wt%Ti/AlB₂ interface is energetically weak.

In case of Al₄C₃ powder the work of adhesion is 45.53% and 47% of cohesion work for Al and Al alloy at 850°C. It can be said that at that temperature for both the system showing

weak interface.

Cohesion work of liquid Al for Al/TiB₂ and for Al/TiC powder system is 45.53% and 35.7% of the work of adhesion respectively, which suggests that Al/TiB₂ interface is energetically stronger than Al/TiC interface.

5.1.4.2 Calculation of Reaction Kinetics

The rate of liquid metal penetration and spreading is related to the rate of change of contact angle. Therefore the constant 'K' in Eq.2.6 can be referred as penetration and spreading constant or rate constant. If 'K' as well as the initial and the equilibrium values of the contact angle are known, the contact angle at any time can be determined for a given system using Eq.2.9. In Eq. 2.9, θ_e is referred as an equilibrium contact angle. In this study, contact angle obtained after 20 minutes are used as reference contact angle (or apparent equilibrium angle which replaces equilibrium angle) because in this case it is impossible to reach equilibrium. It was observed during the experiments that the contact angles do not change significantly after this time. 'K' values show how fast the system reaches to its final contact angle value at a given temperature.

Table 5.7 presents the equilibrium angles used as well as the 'K' values calculated for Al/B₄C system at different temperatures. It is clearly observed that for Al/B₄C powder system the rate constant (K) is highest at 850°C and lowest at 900°C.

Fig. 5.29 compares the experimental contact angle versus time data with those calculated using Eq. 2.9 (model) for Al/B₄C powder system. Curves with higher 'K' are strongly

exponential; consequently, the contact angle reaches equilibrium value faster. Maximum 'K' value is observed at 850°C and contact angle reaches to its reference value quickly at this temperature. At 800°C, 'K' value is next highest and contact angle also decreases very fast. At 800°C, 850°C and 900°C the wetting model represents the experimental data well. However, as it was mentioned before, the samples were highly oxidized at this temperature.

Table 5.7 Contact angle change rate (K) for Al/B₄C powder system at different temperatures

Ceramic	Metal	Temperature(°C)	K(sec ⁻¹)	Equilibrium Contact Angle(°)	Initial Contact Angle(°)
B ₄ C	Al	700	0.00017	126	135
B ₄ C	Al	750	0.00018	127	135
B ₄ C	Al	800	0.00019	124	134
B ₄ C	Al	850	0.0003	126	129
B ₄ C	Al	900	0.00007	128	131

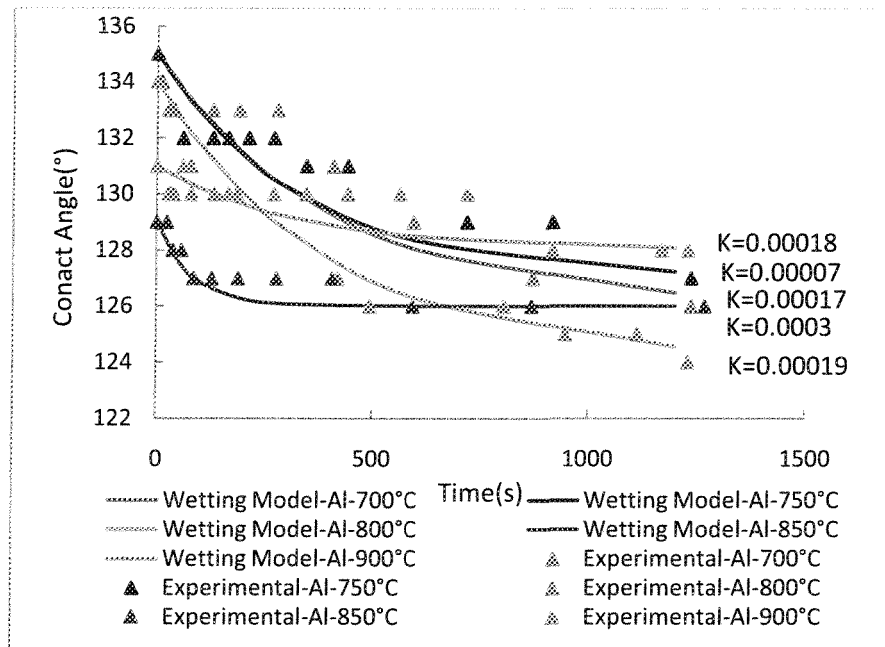


Figure 5.29 Comparisons of contact angle evolution measured experimentally and calculated with wetting model for Al/ B₄C powder system

For Al-1wt%Ti/B₄C powder system, the rate constant 'K' is highest at 900°C and lowest at 700°C. The rate constants are found to be similar at 800°C and 850°C (see Table 5.8).

Table 5.8 Rate constant (K) for Al-1wt%Ti/B₄C powder system at different temperatures

Ceramic	Metal	Temperature(°C)	K(sec⁻¹)	Equilibrium Contact Angle(°)	Initial Contact Angle(°)
B ₄ C	Al- 1wt%Ti	700	0.00008	130	136
B ₄ C	Al- 1wt%Ti	750	0.00012	124	135
B ₄ C	Al- 1wt%Ti	800	0.000129	124	134
B ₄ C	Al- 1wt%Ti	850	0.00013	121	127
B ₄ C	Al- 1wt%Ti	900	0.00031	122	131

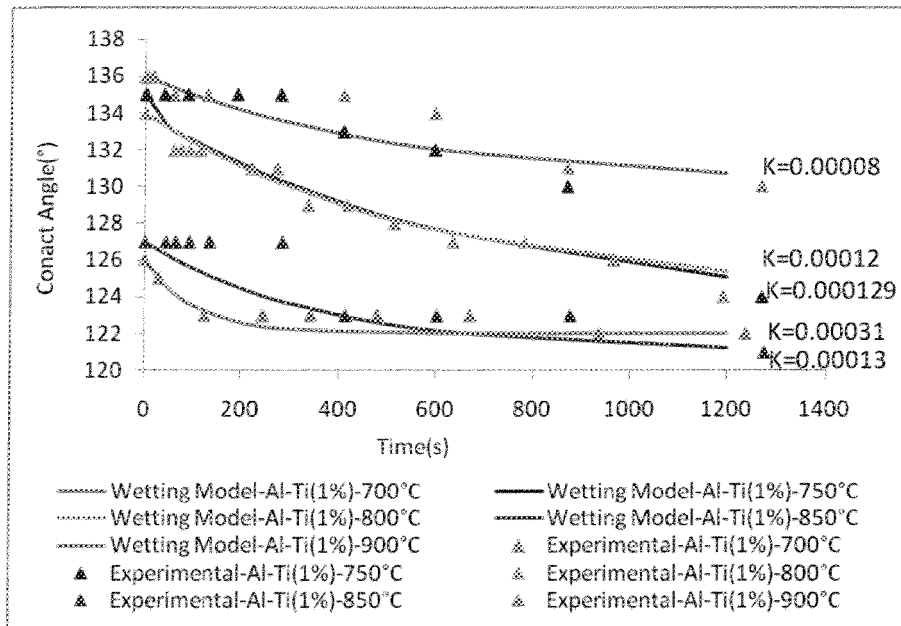


Figure 5.30 Comparisons of contact angle evolution measured experimentally and calculated with wetting model for Al-1wt%Ti/ B₄C powder system

Figure 5.30 shows that wetting model prediction are in good agreement with the data at 800°C, 850°C and 900°C for Al-1wt%Ti/ B₄C powder system. However, the agreement between the model and the data is not as good at lower temperatures (700°C and 750°C).

Table 5.9 Contact angle change rate (K) for Al-1.5wt%Ti/B₄C powder system at two different temperatures

Ceramic	Metal	Temp (°C)	K(sec ⁻¹)	Equilibrium Contact Angle(°)	Initial Contact Angle(°)
B ₄ C	Al-1.5wt%Ti	750	0.00006	122	125
B ₄ C	Al-1.5wt%Ti	850	0.00019	110	118

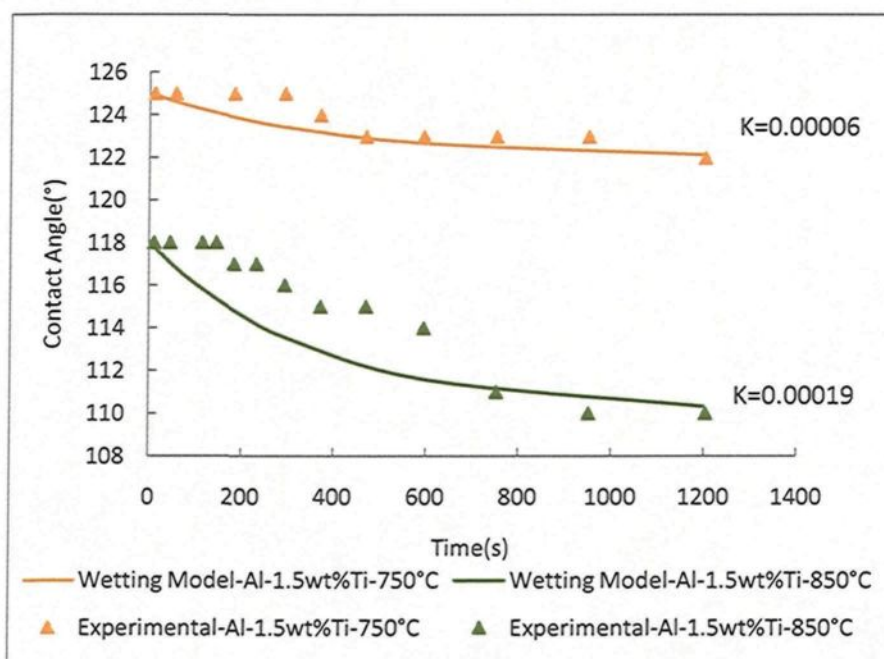


Figure 5.31 Comparisons of contact angle evolution measured experimentally and calculated with wetting model for Al-1.5wt%Ti/ B₄C powder system

At both temperatures, the predicted model provides good accordance with the experimental

results especially at lower temperature Al-1.5wt%Ti/B₄C powder system. 'K' is higher at 850°C compared to that of 750°C for this system (see Table 5.9, Fig.5.31).

Table 5.10 Rate constant (K) for Al-3wt%Ti/B₄C powder system at two different temperatures

Ceramic	Metal	Temp (°C)	K(sec ⁻¹)	Equilibrium Contact Angle(°)
B ₄ C	Al-3wt%Ti	750	0.000033	124
B ₄ C	Al-3wt%Ti	850	0.00008	116

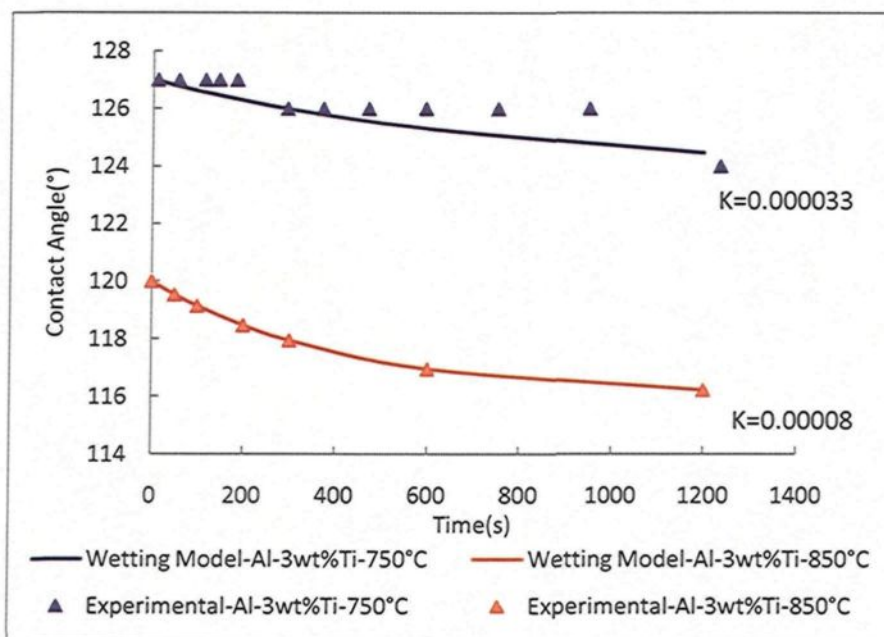


Figure 5.32 Comparisons of contact angle evolution measured experimentally and calculated with wetting model for Al-3wt%Ti / B₄C powder system

At both the temperatures, the predicted model exactly coincided with the experimental results for Al-3wt%Ti/B₄C powder system. 'K' is found to be higher at 850°C compared to that of 750°C for this system (see Table 5.10, Fig.5.32).

All the wetting model prediction curves exhibit three characteristic regions of the contact angle with respect to time. The first region is characterized by a sharp slope where contact angle decreases very fast (0 to 200s). In the second region the slope of the curve is smaller and contact angle continues to decrease with a lower rate compared to the decrease in the first region. In the third region, θ stays nearly constant or reaches to apparent equilibrium (reference value).

5.1.4.3 Calculation of Activation Energy

Since reaction systems can be characterized by change of θ with time and strong temperature dependence, it is possible to calculate the activation energies for the wetting. 'K' values which are predicted by the model (see Eq.2.9) are used to calculate the activation energy using the Arrhenius equation as used by other authors [Contreras *et al.*, 2003; Contreras *et al.*, 2004; Toy *et al.*, 1997]. In general, low values of activation energy are related with strong chemical interactions [Contreras *et al.*, 2003].

Table 5.10 shows the activation energy values obtained from the Arrhenius plot shown in Fig.5.33. Pre-exponential factors (K_0) and the activation energies (E_a) for different systems are calculated from the intercept and the slope of the graphs, respectively. It is possible to calculate the K values of these systems at any temperature by using the activation energies

and K_0 values calculated with the model.

Table 5.11 shows that Al-1wt%Ti/B₄C system has the lowest activation energy indicating that this system is most reactive compared to the others studied. Al-1.5wt%Ti/B₄C system shows highest activation energy which indicates that this system is less reactive than other systems. These results do not agree with the contact angle data since the system was found to be most wettable with Al-1.5wt%Ti (lowest contact angles). If the wetting is controlled by interfacial chemical reaction, ' E_a ' for B₄C/ Al-1.5wt%Ti system should be the lowest. It can be clearly seen that it is not possible to reach a conclusion when the activation energies are calculated from ' K ' values obtained only at two temperatures. It might be true that the system is controlled by some other mechanism than interfacial reaction (such as diffusion or the combination of reaction and diffusion) as suggested from activation energies found. However, it is also possible that the values are erroneous due to the lack of data and the interfacial reaction is the controlling mechanism for wetting. Therefore, these calculations are demonstrated here only to show the usefulness of the model. However, it has to be kept in mind that the values are very rough approximations. Therefore, this model is not applied to all of the data obtained from the wetting experiments using different ceramic powders. If more experiments are carried out at different temperatures this model will yield valuable information.

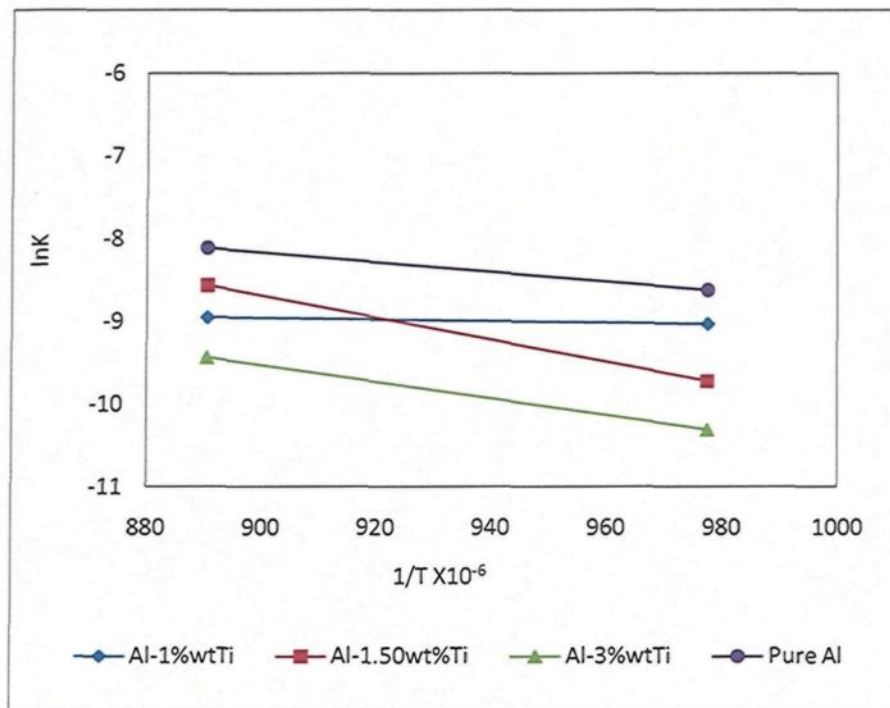


Figure 5.33 Arrhenius plot for Al/B₄C and Al alloys/B₄C systems

Table 5.11 Activation energy of Al/B₄C and Al alloys/B₄C systems

Alloy (wt%)	E _a (kJ/mol)	K ₀
Pure Al	48.71	0.0553
Al-1% Ti	7.45	0.00288
Al-1.5% Ti	110.8	27.279
Al-3% Ti	84.05	0.646

CHAPTER 6

CONCLUSIONS AND RECOMMENDATION

6.1 Conclusions

1. The originality of this project was to study the wetting behavior of boron carbide, some transition metal carbides and borides by aluminum and aluminum alloys under same experimental environment.
2. Wetting between boron carbide powder and molten aluminum as well as Al-1wt% Ti alloy were studied using the sessile-drop technique. Initially, wetting experiments were conducted in the temperature range of 700°C to 900°C. In general, it was observed that contact angle decreases with increasing temperature and with increasing time.
3. In order to understand the effect of interfacial reaction products on wetting, the contact angles between various reaction products of alloying elements (titanium, zirconium, vanadium) and aluminum have been studied at 750°C and 850°C.
4. It is also clear that the presence of zirconium and titanium enhances the wetting in most of the cases. Effect of vanadium on wetting is not very clear. At 850°C, the final contact angle (after 20 min) of pure aluminum on vanadium carbide is 109°, however, at 750°C and 850°C vanadium boride is not at all wetted by pure aluminum.
5. The wettability of the boron carbide by aluminum increases as Ti content increases up to

- 1.5%. The optimum Ti levels lie around 1.5% in order to have the best wettability. Further increase in Ti level towards 3 % decreases the wettability because of formation of Al_3Ti .
6. The microstructure of the interface of Al-Ti Alloy/ B_4C systems consists of B_4C powders and phases such as Al_3BC and TiB_2 . However adequate amount of Ti addition is able to limit the undesirable interfacial reaction. This leads to improvement of wettability.
7. The spreading of Al and Al-Ti alloy drop was observed to occur in accordance with the formation of new phases, leading to a decrease in the contact angle. The work of adhesion increases with decreasing contact angle and increasing temperature except for the Al-3wt%Ti/ B_4C system. Work of adhesion also increases with increasing Ti levels up to 1.5%.
8. No reaction was observed in the cross section of the sessile drop- substrate interface for Al / Al_4C_3 system at 850°C and only physical wetting takes place.
9. The microstructure of the interface for Al /VC and Al/ ZrC systems shows formation of new phases. It can be said that in this case wetting is driven by chemical reaction.
10. All the metal-ceramic systems investigated have low work of adhesion which indicates weakly-bonded interfaces.
11. Surface tension of Al was reduced by increasing temperature and addition of Ti. Surface tension of the Al-Ti alloy decreases as the titanium content increases up to 1.5%. An exception is observed in case of 3wt%Ti.
12. Most of the wetting model predictions are in good agreement with the experimental results. High activation energies values obtained for Al/ B_4C and Al alloys/ B_4C systems, suggests that chemical reaction is the driving force for the spreading of the drop, consequently, wetting. However, more experiments at different temperatures are required in

order to do a kinetic analysis.

13. It is difficult to compare the initial contact angle data with those found in the literature due to the different experimental conditions used. However, the initial contact angles measured during this work seems to be in the same range as those cited in literature for B_4C , TiC and TiB_2 powders and pure aluminum.

6.2 Recommendations

One of the major objectives of this project was to study the wetting behavior of boron carbide, transition metal carbides and borides by aluminum and aluminum alloys under same experimental environment. Morphological analysis of the interface is important for metal matrix composites production technology. In this study, metal-ceramic interface morphologies were not studied for all the powders. Studying all the metal ceramic interfaces in a future investigation would provide a more comprehensive picture.

In this study, 1.5% Ti content was found to be optimal to obtain the best wetting, consequently, mixing of B_4C with Al. The use of this Ti content is recommended for MMC preparation in industry. If other alloys are to be used, the optimum content for the alloying elements should be determined with wetting tests

The reaction products of the Al/VC system were not identified accurately because of the reduced volume of the reaction products. This has to be overcome in future investigations

so as to be able to carry out proper TEM analysis.

In this study, the experiments were carried out with powders. The effects of surface characteristics (granular powders and hot-pressed plates) on wetting were not taken into account. However, these may show the effect of the surface conditions on the contact angle. During this study, Al alloys with different Ti contents were used to study the effect on wetting of B_4C by aluminum. In the same manner, considering different zirconium and vanadium contents could be of interest.

REFERENCES

- Adamson A.W, *Physical chemistry of surfaces*, John Wiley & Sons Inc (1990).
- Askari M, Camerom A.M, Oakley J, *The Determination of Surface Tension at Elevated Temperature by Drop Image Analysis*, High Temperature Tech., V.8(3), pp. 201-207 (1990).
- Assael M.J, Kakosimos K, Dix M.J, *Reference Data for the Density and Viscosity of Liquid Aluminum and Liquid Iron*, J. Phys. Chem. Ref. Data., V. 35(1), pp. 285-300 (2006).
- Bashforth F, Adams J.C, *An Attempt to Test the Theories of Capillary Action*, Cambridge University Press, Cambridge, UK 1883.
- Cassie A.B.D, Baxter S., *Wettability of porous surfaces*, Transaction of the Faraday Society, V. 40, pp 546-551 (1944), DOI: 10.1039/TF9444000546.
- Cazabat A.M, Cohen Stuart M.A, *Dynamics of Wetting: Effect of Surface Roughness*, Journal of Physical Chemistry, V.90, pp.5845-5849(1986).
- Chen X-G, EPD Congress 2005, *Interface Reaction of Boron Carbide in Aluminum Matrix Composites and its Control*, Etd by M.E Schlesinger TMS (The Minarals, Metals and Material Society), pp 101-106 (2005).
- Chen X-G, *Application of Al-B₄C Metal Matrix Composites in the Nuclear Industry for Neutron Absorber Materials*, Solidification Processing of Metal Matrix Composites-Roatgi Honorary Symposium, Etd. By N. Gupta and W.H. Hunt, The Minarals Metals and Material Society, pp. 343-350 (2006).
- Contreras A, Lopez V.H, Leon C.A, Drew R.A.L, Bedolla E. *The Relation Between Wetting and Infiltration Behavior in the Al-1010/TiC and Al-2024/TiC Systems*, Advances in Technology of Materials and Materials Processing Journal, V.3, (1-2), pp.27-34(2001).
- Contreras A, Leon C.A, Drew R.A.L, *Wettability and Spreading Kinetics of Al and Mg on TiC*, Scripta Materialia, V. 48, pp.1625-1630 (2003).
- Conteras A, Bedolla E, Perez R, *Interfacial Phenomena in Wettability of TiC by Al-Mg alloys*, Acta Materialia, V.52, pp 985-994(2004).
- Dorsey N.E, *A New Equation for the Determination of the Surface Tension from the form of a Sessile Drop or Bubble*, J. Wash. Acad. Sci., V.18 (19), pp. 505-509 (1928).
- Drelich J., Miller J.D, J. Colloid Interface Sci., 164 (1994), p. 252

- Ergin G, *The Wettability of the Filter Media by Aluminum Alloys during Aluminum Filtration*, Thesis UQAC, (2006).
- Eustathopoulos N, Nicholas M.G, Drevet B, *Wettability at High Temperatures*, Pergamon Materials Series V.3, Series Editor: R.W. Cahn, Amsterdam (1999).
- Halverson D.A, Pyzik A.J, Aksay I.A, *Processing of Boron Carbide- Aluminum Composites*, J. Am.Soc.,V. 72 (5), pp. 775-780 (1989).
- Hashim J, Looney L, Hashmi M.S.J, *The wettability of SiC Particles by Molten Aluminium Alloy*, J.Mate.Processing.Tech.119, pp 324-328(2001).
- Himbeault D.D, Varin R.A, Piekarski K, *Proceedings of the International Symposium on Advances in Processing of Ceramic and Metal Matrix Composites*, Halifax, Nova Scotia, Canada, pp. 312–323 (1989).
- Ishikawa T, Tanaka J, Teranishi H, Okamura T, Hayase T, US Patent 440 571(1981).
- Keene B.J, *Review of Data for the Surface Tension of Pure Metals*, International mat. Rev., V.38 (4), pp.157-192 (1993).
- Kainer K.U, *Metal Matrix Composites*, WILEY-VCH, (2006).
- Kanian V.S, Millot F, Rifflet J.C, *Surface Tension and Density of Oxygen-Free Liquid Aluminum at High Temperature*, Int. J.Ther.Phy, V. 24(1), pp.277-286(2003).
- Kingery W.D, Humenick Jr. M, *Surface Tension at Elevated Temperature I., Furnace and Methode for use of Sessile Drop Method; Surface Tension of Silicon, Iron, and Nickel*, J. Phys. Chem., V.57(3), pp. 359-63 (1953).
- Keisler C, Lataillade J.L, *The Effect of Substrate Roughness Characteristic on Wettability and on the Mechanical Properties of Adhesive Joints Loaded at High Strain Rates*, J. Adhesion Sci, Technol,V. 9(4), pp.394-411(1995).
- Kennedy A.R, Karantzalis A.E, *The Incorporation of Ceramic Particles in Molten Aluminium and the Relationship to Contact Angle Data*, Mater. Sci. Eng. A264, pp.122-129 (1999).
- Kennedy A.R, Brampton B, *The Reactive Wetting and Incorporation of B₄C Particles into Molten Aluminum*, Scripta Materiala, V.44, pp.1077-1082(2001).
- Kubaschewski O, Alcock C.B, *Materials Thermo- Chemistry*, 6th Ed. (1993).

- Kwok D.Y, Neumann A.W, *Contact angle interpretation in terms of solid surface tension, Colloids and Surfaces , A: Physicochemical and Engineering Aspects* V.161, pp 31–48 (2000)
- Landry K, Rado C, Voitovitch R, *Mechanism of Reactive Wetting: The Question of Triple Line Configuration*, *Acta Materiala*, V. 45 (7), pp. 3079-3085 (1997).
- Lebeau T, Strom-Olsen J.O, *Aluminium Alloy /Aluminium based Ceramic interactions, Material characterization*, V. 35, pp. 11-22(1991)
- Levenspiel O, *Chemical Reaction Engineering*, 3rd edition, pp.27-28(1999).
- Liptáková E, Kúdela J and Sarvaš J, Study of the System Wood - Coating Material, *Holzforschung*, V. 54, No. 2, pp. 189–196 (2000)
- Li J.G, Wetting of Ceramic Materials by Liquid Silicon, *Aluminum and Metallic Melts Containing Titanium and Other Reactive Elements-A Review*, *Ceram. Int.*, Vol. 20, pp.391-412(1994).
- Marmur A, Soft contact: measurement and interpretation of contact angles, *The Royal Society of Chemistry, Soft Matter*, V.2, pp.12–17(2006).
- Maze C, Burnet G, *A Non Linear Regression Method for Calculating Surface Tension and Contact Angle from the Shape of a Sessile Drop*, *Surf. Sci.*, V.13, pp. 451-70 (1969).
- Myres D, *Surfaces Interfaces and Colloids Principles and Applications*, 2nded, 1999.
- Murr L.E, *Interfacial Phenomena in Metals and Alloys*, London (1975)
- Naidich Y.V, Chubashov Y.N, Ischchuk N.F., Krasovskii V.P, *Wetting of Some Nonmetallic Materials by Aluminum*, *Proskovaya Metallurgiya*, V. 6, pp.67-69 (1983).
- Nakae H, Inui R, Hirata Y, Saito H, *Effects of Surface Roughness on Wettability*, *Proceeding of the Third International, Spain, Sept 1996/Proceeding Ed*, pp.2313-2318(1998).
- Neumann A.W, Good R.J., *Surface and Colloid Science*, vol. II, ed. R.J. Good and R.R. Stromberg (New York: Plenum Press, 1979).
- Nizhenko V.I, Floka L.I, *Wetting of Al₂O₃- Based Oxide Ceramics by Molten Aluminum*, *Powder Metallurgy and Metal Ceramics*, V.40(5-6), pp.271-276 (2001).
- Nowok J. W., *Mass Transport Phenomena at the Liquid Metal/Substrate (Metal/Carbide) Interface*, *Materials Science and Engineering*, A232, pp. 157-162(1997).

- Okamoto H, *Desk Handbook: Phase diagrams for binary alloys*, pp.46 (2000)
- Onuhama I, Fujita Y, Mitsui H, Ishikawa K, Kainuma R, and Ishida K, *Phase Equilibria in the Ti-Al Binary System*, *Acta Material.*, V.48(12), pp.3113-3124(2000).
- Paddy J.F, *Surface and Colloid Science*, V.1, Ed. Egon Matijevic, Jhon Wiley and Sons, N.Y, pp.101-149 (1960).
- Pai B.C, Rohatgi P.K, *Preparation of Cast Aluminium-Silica Particulate Composites*, *Mater. Sci. Eng.*, V. 21, pp. 161 (1975).
- Passerone A, Sangiorgi R, Valbusa G, *Surface Tension and Density of Molten Glasses in the System $La_2O_3-Na_2Si_2O_5$* , *Ceram. Int.*, V.5, pp 18-22(1979).
- Passerone A, Passerone D, Muolo M.L, *Wetting of Group IV diborides by Liquid Metals*, *J.Mater. Sci*, V. 41, 5088-5098 (2006).
- Quere D, *Wetting and Roughness*, *Annual Review of Materials Research*, V.38, pp.71-99 (2008).
- Rajan T. P. D, Pillai R. M, Pai B. C, *Review Reinforcement coatings and interfaces in aluminum metal matrix composites*, *Journal of Materials Science*,V.33, pp 3491-3503 (1998).
- Ramani G, Pillai R.M, Pai B.C, Satyanarayana K.G, *Stir Cast Aluminium Alloy Matrix Composites*, M.Tech. Dissertation, IIT, Kanpur, India, V. 12, p. 117(1993).
- Rangel E.R., Becher P.F, *Influence of Carbon on the Interfacial Contact Angle between Alumina and Liquid Aluminum*, *Surf. Interface Anal*, V.35, pp.151-155(2003).
- Ray S, *Casting of composite components*, in: *Proceedings of the 1995 Conference on Inorganic Matrix Composites*, Bangalore, India, pp. 69–89 (1996).
- Rotenberg Y, Boruvka L, *Determination of Surface Tension and Contact Angle from the Shapes of Axisymmetric Fluid Interfaces*, *Colloid Interface Sci.*, V. 93(1), pp. 169-83 (1983).
- Rhee S.K, *Wetting of Ceramics by Liquid Aluminum*, *J. American. Soc.*, V. 53(7), pp. 386-389 (1970).
- Saiz E, Cannon R.M, Tomsia A.P, *Wetting and Diffusion Process at Liquid Metal/Ceramic Interfaces*, Proc. 6th Japan International SAMPE Symposium, V. 26-29, pp.863-866(1999).
- Sangiorgi R, Caracciolo G., Passerone, *Factors Limiting the Accuracy of Measurements of Surface Tension by the Sessile Drop Method*, *J. Mater. Sci.*, V.17, pp.2895-901(1982).
- Saravanan R.A, Molina J.M, Narciso J, Garcia-Cordovilla C, E. Louis., *Surface Tension of*

Pure Aluminum in Argon/Hydrogen and Nitrogen/Hydrogen Atmospheres at High Temperatures, J. Mat. Sci. Lett., V.21, pp. 309-311(2002).

Sarou-Kanian V, Millot F and Rifflet J.C, Surface Tension and Density of Oxygen-Free Liquid Aluminum at High Temperature, international Journal of Thermophysics, Vol.24, No.1, pp.277-296(2003).

Schoennahl J, Willer B, Daire M, *The mixed carbide Al_4SiC_4 -preparation and structural data*. J. Solid State Chem. V.52, pp. 163–173 (1984).

Semal S, S. Blake S, Geskin V, Ruijter M.J. de, Castelein G, *Influence of Surface Roughness on Wetting Dynamics*, The ACS J. Surf. Collid., V.15, pp.8765-8770(1990).

Shi S.Q, Gardner D.J, *Dynamic Adhesive Wettability of Wood*, Wood and fiber sciences, V.33 (1), pp. 58-68 (2001).

Stehr M, Gardner D.J, *Dynamic Wettability of Different Machined Wood surfaces*, J.Adhesion, V.76, pp.185-200 (2001).

Toy C, Scott W.D, *Wetting and Spreading of Molten Aluminium against AlN surface*, J. Mat. Sc., V.32, pp.3243-3248 (1997).

Tafto J, Kristiansen K, Westengen H, Nygard A., Borradaile J.B, Karlsen D.O, Proceedings of the International Symposium on Advances in Cast Reinforced Metal Composites, pp.71-75(1988).

Vainshtein B.K, *Modern Crystallography: Fundamentals of crystals, symmetry and methods of structural crystallography*, Spinger-Verlag Berlin Heiedlberg, 2nd Etd.,(1996).

Viala J.C, Bouix J, Gonzalez G, Esnouf C, *Chemical Reactivity of Aluminum with Boron Carbide*, J. Mater. Sci., V.32, pp.4559- 4573 (1997). doi:10.1023/A:1018625402103).

Warren R, Anderson C.H, *Silicon Carbide Fibers and Their Potential for Use in Composite Materials*, Part II, Composites, pp. 101–111(1984).

Weirauch. Jr. D. A , Krafick W. J, *The Effect of Carbon on Wetting of Aluminum Oxide*, Metallurgical Transaction A, V. 21A(6), pp.1745-1751(1990).

Weirauch Jr. D.A, Zigler D.P, *An Improved Method for the Determination of the Surface Tension of Silicate Melts*, 12 th University Conference on Glass Science, Alfred, NY, July pp. 25-29 (1993).

Weirauch D.A, Balaba W.M, Perrotta A.J, *Kinetics of the Reactive Spreading of Molten Aluminum on Ceramic Surfaces*, J. Mater. Research, V. 10(3), pp.640-650(1995).

Weirauch D.A, Ziegler D.P, *Surface Tension of Calcium Aluminosilicate Glass Using Computerized Drop Shape Analysis*, J.Am.Ceram. Soc., V.78 (4), pp.920-926 (1996).

Weirauch D.A, Krafick Jr. W.J, Ackart G, Ownby P.D, *The Wettability of Titanium Diboride By Molten Aluminum Drops*, J. Mater.Sc.,V.40, pp.2301-230(2005).

Wenzel R. N, *Resistance of Solid Surfaces to Wetting by Water*, Industrial and Engineering Chemistry, V. 28 (8), pp 988-994(1936).

Yasinkaya G.A, *The Wetting of Refractory Carbides, Borides, and Nitrides by Molten Metals*; Poroshkovaya Metallurgiya, V.7(43), pp.53-56(1965).

Zhang G.J, Ando M, Yang J.F, Ohji T, Kanzak S, *Boron Carbide and Nitride as Reactants for in situ Synthesis of Boride-Containing Ceramic Composites*, J. Eur.Ceram.Soc., V.24, pp. 171-178(2004).

Zhang Z, Chen X-G, Charette A, *Powder distribution and interfacial reactions of Al-7%Si-10% B₄C die casting composite.*, J Mater Sci ,V.42,7354(2007),DOI 10.1007/s 10853-007-1554-5.

Zhang Z, Chen X-G, Charette A, *Fluidity and Microstructure of an Al-10% B₄C Composite*, J.Mater Sci., (2008a) DOI 10.1007/s 10853-008-3097-9.

Zhang Z, Fortin K, Chen X-G, Charette A, *Metal Flow and Semi Solid Processing: Effect of Titanium on Castability of Al- B₄C Composites*, Aluminum Alloys, Etd. by Jürgen Hirsch,Günter Gottstein, Birgit Skrotzki, ,V.1, pp. 434-440(2008b).

Zhou W, Xu Z.M, *Casting of SiC reinforced metal matrix composites*,J.Mater. Process.Technol.,V.63,pp.358-363(1997)